JOINT TRANSPORTATION
RESEARCH PROGRAM
INDIANA DEPARTMENT OF TRANSPORTATION
AND PURDUE UNIVERSITY

Predictive Analytics for Quantifying the Long-Term Costs of Defects During Bridge Construction

Nichole Marie Criner, Manuel Salmeron, Xin Zhang,
Shirley J. Dyke, Julio A. Ramirez, Benjamin Eric Wogen

SPR-4526 • Report Number: FHWA/IN/JTRP-2023/08 • DOI: 10.5703/1288284317615

RECOMMENDED CITATION

Criner, N. M., Salmeron, M., Zhang, X., Dyke, S. J., Ramirez, J. A., & Wogen, B. E. (2023). *Predictive analytics for quantifying the long-term costs of defects during bridge construction* (Joint Transportation Research Program Publication No. FHWA/IN/JTRP-2023/08). West Lafayette, IN: Purdue University. https://doi.org/10.5703/1288284317615

AUTHORS

Nichole Marie Criner
Graduate Research Assistant
Lyles School of Civil Engineering
Purdue University

Manuel Salmeron
Graduate Research Assistant
School of Mechanical Engineering
Purdue University

Xin Zhang
Graduate Research Assistant
Lyles School of Civil Engineering
Purdue University

Shirley J. Dyke, PhD
Professor of Mechanical and Civil Engineering
Lyles School of Civil Engineering
(765) 494-7434
sdyke@purdue.edu
Corresponding Author

Julio A. Ramirez, PhD
Kettelhut Professor of Civil Engineer and NHERI-NCO Center Director
Lyles School of Civil Engineering
(765) 494-2716
ramirez@purdue.edu
Corresponding Author

Benjamin Eric Wogen
Graduate Research Assistant
Lyles School of Civil Engineering
Purdue University

JOINT TRANSPORTATION RESEARCH PROGRAM

The Joint Transportation Research Program serves as a vehicle for INDOT collaboration with higher education institutions and industry in Indiana to facilitate innovation that results in continuous improvement in the planning, design, construction, operation, management and economic efficiency of the Indiana transportation infrastructure. https://engineering.purdue.edu/JTRP/index_html

Published reports of the Joint Transportation Research Program are available at http://docs.lib.purdue.edu/jtrp/.

NOTICE

TECHNICAL REPORT DOCUMENTATION PAGE

1. Report No. FHWA/IN/JTRP-2023/08	**2. Government Accession No.**	**3. Recipient's Catalog No.**
4. Title and Subtitle Predictive Analytics for Quantifying the Long-Term Costs of Defects During Bridge Construction		**5. Report Date** January 2023 **6. Performing Organization Code**
7. Author(s) Nichole Marie Criner, Manuel Salmeron, Xin Zhang, Shirley J. Dyke, Julio A. Ramirez, and Benjamin Eric Wogen		**8. Performing Organization Report No.** FHWA/IN/JTRP-2023/08
9. Performing Organization Name and Address Joint Transportation Research Program Hall for Discovery and Learning Research (DLR), Suite 204 207 S. Martin Jischke Drive West Lafayette, IN 47907		**10. Work Unit No.** **11. Contract or Grant No.** SPR-4526
12. Sponsoring Agency Name and Address Indiana Department of Transportation (SPR) State Office Building 100 North Senate Avenue Indianapolis, IN 46204		**13. Type of Report and Period Covered** Final Report **14. Sponsoring Agency Code**

15. Supplementary Notes

Conducted in cooperation with the U.S. Department of Transportation, Federal Highway Administration.

16. Abstract

During the lifecycle of a bridge, deterioration of the concrete deck originates from many sources, e.g., corrosion due to water infiltration in conjunction with chlorides from the use of de-icing salts. Such deterioration may be affected by any one of the following six actions relevant to a bridge from conception to demolition: design, construction, in-service conditions, maintenance, repair and rehabilitation, and replacement. Many researchers have studied the relationships between these sources and their consequences. However, the relationship between construction defects and inspection practices, and its impact on the deterioration process has not yet been identified. This project focuses on the development of predictive models to assess the impact that defects present during concrete bridge deck construction may have on the lifecycle performance of the bridge deck in terms of the chemical and environmental deterioration relevant to Indiana. Based on the relevant cost information from the Indiana Department of Transportation (INDOT), a methodology is developed here to determine the potential costs associated with this deterioration. Recommendations relevant to construction and inspection and data collection practices are discussed to improve future bridge construction and inspection practices. The models and methods developed in this work will enable INDOT to better predict the accelerated deterioration of a concrete deck when a construction defect has been identified and the associated additional cost.

17. Key Words bridge deterioration, physics-based model, data-driven model, lifecycle cost analysis, construction defects	**18. Distribution Statement** No restrictions. This document is available through the National Technical Information Service, Springfield, VA 22161.

19. Security Classif. (of this report) Unclassified	**20. Security Classif. (of this page)** Unclassified	**21. No. of Pages** 92 including appendices	**22. Price**

EXECUTIVE SUMMARY

Introduction

During the lifecycle of a bridge, many factors influence the deterioration of a concrete bridge deck. Deterioration may be impacted by actions in any of the following six stages relevant to a bridge deck: design, construction, in-service conditions, maintenance, repair and rehabilitation, and replacement. During the construction of a bridge deck, there are occasions when defects in workmanship or materials might occur, e.g., inadequate mixing of the concrete. These defects may seem innocuous initially but in the long run can have a negative impact on the bridge deck's lifecycle performance and the associated cost of maintaining the bridge over its service life. Additionally, environmental and usage conditions may amplify the impact of these defects. In Indiana, these conditions include chemical and environmental factors (e.g., use of de-icing salts, and resultant corrosion, carbonation, and freeze-thaw cycles), daily traffic (e.g., average daily traffic and average daily truck traffic), and inspection-related issues (e.g., the missing information during inspection). Such defects and its consequences place an additional monetary burden on the bridge owner, INDOT.

This project focused on developing predictive models and methods to assess the impact of a concrete bridge deck that has construction defects on its lifecycle performance. Chemical and environmental deterioration factors were selected to be relevant to Indiana. A predictive degradation model for a concrete deck was developed and defects that may occur during construction and their corresponding consequences were considered when building the model. To evaluate the added life cycle costs from deterioration, a cost evaluation was also performed. The models and findings developed in this project will provide INDOT with necessary information to support decisions related to planning interventions and assigning costs. We also gathered recommendations relevant to data collection and construction inspection procedures for INDOT's consideration when they improve these models in the future.

Findings

- This study provides a procedure to predict the deterioration and resultant degradation of concrete bridge decks. The predictive degradation model developed consists of (1) a physics-based model for simulating the impact of physical processes on the concrete bridge deck, and (2) a data-driven model for considering the influence of external factors based on historical data.
- A cost model was developed to estimate the added costs associated with the deterioration of the concrete bridge deck when defects were present at the time of construction.
- Ten bridges were selected for the case study. These bridges were distributed geographically within Indiana. The degradation and additional cost incurred by the owner over its lifecycle was estimated for these bridges.
- The concrete bridge deck's sensitivity to the deterioration due to several relevant factors was investigated through the case studies. These factors included the region, the concrete deck defects, and a host of relevant hazard ratios for Indiana.
- Data needed for improving these estimates has been identified and is recommended for inclusion in future data collection procedures. Having this data will empower INDOT to better quantify bridge deck deterioration prediction, subsequent degradation, and cost analysis.
- Recommendations are provided for improving standards and procedures. These recommendations consider different stages of a bridge life cycle, including the bridge deck construction, inspections during the construction of the deck, maintenance actions taken while the bridge is in-service, and the relevant standards.

Implementation

This research culminated in the development of an Excel-based tool named INSPEC, which empowers INDOT to rapidly predict the deterioration of a concrete bridge deck and estimate the additional costs associated with substandard construction. Currently, this tool is only designed to serve as an estimation instrument because of gaps in the available data items, e.g., average surface chloride concentration. The collection of these data items should be prioritized for improving the robustness of the developed approach. In addition, INDOT should clarify and improve the standards for handling epoxy-coated bars to provide more specific, clear epoxy-coated rebar handling instructions, which is vital to the process of developing the proposed model. The procedures for inspection during construction should be adjusted for enriching the information needed for analysis. Finally, INDOT can implement the approach developed in this study and monitor a broader sample of bridges to calibrate the model parameters and refine the estimated costs.

The methodology developed in this study is directed to bridges built using current standard construction practices. Should these practices be improved, e.g., changing the standard concrete mix in the deck, increasing minimum cover, or increasing the thickness of epoxy coating applied to the bars, there would be a need to reevaluate the predictive models and collect data on those bridges to also evaluate the results from the data-driven model.

CONTENTS

LIST OF TABLES

LIST OF FIGURES

1. INTRODUCTION

During the lifecycle of a bridge, deterioration of the concrete deck often originates from one or more of the following sources: (1) corrosion due to water infiltration, which is worsened by weather and application of de-icing salts during the winter months; (2) delamination caused by freeze/thaw cycles, when applicable; (3) improper curing conditions that result in earlier cracking; and (4) carbonation and potential reinforcement corrosion by destroying the passive environment due to increased acidity. These processes may occur together and are affected by six actions relevant to a bridge from conception to demolition: design with associated specifications; construction and proper inspection of the construction processes; in-service conditions; maintenance; repair and rehabilitation; and replacement. For example, the amount and mix of deicing salt and sand used will influence how fast the alkaline environment is destroyed around the epoxy-coated rebar, and further causes deterioration of the rebar condition (Li et al., 2019; Martín-Pérez et al., 2000); or the cracking due to differential curing in the construction phase will open up paths for chloride penetration (Chen & Mahadevan, 2008). The relationship between some of these phenomena and their consequences in the lifecycle of a bridge deck have been extensively studied by previous researchers and can be found in the literature (Mangat & Molloy, 1994; O'Reilly et al., 2011; Sajedi & Huang, 2019). However, the relationships between construction and inspection practices and its impact on the aforementioned degradation processes deserves further research (Kim et al., 2013; Leiva Maldonado et al., 2019; Samples & Ramirez, 2000a, 2000b). Actually, it is the understanding of the influential factors in such relationships that can in turn help asset managers, inspectors, and field engineers to improve their practices and procedures.

This project focuses on the development of predictive analytics to assess the impact that defects in concrete bridge deck construction may have on the lifecycle performance of a bridge with regard to chemical and environmental deterioration relevant to Indiana. We consider the impact of potential defects that may occur during construction as well as the corresponding consequences using predictive models of the deterioration due to chemical and environmental causes, specifically, chloride-induced corrosion, carbonation, and freeze-thaw cycles. While we do not attempt to model and quantify the extent of cracking associated with improper curing, the data from the Indiana Department of Transportation (INDOT) inspection records showed that improper curing might have a significant deleterious effect on the durability of such concrete decks. We provide a method to estimate the additional lifecycle costs that are imposed as a direct result of these construction defects. To determine potential costs associated with this deterioration, we extract the relevant cost information from INDOT records, and relate it to expected time to and extent of deterioration obtained from the models. A simple procedure of the processes of the study is illustrated in Figure 1.1.

We also provide recommendations related to construction inspection procedures and priorities. The outcomes of the project will provide INDOT with information needed to support decisions related to setting appropriate allowances for pay items. We also identify the value of collecting data towards asset management going forward to provide guidance to INDOT on how to improve such cost estimates in the future. Recommendations related to additional maintenance needs for particular defects are also included.

An implementation is provided which specifically considers improvements for epoxy coated reinforcement handling, storage, construction, and inspection during construction as appropriate, approaches to weigh costs vs. tolerances when accepting allowances for known defects, construction practices, and suggestions for leveraging data collected during inspections over the lifetime of the bridge to collect additional data needed to refine the predictive analytics.

1.1 Factors Affecting the Lifecycle Performance of Concrete Bridge Decks in Indiana

The condition of a bridge deck in service depends on several factors. ACI365.1R-17 (ACI Committee 365, 2017) lists several factors that affect the service life performance of new and existing concrete structures. Interviews with INDOT personnel helped to establish the relative contribution of these factors on the performance of a typical cast in place concrete bridge deck. The interviews also helped to delineate additional factors observed by asset managers during routine inspections. Some of these factors are common to all bridge decks in Indiana, while others specific to the geographic location of the bridge. The common factors are the following:

- traffic/loading levels,
- presence of expansion joints,
- presence of wearing surface,
- maintenance,
- use of epoxy coated rebar,
- occurrence of carbonation corrosion, and
- presence of effective positive drainage.

In addition, the following factors may influence the performance of the bridge deck depending upon the geographic location of the bridge:

- rate of chloride-induced corrosion (use of deicing salts),
- delamination exacerbated by freeze-thaw cycles, and
- bridge is over a waterway.

Such factors can be classified as chemical and environmental, and external usage factors.

1.1.1 Chemical and Environmental Factors

The use of deicing salts on routes with heavy snow leads to chloride-induced corrosion on the bridge deck.

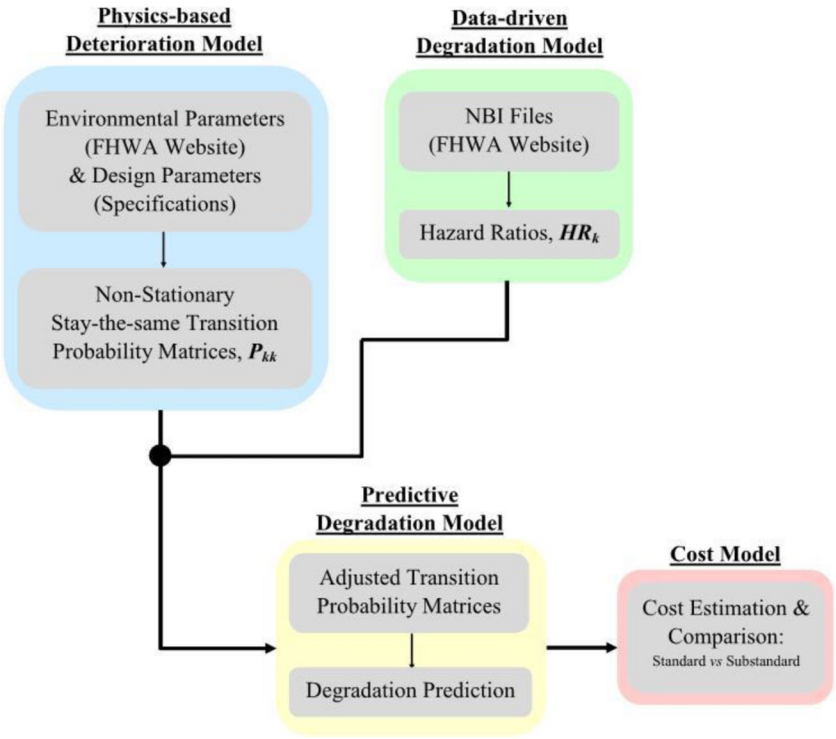

Figure 1.1 Simple graphical procedure of predictive degradation model.

Chloride penetrates the concrete surface and damages the passive film made of high alkali solution at the surface of steel bars (Olek & Liu, 2001). Example 10 of ACI365.1R-17 estimates the chloride content at various reinforcement levels for bridge decks exposed to deicing salts. An increase in total chloride content leads to corrosion of the black steel bar once a concentration of 0.05% of dry mass concrete is reached. Inspection reports in BIAS revealed delamination in several bridge decks. This delamination often is the result of corrosion-induced tensile strains, a by-product of the same corrosion. If not treated in time, it will accelerate the deterioration of the bridge deck. Contractions and expansions of the deck's internal moisture as a result of the cyclical nature of freezing and thawing lead to additional cracking. Freeze-thaw cycles allow for more surface delamination and further expose the rebar to the chlorides of deicing salts, causing more chloride-induced corrosion. The interviews with INDOT personnel also revealed that a bridge deck over a waterway could have some problems related to moisture. However, the conclusion was that the presence of this additional moisture alone does not typically result in significant problems with the overall condition of the bridge deck.

Corrosion due to carbonation of the bridge deck starts with an initiation phase followed by a propagation phase. A reduction in pH of the concrete (lower than 12.5) leads to the corrosion of the reinforcement (Olek & Liu, 2001). The carbonation starts at the surface of the concrete and eventually reaches the level of the reinforcement, leading to the initiation of corrosion. The propagation of corrosion after its initiation depends on both the strength of the concrete and the temperature (Stewart et al., 2011). A higher rate of carbonation leads to more extensive propagation of corrosion, and thereby compromises the overall health of the bridge deck.

1.1.2 External Usage Factors

External usage factors can affect the expected life of a bridge deck. However, these factors are all externally applicable to the deck, compared to the chemical and environmental factors mentioned in the previous section, which are internally applicable to the concrete of the bridge deck. Some examples of external usage factors that may affect expected life include but are not limited to average daily traffic counts, average daily truck traffic counts, the geographic location of the bridge, whether or not the bridge is located over a waterway or a roadway, whether or not the bridge is maintained by the state or the local county, as well as the age, width and length of the bridge and the degree of skew.

The Federal Highway Administration (FHWA) requires each state to collect and report a large amount of bridge inspection data on a yearly basis. Some of the collected data include external usage items like those mentioned above, making the analysis of their effect on the expected life, possible in this study.

1.1.3 Inspection Records and Material Defects

Common material defects and inspection practices are illustrated using an example provided by INDOT

personnel (see Figure 1.2). The original deck of the bridge, located on US-20, was built in 1975. It was replaced with a new deck in 2019, but that deck began to deteriorate much sooner than would be expected. Significant cracking is visible on the deck surface and in Figure 1.2, and this cracking extends across its width. Based on the inspection reports, the cracking includes both longitudinal and transverse cracks, and the majority were more than just hairline cracks. The deck of this bridge also has stay-in-place pans, so is not possible to assess the underside.

The design, construction, and inspection teams conducted an assessment on its condition and findings are summarized in Table 1.1. This summary describes the observed defects in this particular bridge deck and possible causes of those defects that may be associated with design, construction, or materials.

In this project we are focused mainly on understanding the impact of *construction defects*. Table 1.1 illustrates that concrete defects that occur as a result of mixing or curing will strongly influence the performance of the deck. This dependence is because the concrete mixture and curing process will influence the strength gain and extent of cracking in the concrete due to restrained shrinkage. Also, having a good void matrix in the concrete is known to protect the deck against delamination due to free-thaw action. The size and distribution of voids is the result of the amount of water and chemical admixtures present in the mix. Considering these various relationships, material defects associated with the mix design and construction are important issues that must be considered when modelling degradation.

Figure 1.2 Cracks on the deck surface.

TABLE 1.1
Assessment of the defects in the US-20 bridge

Problem Type	Description
Design	Insufficient bottom longitudinal steel. It specified #4 @ 8″. However, based on current American Association of State Highway and Transportation Officials (AASHTO) *Bridge Design Specifications* (2017), it should be #5 @ 8″. The design of other bars was adequate.
Construction and Concrete Material	1. There is an issue with too many air voids in the concrete. It looked like a sponge. The cause(s) could be the following: a. air entrainment admixture over dosage, b. superplasticizer over dosage, creating large bubbles, and c. sand is too coarse and created excessive bubbles. 2. Insufficient hydration of cement particles perhaps resulting from improper curing. 3. Weak interfacial transition zone around the aggregate, which means that the concrete did not cure properly. 4. A combination of bad mix design of concrete and bad construction practices, especially concrete curing.
Other	The diaphragms were not removed before casting of the concrete deck. This may result in discontinuous cracks between the lanes.

1.2 Existing Models

Bridge deterioration is a time dependent process influencing bridge performance, routine inspection and maintenance actions, and associated costs. Thus, in the past few years, researchers have focused on developing methods to estimate bridge lifecycle deterioration. The FHWA developed a simple model relying on regression analysis on preselected bridge datasets (FHWA, 1995, 2019). Other researchers adopted a proportional hazards deterioration model and utilized survival analysis to identify major factors affecting the condition rating (CR) durations to predict future CRs (Cavalline et al., 2015). An important constraint in most of these models is the assumption that the bridge starts in a "perfect" condition. However, during the construction of a bridge, defects in workmanship or materials may occur. These defects may seem innocuous at first, but in the long run can have deleterious impact on bridge lifecycle and increase costs of repair/rehabilitation due to their influence on the bridge's deterioration process.

Here we aim to assess the long-term impact of construction defects on the maintenance cost of bridge decks. To that end, modeling is conducted of the impact of the chemical, environmental and external factors in the lifecycle of the bridge deck. Several models exist in the literature for capturing the sources of deterioration mentioned in Section 1.1. These models are classified in this study in two categories. First, *physics-based deterioration models* are used to simulate the chemical processes in concrete and the environmental factors that influence this behavior. A second category consists of *data-driven degradation models* to capture the state of the deck over time using historical data gathered during inspections and account for relevant external usage factors. In this section the models are briefly described, and subsequently we illustrate how they are adopted and adapted for this research. Finally, a cost model is presented to estimate intervention costs, replacement costs, and total costs associated with the bridge deck during its lifecycle.

1.2.1 Physics-Based Deterioration Models

Three main chemical and environmental mechanisms affect the performance of a concrete deck, including: chloride-induced corrosion, which causes the rebar to corrode and damage the concrete; freeze-thaw cycles, that shrink and expand the pores of the concrete, thus inducing additional cracking; and, carbonation, a process that wears down the concrete cover, either exposing the rebar directly to the elements or shortening the path for the moisture and corrosive agents to reach the rebar.

Existing models found in literature are able to capture or simulate these three phenomena separately. Chloride penetration is usually simulated by solving Fick's second law of diffusion (Claisse, 2020). For instance, Martín-Pérez et al. (2000) studied the impact of chloride binding in the penetration speed for different environments. Chen and Mahadevan (2008) used a finite element approach and an analogy to a thermal process to solve the equation. Glass and Buenfeld (2000) mentioned in their review that although a closed-form solution is usually used, this approach is not accurate if the diffusion coefficient changes with time. They also indicate that some researchers have substituted the solution of the Fick's second law with probabilistic approaches and neural networks (Enright & Frangopol, 1998; Faber, 2000; Liu & Yunfeng, 2020; Vu & Stewart, 2000).

Following Chen et al. (2020), there have also been several efforts to numerically model the effect of the freeze-thaw cycles in the chloride-transportation process. These include simplified models in which the concrete is taken as a homogeneous material (Jiang et al., 2018; Wang et al., 2019; Xu & Li, 2017); models for the frost-induced cracks (Ueda et al., 2009); and models that account for the diffusivity change in concrete due to the freeze-thaw cycles (Chen et al., 2020; Zhang et al., 2014).

Finally, Zambon et al. (2019) presents an analytical model for simulating the carbonation. This phenomenon is modelled by means of a carbonation front that wears the deck cover with time. The advance of such front depends on environmental conditions, i.e., relative humidity and CO_2 concentration, and design parameters, such as cover and curing time.

1.2.2 Data-Driven Degradation Models

In this study, the term *degradation* will be used to describe the loss of grading, or CR, of a concrete bridge deck over time. The modeling of such a loss is referred to as a degradation curve. A data-driven model can be created using the available historical data for the state of Indiana. The historical data allows for an analysis of the degradation patterns within the state and thus for the prediction of future CRs of a bridge deck. This type of prediction is useful to bridge asset engineers and managers as it aids them in better planning for preventative maintenance and new construction actions in the future.

A recent study performed by the University of North Carolina at Charlotte in partnership with the North Carolina Department of Transportation utilized the historical data collected and reported to the FHWA to develop the basic procedure along with a case study for probabilistic deterioration modeling (Goyal, 2015). They defined this as a combination of semi-parametric multi-variable proportional hazards modeling (Cox, 1972) and semi-Markov theory (Jiang et al., 1988). The model is based on a survival analysis followed by a regression using the Cox multivariable proportional hazards model (Cox, 1972). The survival analysis results are then transformed into a probabilistic deterioration model using the well-established Markov-chain approach. These probabilistic deterioration models reflect the degradation that occurs between

subsequent CRs and the influence of external usage factors on degradation rates. This yields a North Carolina-specific analysis of external usage factors and their effect on overall degradation within the state. The dataset included approximately 17,000 bridges in North Carolina over a time period of 35 years. The historical data utilized in the creation of the model include external usage factors like those mentioned in Section 1.1.

1.3 Proposed Approach

1.3.1 Modeling

This study aims to develop and approach for generating *predictive degradation curves* for a concrete bridge deck by merging physics-based deterioration models with a data-driven degradation model (see Figure 1.1), and then apply a cost model to those outcomes to evaluate the cost differences when a bridge deck is built in a standard construction case in contrast with a substandard or defective construction case. The models introduced in Section 1.2 must be integrated to establish the predictive degradation capabilities needed. The uncertainties in the physics-based deterioration model are incorporated by assuming expected probability distributions for the parameters of the model and sampling over those parameters. This sampling is used to perform a Monte Carlo simulation, a technique relying on random sampling over a model's parameters for a given number of times to obtain random outcomes from a model (Zambon et al., 2019). The random outcomes are then used to generate probability transition matrices representing the change from one state or CR to another. The data-driven degradation model utilizes historical data for the state of Indiana to create state specific hazard ratios and thus allows the application of two-dimensional physics-based models to the three-dimensional conditions of a real concrete deck in Indiana. The CR prediction is finally used to compute the expected replacement and intervention costs associated with an individual bridge, which is illustrated in Section 5. A more detailed version of the procedure described in Figure 1.1 is provided in Figure 1.3. The remainder of this report discusses the development of this model. Section 2 describes the physics-based model, the data-driven model is described in detail in Section 3. The integration of both models is explained in Section 4, and the details of the cost model and application are given in Section 5.

1.3.2 Bridges Identified for Case Studies

Considering the variety of the bridge characteristics across the state of Indiana, it is desirable to designate a reduced, yet representative, set of bridges to work with. Such a set should be composed of bridges with common properties while still representing a variety of conditions. Both objectives would allow for an easier and clearer identification of the factors that have the greatest and least effect on the lifecycle performance of the bridges and allow for the prioritization of those factors.

Some preliminary proposals of bridges were provided by INDOT personnel. According to their description, the lists contained relatively new bridge decks with unexpected underperformance shortly after its construction. Inspection reports from such bridge decks were extracted from the Indiana Bridge Inspection Application System (BIAS) and the information gathered was documented and analyzed. It was observed that most bridge decks provided by INDOT personnel shared the following common characteristics.

- The main span superstructure is mostly "Tee beam" or "Stringer/Multi-beam or Girder."
- All of the decks fall under the category "Concrete Cast-in-Place."
- Most of them have a "Monolithic Concrete" wearing surface.
- None of them have a membrane.
- All of the decks have "Epoxy coated reinforcing" as protection.

In this study, bridges with the characteristics described above will be referred to as *nominal cases*, while bridges without one or more of these characteristics will be referred to as *non-nominal cases*. The complete set of nominal case study bridges is described in Appendix A.1, but a summary is shown in Table 1.2. The purpose of having this set of case study bridges is to evaluate the effect of the modeled phenomena under different conditions, for instance: (1) different combination of defects; (2) different environmental conditions, i.e., geographic distribution in the state; and (3) different intensities on each of the studied external factors. That is, every bridge in the catalog of case studies represents a distinct possible scenario that INDOT personnel must deal with in field. The asset name and location correspond to the same designation in the National Bridge Inventory (NBI) number.

1.3.3 Cost Model

The ability to associate a predicted condition state with an incurred cost is vital for evaluating the overall effect that a construction defect has on the lifecycle of a bridge deck. Following Kleiner's (2001) approach, one can compute the expected results of the cost of reconstruction of a bridge deck, the cost of intervention at every CR stage, and finally the total cost of these combined over time. The calculations of the two individual costs are based on one vector of the probability of being in each CR at a given year, and a second constant vector of the presumed costs associated with interventions and reconstruction for each of the CR stages. The total cost then is determined as the sum of both values, and it is multiplied times an exponential term with a discount rate to account for inflation. This process is further explained in Section 5.1 and illustrated through application in Section 5.2.

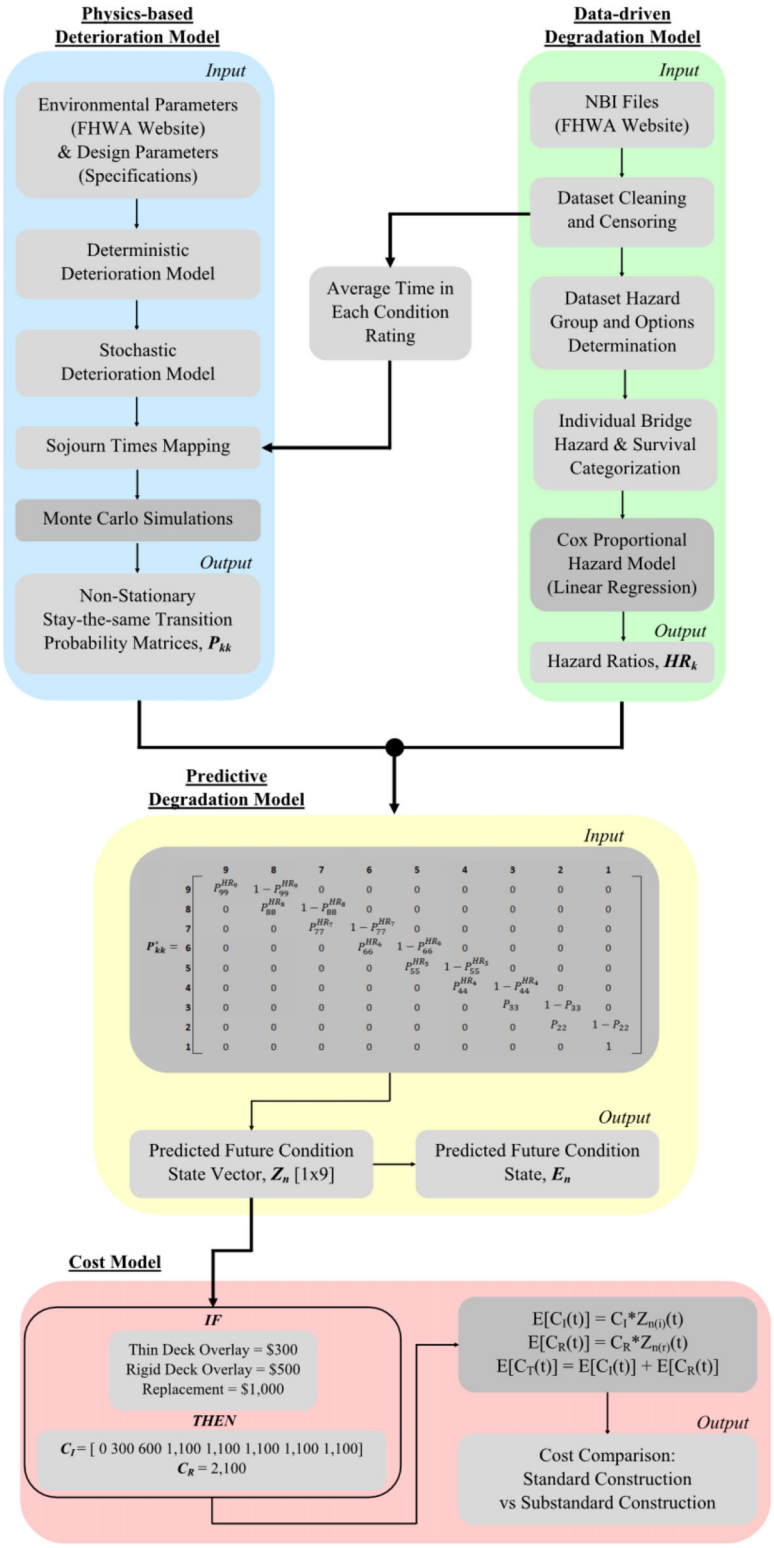

Figure 1.3 Graphical procedure of the predictive degradation model.

TABLE 1.2
List of bridges in the catalog of case studies

NBI	Asset Name	Location
4081	015-43-10215	SR 15 over Tippecanoe River
11980	037-47-05934	SR 37 NB over Salt Creek
15651	041-45-02808	US 41 NB/SB over GTW RR
18911	051-45-09797 SBL	SR 51 SB over Burns Ditch (Deep River)
19571	054-77-08692	SR 54 over Coulson Drain
33440	I64-18-05205 BEBL	I-64 EBL over Lower Big Creek
36033	I65-106-10142 NBL	I-65 NB over I-465 EB/WB
44080	33-04944 FWBL	I74 WB over US 231 SB/NB
50521	I465-132-09971	Ditch Road over I-465 EB/WB
79848	031-71-08944	US 31 NB/SB over Kern Road

2. PHYSICS-BASED DETERIORATION MODEL

The objective of the model discussed in this section of the report is to quantify how issues during construction influence the degradation process in concrete bridge decks. The first step is to develop a *physics-based deterioration model* for standard-construction cases aimed at capturing the effect of carbonation, freeze-thaw cycles, and cracking on a bridge's deck. This model will be extended to include the impact of construction defects on the long-term performance. Second, the model is turned into a stochastic version that captures the uncertainty on its intervening parameters. Finally, using Monte Carlo simulations, this stochastic physics-based deterioration model is used to obtain the probabilities of a bridge changing condition rating (CR) during its life.

First, the model used to establish physical deterioration of the concrete deck in a standard, non-defective case is presented. Once this model is verified, the effects of four common construction defects are studied. These defects are (1) improper curing, (2) improper mixing, (3) insufficient concrete cover, and (4) damage to the epoxy coating of the reinforcing bar (Samples & Ramirez, 2000a, 2000b). The impact of these construction defects on the deterioration and lifecycle of a bridge deck is quantitatively examined.

2.1 Deterministic Physics-Based Deterioration Model

In the development of the deterioration model, the following four critical mechanisms relevant to decks in Indiana will be considered: (1) rebar corrosion, (2) carbonation, (3) freeze-thaw cycles, and (4) cracking.

2.1.1 Rebar Corrosion

Chloride induced corrosion is one of the major causes of rebar corrosion in reinforced concrete (Martín-Pérez et al., 2000). This mechanism is of utmost relevance for bridge decks treated with deicing salts to prevent freezing during winter. This phenomenon is illustrated in Figure 2.1 where a concrete deck with a rebar is shown. The steel rebar in concrete has a protective passivation layer of iron oxides (Fe_2O_3 and Fe_2O_2) which is naturally created due to the interaction with the concrete (see a in Figure 2.1). Given that concrete is a porous media, the chlorides contained in the accumulated chloride solution on the deck's surface gradually infiltrate until they reach the rebar. Cracking can certainly facilitate the access of chlorides in the concrete mass. Once the chloride concentration threshold is surpassed, the protective passivation layer of the rebar is broken (b in Figure 2.1) and corrosion starts, with the subsequent rust accumulation (c in Figure 2.1) and cracking due to the increased stresses as a result of rust accumulation on the surrounding concrete (d in Figure 2.1).

The times for each of the aforementioned stages to occur are often termed *time to initiation*, t_i, which encompasses (a) and (b) in Figure 2.1, and *time to cracking* or, hereafter, *time to spalling*, t_s, which includes (c) and (d).

To model the initiation stage, the flux of water through the concrete deck must be modeled. The common approach to do this is with Fick's second law of diffusion (Chen & Mahadevan, 2006; Claisse, 2020; Martín-Pérez et al., 2000):

$$\frac{\partial c}{\partial t} = \frac{\partial}{\partial x}\left(D\frac{\partial c}{\partial x}\right) \qquad \text{(Eq. 2.1)}$$

where $C = C(x, t)$ stands for the chloride concentration at time t and at x depth, and D is the chloride's diffusion coefficient in concrete. Typically, values of D range from 3.28×10^{-12} to 3.28×10^{-10} ft/s^2 (10^{-12} and 10^{-10} m/s^2; Wang & Zhang, 2016). A closed-form solution for Equation 2.1 does exist, but it assumes a linear behavior on the parameter D, thus discarding any possible modifications due to, for example, freeze-thaw cycles or cracking. Hence, in this report, to account for the effect of those parameters, Equation 2.2 is solved numerically using a Crank-Nicolson scheme, a method that allows more flexibility for such modifications, which will be evaluated in Section 2.1.5. After running a simulation for some time period, t_i is obtained as the first-time chlorides reach the upper rebar level.

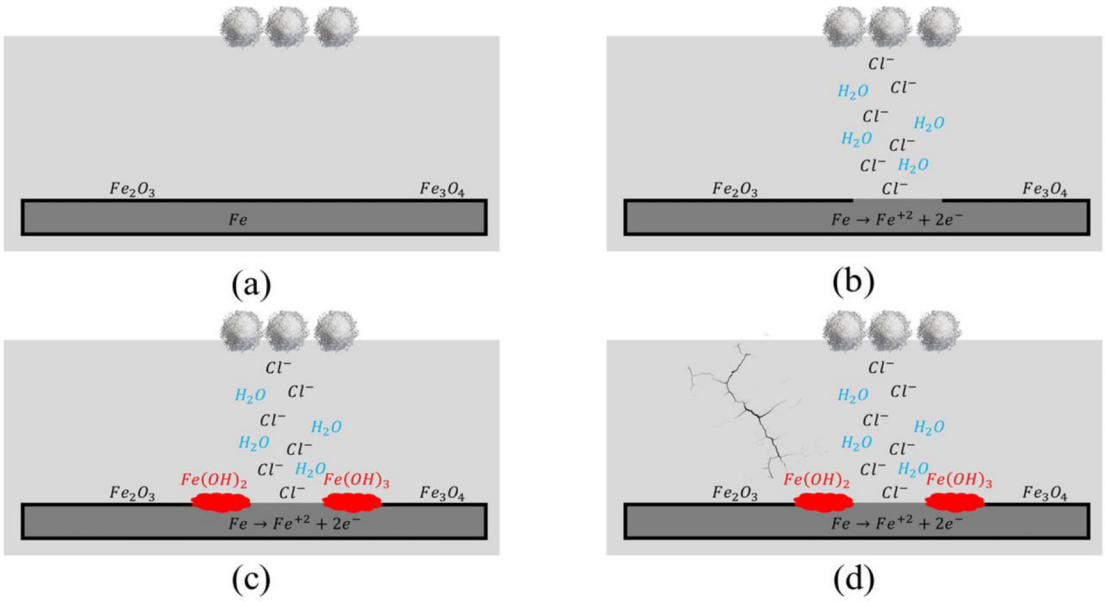

Figure 2.1 Process of corrosion due to chloride penetration: (a) deicing salts are spread on the concrete deck's surface; (b) chlorides diffuse through the concrete and breaks the passivation layer of the rebar; (c) rust accumulation begins; and (d) the stress increase leads to cracking.

Once the chloride concentration has surpassed a threshold C_{th}, the corrosion process starts. The threshold is taken, according to the ACI 318 (ACI Committee 318, 2016), as the 0.15% of the cement weight per mix volume. Let t_n be the current simulation time, that is, the current timestep when solving Equation 2.1. The corrosion evolution is modeled through the following equation (O'Reilly et al., 2011):

$$\varphi(t_n) = r_c t_n \qquad \text{(Eq. 2.2)}$$

where $\varphi(t_n)$ is the rebar loss due to corrosion at time t_n and r_c is the corrosion rate. O'Reilly et al. (2011) found that the corrosion rate value depends on the severity of the cracking in the concrete. Thus, in this study, an uncracked corrosion rate value is adopted when the rebar loss due to corrosion is below the critical value φ_c, while cracked, higher corrosion rate value corresponding to cracked concrete is used otherwise. The critical corrosion loss, φ_c, i.e., the amount of rebar loss required for the deck to start cracking, is given by (*ídem.*):

$$\varphi_c = 45\left[\frac{c^{2-a_f}}{d_b^{0.38} l_f^{0.1} a_f^{0.6}} + 0.6\right] \times 3^{a_f - 1} \qquad \text{(Eq. 2.3)}$$

φ_c is the critical corrosion loss in *mil* and l_f and a_f are the non-dimensional fraction of epoxy-coating damage length and area, respectively, and d_b is the rebar diameter in inches.

With the definitions made above, the time to spalling, t_s, can be defined as the timestep such that the critical corrosion loss has been reached, that is:

$$\varphi(t_s) = \varphi_c \qquad \text{(Eq. 2.4)}$$

2.1.2 Carbonation

Carbonation is an electrochemical process by which atmosphere's carbon dioxide and moisture react with concrete's calcium hydroxides. It begins when the deck's surface comes into contact with the atmosphere, i.e., as soon as the formwork is removed. The main consequence of such process is the loss of concrete's surface by means of the so-called carbonation front (Zambon et al., 2019). A reduced concrete cover will thus lead to a shorter path for the chlorides to get the rebar and, as a consequence, a reduced time to initiation of corrosion.

The carbonation front (or depth) at time t_n, $x_c(t_n)$, can be computed using (Zambon et al., 2019):

$$x_c(t_n) = k_{NAC} \cdot \sqrt{k_e \cdot k_c \cdot k_a} \cdot \sqrt{t_n} \cdot W(t_n) \qquad \text{(Eq. 2.5)}$$

where k_{NAC} is the carbonation rate, k_e describes the environmental effect of relative humidity, k_c describes the effect of curing execution, k_a describes the effect of CO_2 concentration in the ambient air, t_n is the current timestep of calculation, and $W(t_n)$ describes the wetting events:

$$W(t_n) = \left(\frac{t_0}{t_n}\right)^{\frac{(p_{dr} \cdot T_0 W)^{b_w}}{2}} \qquad \text{(Eq. 2.6)}$$

where t_0 is the reference year or initial year of the analysis, p_{dr} is the probability of driving rain, that is, the probability of the deck to get wet during rains, $T_0 W$ is number of rainy days per year and b_w is a regression parameter equal to 0.446. The values of the remaining constants in Eq. 2.5 are computed as indicated in Table 2.1.

TABLE 2.1
Calculation of constants in Equation 2.5

Effect	Equation	Parameters
Relative Humidity	$k_e = \left[\frac{1-(RH_a)^{f_e}}{1-(RH_l)^{f_e}}\right]^{g_e}$	RH_a : relative humidity of ambient air (%) RH_l : reference relative humidity (%) f_e = 5.0: regression exponent g_e = 2.5: regression exponent
Curing Execution	$k_c = \left(\frac{t_c}{7}\right)^{b_c}$	t_c: curing time (days) b_c = –0.567
Ambient CO_2	$k_a = \frac{c_a}{c_l}$	c_a: CO_2 concentration in ambient (%) c_l: CO_2 reference concentration (%)

During the simulation, the top concrete cover to the top reinforcement in the deck is modified to account for the carbonation wear:

$$c(t_n) = c(t_{n-1}) - x_c(t_n) \qquad \text{(Eq. 2.7)}$$

2.1.3 Freeze-Thaw Cycles

As described in Section 2.1.1, concrete decks collect moisture throughout their lifecycle. During the cold season, the water inside the concrete's pores freezes during frosts and, therefore, expands. Such expansion puts additional stresses on concrete. When the frost ends, water thaws and keeps on infiltrating the deck until another freeze occurs and the cycle repeats. After several freeze-thaw cycles the concrete accumulates damage that ultimately leads to a reduced ability to contain the water flux (Chen et al., 2020).

Based on the model developed by Chen et al. (2020), this phenomenon may be included as a modification of the chloride's diffusion coefficient:

$$D_{FT}(t_n) = D + 26.25 \times 10^{-9}\left[1 - \frac{1}{1+(2.5d_N(t_n))^5}\right] \qquad \text{(Eq. 2.8)}$$

where $d_N(t_n)$ is a damage factor at time t_n determined by the maximum expected number of cycles in the year (N_{max}):

$$d_N(t_n) = 1 - \frac{0.6\log N_{\max}}{\log N_{\max} - 0.4\log(N_{\max} - N)} \qquad \text{(Eq. 2.9)}$$

with N being the number of cycles that have occurred up to time t_n.

2.1.4 Cracking

Even if the reinforced concrete deck meets specifications, it will eventually deteriorate throughout its lifecycle due to the corrosion process, and the impact of traffic loads. Such factors inevitably lead to cracking of the deck, and a cracked deck allows for more water and thus more chlorides to penetrate.

The cracking process of the bridge deck is represented by a simplified linear cracking pattern described by the equation:

$$\omega(t_n) = mt_n + \omega_0 \qquad \text{(Eq. 2.10)}$$

where ω and ω_0 are the cracking at time t_n and at time 0, respectively, and m is the cracking slope. Based on this pattern, the diffusion coefficient of cracked concrete, D_{cr}, at each time step is computed as follows (Wang & Zhang, 2016):

$$D_{cr}(t_n) = \begin{cases} D_{FT} & \omega < 1.18\,mil \\ 28.3 - 35.6e^{-0.00835\omega} & 1.18\,mil \le \omega \le 3.94\,mil \\ D_{H_2O} & \omega > 3.94\,mil \end{cases} \qquad \text{(Eq. 2.11)}$$

where D_{H_2O} is the diffusion coefficient of water in concrete, typically $4.10 \times 10^{-9}\ ft^2/s$ ($1.25 \times 10^{-9}\ m^2/s$; Jin, 2010).

To determine the crack depth, a factor λ given by Zhu et al. (2020) is used:

$$\lambda = \frac{h}{\omega} = \begin{cases} -39\omega + 56 & 60\,\mu m\ (2.36\,mil) \le \omega < 300\,\mu m\ (11.81\,mil) \\ 43 & \omega < 300\,\mu m\ (11.81\,mil) \end{cases} \qquad \text{(Eq. 2.12)}$$

where h is the crack depth in μm.

2.1.5 Integration of the Deterioration Model

The model for chloride-induced corrosion described in Section 2.1.1 is coupled with the carbonation (Section 2.1.2), freeze-thaw cycles (Section 2.1.3) and cracking (Section 2.1.4) models as illustrated in Figure 2.2 for a total simulation time of T; each timestep corresponding to a time t_n. First, the chloride diffusion coefficient is affected by the freeze-thaw cycles and by the cracking by means of Equations 2.8 and 2.9. Using this result, the chloride concentration at each point x of the deck is computed by solving Equation 2.1. In a third step, the carbonation front x_c at the time t_n is computed using Equation 2.5. During the execution of this loop, the time to initiation is registered as the instant at which the chloride concentration at rebar

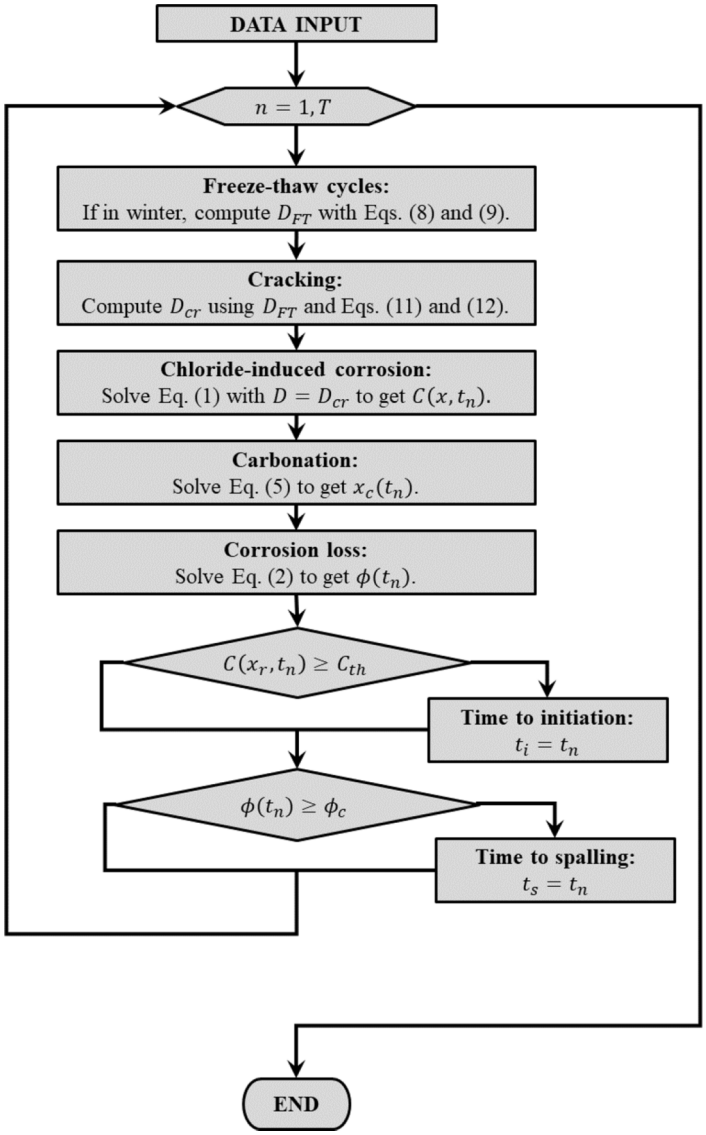

Figure 2.2 Flow chart describing the corrosion process incorporating carbonation, freeze-thaw cycles, and cracking effects.

level, $C(x_r, t_n)$, first exceeds the chloride threshold for corrosion (C_{th}); and the time to spalling is registered as the first time the corrosion loss surpasses its critical value. Note that, at each calculation step the following is true.

- D_{FT} is dependent upon the last step's D (see Equation 2.8).
- D_{cr} contains both freeze-thaw cycles and cracking effects ($D = D_{FT}$ in Equation 2.11).

2.1.6 Validation of the Physics-Based Deterioration Model

Herein, the physics-based deterioration model developed in this study will be validated. Here validation focuses on the agreement between the model outcomes and field observations. Moreover, this agreement heavily depends on the ability of each collected parameter, be an environmental or a design one, to represent one or another physical phenomena. For instance, there is no information available about the carbon concentration in Indiana. Hence, data from the nearest location (Homer, Illinois) with known CO_2 indices was used instead.

The scope of this project includes the quantification and prediction of the impact of construction defects on the lifecycle of a bridge deck. As such, an index for measuring a deck's performance as a function of time is needed. Following O'Reilly et al. (2011), once the initiation and spalling times have elapsed the damage in the deck will be evident and thus form of intervention (repair) may be needed to return it to proper service. So, for purposes of this study the sum of t_i and t_s is the time it takes for the first rust-induced crack to appear on the surface of the deck. This assumption implies that

the deck has extensive cracking and major intervention is required.

$$t_1 = t_i + t_s \qquad \text{(Eq. 2.13)}$$

Equation 2.13 represents the *time to first repair*. This parameter will be considered as the main deterioration index for the physics-based models: the larger t_1 is, the better the deck performance will be, on the other hand as t_1 decreases the condition of the deck also degrades.

There is potential for intermediate actions to be performed on the deck before the first major repair is needed, but it must be noted that the models in this study are not able to accommodate any intervention that changes the properties of the originally constructed deck in the prediction of CR after the intervention. The current literature on deck deterioration due to corrosion does not account for those modifications and the physics-based models presented herein do not allow for any intermediate interventions. In this study, we envision that significant interventions to extend the lifetime of the deck will be incorporated within the cost-analysis presented in Section 5 of this report.

To validate the proposed model, a simulation of a nominal non-defective concrete deck is conducted. The non-defectiveness of the bridge is considered by setting a cracking pattern going linearly from the initial crack width in the surface to 0.040″ at the final time. Such end value corresponds to the cracking pattern in a deck with CR 5 or 4 (INDOT, 2020a), which would be indicative of a need for urgent maintenance intervention, thus coinciding with the definition of the time to first repair. The initial crack width is set to 0.006″ (15μm), which corresponds to a CR of 9 or 8 according to *INDOT Bridge Inspection Manual* (INDOT, 2020a).

The simulation parameters for the deck are summarized in Table 2.2. The weather-related parameters here were estimated for the National Weather Service's (Weather Atlas, n.d.) North Indiana region and the South Bend International Airport's weather station (Weather Underground, 2021). When no information on such sources was found, the nearest location with available data was considered instead. The bridge design parameters are from the bridge with NBI number 79848 belonging to the case study catalog assembled in Section 1.3.2. It must be noted that this simulation is not aimed at replicating the bridge's CR evolution: it is only used to illustrate the selection of the design and weather parameters.

Finally, the chloride concentration at the surface of the deck ($x = 0$) is obtained at each timestep using the expression given by Kassir and Ghosn (2002), in Equation 2.14

$$C(0,t) = C_0[1 - e^{-\alpha t}] \qquad \text{(Eq. 2.14)}$$

with an initial surface concentration $C_0 = 9$ lb/yd^3 (5.3 kg/m^3) and a deposition rate of $\alpha = \frac{0.25}{year}$. This expression is developed using measured chloride profiles from 15 bridges in the region near the Great Lakes of North America, also known as the *snowbelt*, where the snowfall is heavy during the winter. Given the proximity of the state of Indiana to such region, Equation 2.14 is considered applicable.

Figures 2.3 and 2.4 show the results of the simulation. Figure 2.3 illustrates the chloride profiles of the deck at selected times: the first year of service, the time to initiation, the time to spalling and, finally, the time to first repair. A gray shaded area representing the "equivalent cover" from the carbonation front is also displayed. Figure 2.4 displays the chloride concentration profile at rebar level for the entire simulation time span; the same selected times are also indicated. The chloride threshold is shown in both figures. *It is clear that the effect of the carbonation is to accelerate the initiation time by making the distance from the surface to the top rebar shorter.*

The model estimated time to first repair of the bridge considered is shown in the bottom row of Table 2.3. First-intervention values from interviews with INDOT personnel are also indicated. Clearly the simulation result is within the range of expected service time before the first intervention from the various interviews.

2.1.7 Modeling of Construction Defects

2.1.7.1 Improper curing. An improper curing technique leads to shrinkage of the concrete in the deck. Even though shrinkage cracks are considered nonstructural (FHWA, 2012), they facilitate water infiltration and, consequently, chloride penetration, which will in turn accelerate the corrosion process (ACI Committee 308, 2016).

To show the effect of early cracking in concrete due to improper curing, five simulations of the same deck described in Section 2.1.5, varying the initial crack width, ω_0, were run. The simulation cases are described in Table 2.4. Each of these cases corresponds to a possible assigned CR number, as specified in INDOT's *Bridge Inspection Manual* (INDOT, 2020a). An initial crack width of 0.006″ (0.1524 mm) is considered the standard case. Figure 2.5 shows that a worse initial condition, i.e., a deck with extensive cracking, will lead to a faster chloride infiltration and eventually to an earlier corrosion. The time to initiation, t_i, (blue-shaded area of the plots) is the time it takes for the chlorides to reach the upper rebar for the first time, while the time to spalling, t_s, (orange-shaded area of the plots) is the time it takes for the rust to generate a crack after corrosion started.

2.1.7.2 Insufficient concrete cover. Casting an insufficient amount of concrete cover over the top rebar is another common construction defect. A thinner cover implies a shorter distance between the surface and the upper rebar and, clearly, could result in an earlier corrosion initiation at such level.

Several cases of insufficient concrete cover are simulated to evaluate their impact on the chloride-

TABLE 2.2
Parameters used in the concrete deck corrosion process in case study bridge #79848

Parameter	Value	Comments	Source
Concrete Chloride Diffusion Coefficient, D	22.96×10^{-12} ft/s^2 (7.00×10^{-12} m/s^2)	For sound concrete and a water/cement ratio of 0.45	Kim et al., 2014
Concrete Water Diffusion Coefficient, D_{H_2O}	4.10×10^{-9} ft^2/s (1.25×10^{-9} ft^2/s)	For sound concrete and a water/cement ratio of 0.45	Jin, 2010
Ambient Temperature, T	$50.4°F$ (285 K)	Historic average	Weather Underground, 2021
Top Rebar Diameter, d	0.75″ (19.05 mm)	Rebar diameter	Structural drawings
Deck's Thickness	8″ (203.20 mm)	–	Structural drawings
Concrete Cover	2.5″ (63.50 mm)	–	Structural drawings
Carbonation Rate, k_{NAC}	0.315″ (8 mm)	–	Zambon, 2019
Relative Humidity of Ambient Air, RH_a	80%	Historic average	Weather Underground, 2021
Curing Time, t_c	7 days	Guidelines for structural concrete	*Indiana Department of Transportation Standard Specifications 2020*, Section 702.22
CO_2 Concentration in Ambient, c_a	0.040%	Urban area considered	Zambon, 2019
Maximum Number of Freeze-Thaw Cycles, N_{max}	14	Data for Indianapolis International Airport's (IIA) station	Purdue University, n.d.
Chloride Threshold, C_{th}	0.15% of the cement weight per mix volume	–	ACI Committee 318, 2022

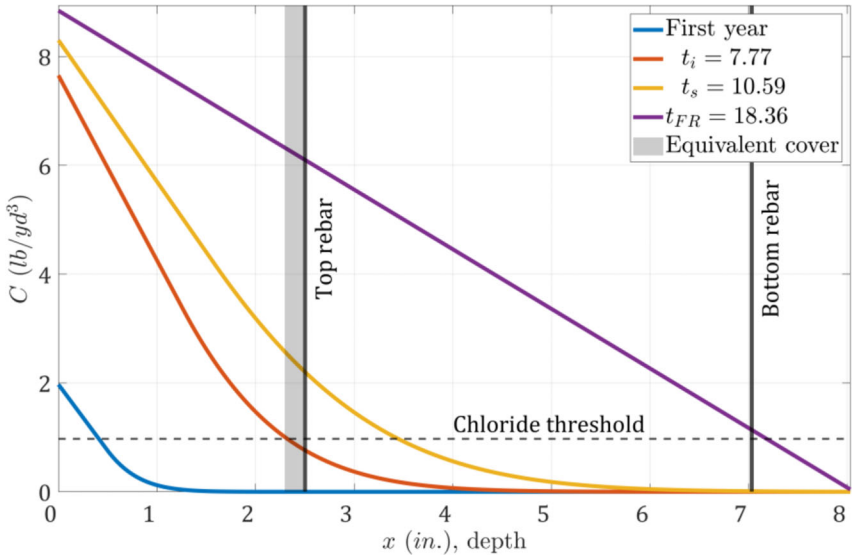

Figure 2.3 Deck chloride profile at different times during the lifecycle.

penetration process. The chloride diffusion coefficient is fixed to be that of sound concrete as in Section 2.1.1. In Figure 2.6 the associated times to first repair for each cover scenario are shown; these are lower for smaller covers and vice versa, as expected. For the standard case (2.50″, as required by INDOT's *Indiana Design Manual* (INDOT, 2013), the time to initiation is the largest (7 years).

2.1.7.3 Water/cement ratio. Several researchers have shown that the proportion of water and cement in the mix has a direct impact on the porosity and, therefore, on the diffusion coefficient value (Claisse, 2020; Kim et al., 2014; Takiya et al., 2014). Takiya et al. (2014) determined a relationship between both variables, which is shown in Table 2.5. Being $w/c = 0.45$ the closest to INDOT's requirement for structural concrete ($\frac{w}{c} = 0.443$, *Indiana Department of Transportation Standard Specifications 2020*), it was considered as the non-defective case. The change in the time to first repair as the w/c ratio changes is illustrated in Figure 2.7.

2.1.7.4 Rebar coating damage. The final defect considered herein is that of damage to the epoxy-

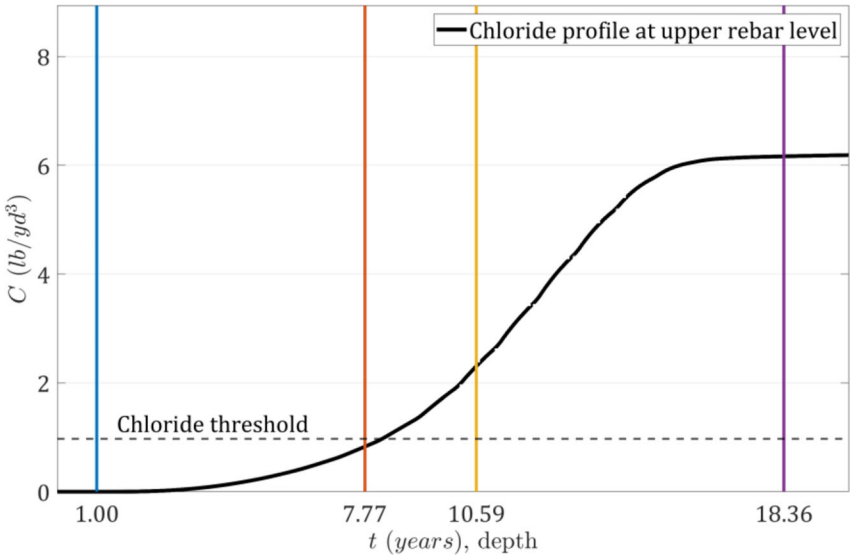

Figure 2.4 Chloride concentration profile at rebar level (2.50″) for the whole time of simulation.

TABLE 2.3
Time to first repair estimated using the proposed model assembled from different sources

Source	Time to First Repair, t_1 (years)
Interviewee 1	10–15
Interviewee 2	15–20
Interviewee 3	15
Interviewee 4	10–20
Barrett et al., 2015	18
Proposed Model	18.36

TABLE 2.4
CR description and related crack width (INDOT, 2020a)

CR	Description
9	No significant defects.
8	Hairline cracking less than 0.012″ nominal width and widely spaced.
7	Cracking less than 0.016″ nominal width, widely spaced, and less than 5% delamination.
6	Cracking less than 0.020″ nominal width and nominal on center spacing greater than 10 feet. Delamination less than 10%.
5	Cracking greater than 0.020″ and less than 0.040″ nominal width and nominal on center spacing not greater than 10 feet. Delamination less than 20%.
4	Cracking greater than 0.040″ nominal width and nominal on center crack spacing less than 10 feet. Delamination greater than 20%. Unpatched or unsound patching, or spalled areas, visible intermittently.

coating of the rebar. Epoxy-coating is directly related to the chloride threshold the rebar can bear before start corroding. Such threshold varies on a project-by-project basis due to design, workmanship, and the quality of concrete (Wiss, 2005). For instance, a defective workmanship will damage the epoxy protective coating, hence permitting the chlorides to corrode the steel rebar faster once they reach it (Samples & Ramirez, 2000a, 2000b). This acceleration will, in turn, decrease the time to initiation of corrosion compared to that in bars with undamaged coating (Holland, 1998; Wiss, 2005).

The standard threshold given by the American Concrete Institute (ACI) is a concentration equivalent to 0.15% of the cement weight in the mix (Holland, 1998). To model the defective cases, the chloride concentration threshold is reduced to that of the black rebar (ACI 365 1R-17), 0.05% of the mix's cement weight. This modification affects the time to initiation, which becomes shorter in comparison with that of the standard case.

However, a damaged rebar also has a faster corrosion process due to a decreased critical corrosion loss (see Equation 2.3). This modification is achieved by

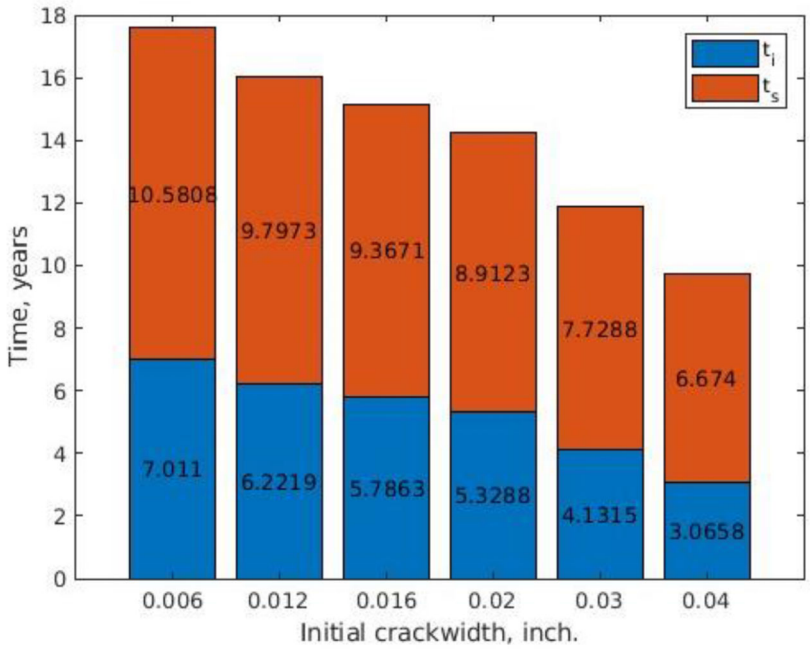

Figure 2.5 Time to first repair for different simulations that vary the initial crack width.

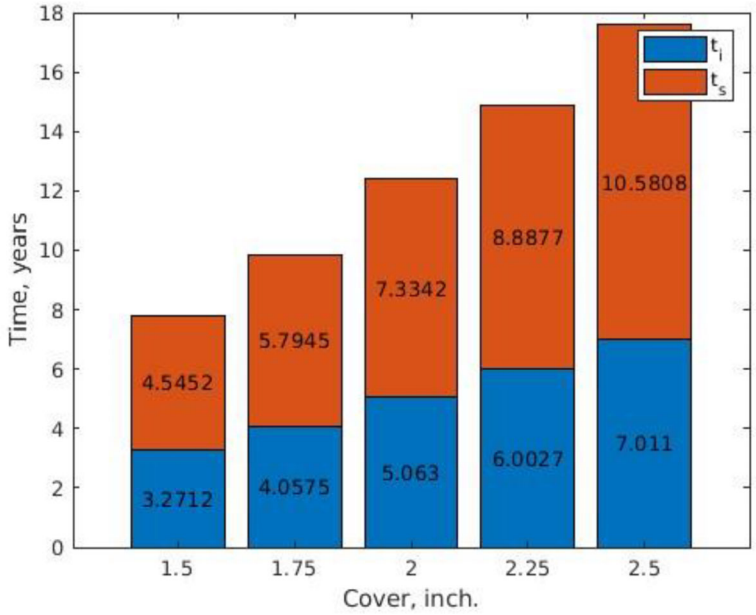

Figure 2.6 Time to first repair for different concrete cover scenarios.

TABLE 2.5
Chloride diffusion coefficients for different w/c ratios

w/c	*D*, $ftls^2$ (mls^2)
0.45	22.97×10^{-12} (7.00×10^{-12})
0.50	24.60×10^{-12} (7.50×10^{-12})
0.55	29.53×10^{-12} (9.00×10^{-12})
0.60	35.43×10^{-12} (10.80×10^{-12})

changing the fraction of the corroded length of the rebar and area. In the standard case, am admissible diameter of the pitting holes and spacing of 0.15″ and 3/8″ were adopted (INDOT, 2020b; see Section 2.2.3 for details). Further, two substandard cases were defined from in-field observations: pitting holes on each of the corrugations of the rebar in a spread pattern; and pitting holes concentrated on the tips of the rebar. From in-field measurements, the diameters for each case are 0.0375″ and 0.1875″, respectively. The spacing was set as 3/8″ for both cases.

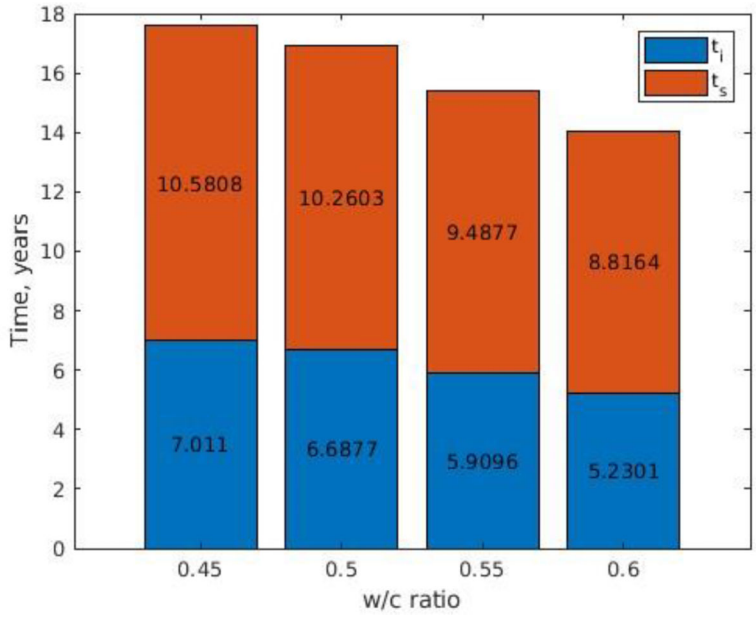

Figure 2.7 Time to first repair for different water-cement ratios.

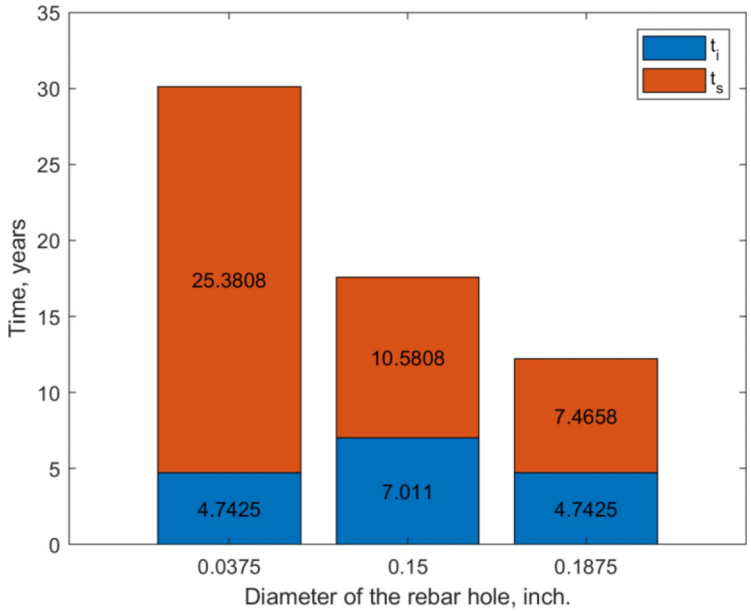

Figure 2.8 Time to first repair for different rebar damage diameters.

The consequences of these non-standard cases in the initiation time are shown in Figure 2.8. Notice that the substandard, spread-pattern case (diameter of 0.0375″) has better performance than the standard case (diameter of 0.30″) during the spalling phase. On the other hand, the substandard, tip-pattern case (diameter of 0.1875″) has a worse behavior. This outcome may suggest that the standard case, that is, the current specification, could be greatly improved if a more restrictive tolerance is set in the allowed diameters of the pitting holes.

2.2 Stochastic Physics-Based Deterioration Model

To account for the variability and uncertainty present in a real-life deterioration process, the deterministic model described in Section 2.1 is converted into a stochastic model. That is, the model parameters are represented as random variables following a probability density function intended to capture their uncertainty. For each run of the simulation the parameters are sampled to generate a unique time history (hereafter, a *realization*). Parameters that can take on continuous

TABLE 2.6
Probability distributions used for environmental parameters

Parameter	Probability Distribution	Source	Observations
Average Relative Humidity (%)	Lognormal	NBI (FHWA, 2023)	–
Number of Freeze Thaw Cycles	Poisson	NBI (FHWA, 2023)	The maximum number of the historical records was also used.
Number of Rainy Days	Poisson	NBI (FHWA, 2023)	–
Number of Winter Days (Days with Temperature Below 0°C)	Poisson	NBI (FHWA, 2023)	–
CO_2 Concentration in Ambient Air	Lognormal	Global Monitoring Laboratory of NOAA (NOAA, 2023)	No information for the state of Indiana. Data from a nearby location (Homer, IL) was used.

values are represented with lognormal distributions, and discrete parameters use Poisson distributions. When data are available, the mean values and standard deviations for the former and the λ-values for the latter are obtained from historical records. The details associated with each distribution are explained in the following sections.

2.2.1 Environmental Parameters

For this set of sampled variables, the descriptors were obtained from historical climate records included in the NBI (FHWA, 2023). Such parameters vary with the region in which a particular bridge is located. In the case of CO_2 concentration in ambient air, the data was collected from the Global Monitoring Laboratory of the National Oceanic and Atmospheric Administration of the U.S. Department of Commerce (NOAA, 2023). In the absence of data for Indiana, a nearby location (Homer, Illinois) was used as a reference. A summary of the environmental parameters, their chosen distributions, and the observations available are shown in Table 2.6.

2.2.2 Cracking and Corrosion Parameters

There are two sources of cracking in the model developed: the cracking due to environmental and traffic parameters, represented by Equation 2.10; and the cracking due to corrosion, which is described using Equations 2.2 and 2.3. Both processes are sampled as described herein.

The slope of the cracking model in Equation 2.10, m, is represented as a random variable. This parameter is unique in that it changes (it is sampled) not only for each realization but also at each timestep of the simulation. This approach is adopted to represent the highly random nature of cracking without the need for a complex model. Figure 2.9 shows one realization of the crack width history using this approach.

The mean value and the standard deviation of the slope were obtained from Indiana's BIAS dataset. Specifically, bridges with a starting CR of 9 or 8 were first extracted. This filtering was meant to identify the average cracking rate of standard-constructed bridges. Hence, the assumption was made that every bridge starting its life cycle at CR 9 or 8 was constructed following the standards. The total number of bridges meeting these criteria is 788. The initial and final CRs of these filtered bridges were obtained and paired with their respective crack width using INDOT's *Bridge Inspection Manual* (INDOT, 2020a) (see Table 2.4). The slope was computed for each deck in this group, m_k, using the geometric definition

$$m_k = \frac{\omega_f^k - \omega_0^k}{T_k} \qquad \text{(Eq. 2.15)}$$

where ω_f^k, ω_0^k and T_k are the final and initial crack widths of the k^{th} deck, and the duration of its history in years, respectively. Once the 788 slopes were computed, the mean value and standard deviation were obtained as follows:

$$\bar{m} = \frac{1}{N}\sum_{k=1}^{N} m_k \quad \sigma = \sqrt{\frac{1}{N}\sum_{k=1}^{N}(m_k - \bar{m})^2} \qquad \text{(Eq. 2.16)}$$

where $N = 788$ is the total number of bridges after the filtering was applied. The point estimates of the distribution parameters were $\bar{m} = 5.0523 \times 10^{-6}$ inch/day and $\sigma = 6.5059 \times 10^{-6}$ inch/day.

Alternately, the cracking due to corrosion depends on the corrosion rate of the rebar, described by Equation 2.2. The evolution of this cracking process is not explicitly modeled. Instead, the time at which the first cracks caused by corrosion appear (a.k.a. time to spalling) is defined using the rebar section loss threshold given in Equation 2.3. Hence, the parameter controlling this phenomenon is the corrosion rate. O'Reilly et al. (2011) performed a series of studies to determine the value of this parameter for different types of reinforcement. For epoxy-coated rebars, the corrosion rates obtained were 0.7 mil/year for uncracked concrete and 3.87 mil/year for cracked concrete, with standard deviations of 0.50 and 2.32 mil/year, respectively. With this information, the

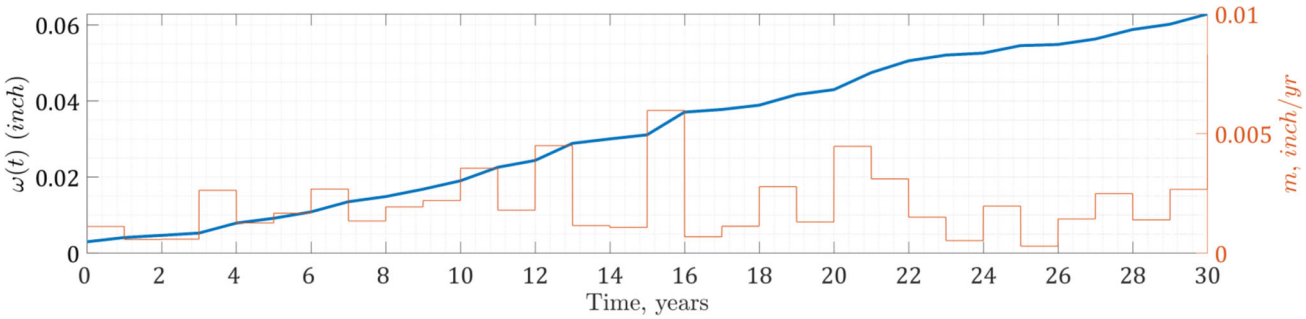

Figure 2.9 Left axis (blue): crack width history for a deterministic simulation. Right axis (orange): slope changed at every year.

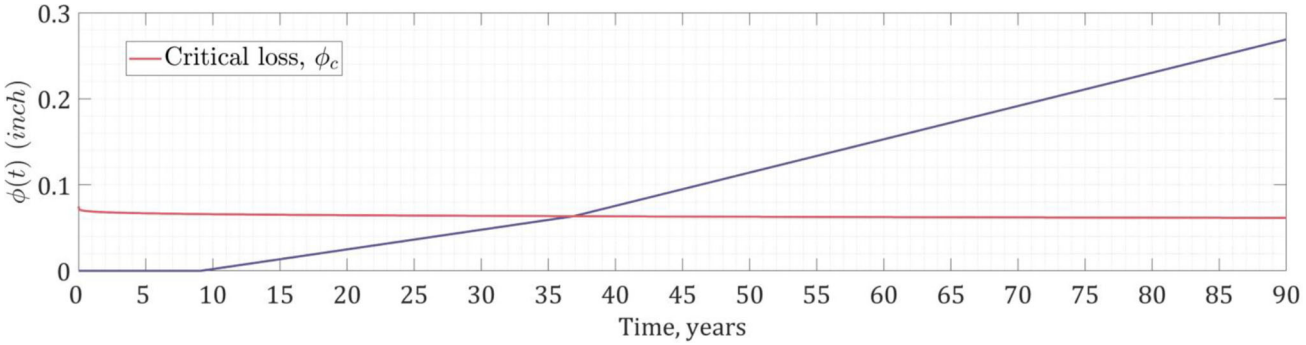

Figure 2.10 Rebar loss due to corrosion and critical corrosion loss for spalling.

corrosion rate r_c was defined as a random variable with two possible distributions depending on the presence of cracking:

$$R_c(t) \sim \begin{cases} \text{Lognormal } (0.70,0.50) & \text{if } \varphi\ (t) < \varphi_c \\ \text{Lognormal } (3.87,2.32) & \text{if } \varphi\ (t) \geq \varphi_c \end{cases} \quad \text{(Eq. 2.17)}$$

This model implies that the rate of the corrosion loss changes once the deck shows extensive cracking. This change in slope is shown in Figure 2.10, which shows the rebar loss due to corrosion for a single realization.

2.2.3 Design Parameters

These variables include those directly related to the defective behavior for the different substandard construction cases defined in the deterministic model. Improper mixing, which refers to a non-standard water/cement ratio, was modeled via a change in the nominal value of the diffusion coefficient. Several researchers have shown that the proportion of water and cement in the mix has a direct impact on the porosity and, therefore, on the diffusion coefficient (Claisse, 2020; Kim et al., 2014; Takiya et al., 2014). Therefore, the standard-construction case was assigned a diffusion coefficient of $D = 22.97 \times 10^{-12}\ ft/s^2$, corresponding to a water/cement ratio of 0.45, which is the closest value available in the literature to INDOT's standard of 0.443. The substandard construction case was assigned a water/cement ratio of 0.60, and $D = 35.43 \times 10^{-12}\ ft/s^2$. Both values were experimentally determined by Takiya et al. (2014). As mentioned by Claisse (2020), the diffusion coefficient of concrete varies considerably and may actually change as much as one order of magnitude from one sample to another. Thus, the standard deviation of this parameter was assumed to be equal to its mean to account for such variability.

Improper curing leads to early cracking of the deck's surface. Hence, it was modeled by increasing the initial crack width, ω_0, in Equation 2.10. For example, a properly cured deck would have expected initial shrinkage cracking with a width smaller than 0.003″, which is the maximum crack width for a deck to be given a CR of 9 (INDOT, 2020a). On the other hand, an improperly cured deck was modeled to have an initial crack width of 0.040″, which corresponds to a CR of 4. In both cases, the standard deviation was defined by assuming it takes on the value equal to the difference between the crack width in a hypothetical totally non-defect deck and a standard constructed deck with CR 9, that is, 0.003″.

Casting an insufficient amount of concrete cover over the top rebar is another common construction defect. An insufficient cover implies a shorter distance between the surface and the upper rebar and, clearly, could result in an earlier corrosion initiation at such level. The standard-construction cover, 2.50″, was taken from INDOT's specifications. The cover for the substandard case was taken to be 1.50.″ For both, a standard deviation of 10% of the non-defective cover, that is, 0.25″, was chosen.

Finally, improper handling of the reinforcement rebars lead to a reduction in their protective epoxy coating. This damage reduces the critical corrosion loss needed for the cracks due to corrosion to appear at the deck's surface (O'Reilly et al., 2011). Defining d_h as a hypothetical rebar pitting, the terms a_f and l_f in Equation 2.3 can be expressed as

$$a_f = \frac{2\pi\left(\frac{d_h}{2}\right)^2}{\pi d_b l} \quad l_f = \frac{d_h}{l} \qquad \text{(Eq. 2.18)}$$

where d_b is the diameter of the rebar and l is the spacing of the pitting holes. According to INDOT's standards and specifications, the maximum allowable pitting hole area should not surpass $0.25'' \times 0.25''$ and the ratio of the damaged area to total area should be less than 0.02. The parameters d_h and l are thus represented as random variables. To generate random distributions, the former was fixed to meet the specification of a maximum damaged area of $0.25'' \times 0.25''$ and the latter was set so that the damaged area to non-damaged area ratio is lesser than 0.02, as indicated in the standards. Symbolically, this means that the following relationships were to be held:

$$A_h = \pi\left(\frac{d_h}{2}\right)^2 < (0.25)^2 \quad \frac{2A_h}{A} = \frac{2\pi\left(\frac{d_h}{2}\right)^2}{\pi d_b l} < 0.02 \qquad \text{(Eq. 2.19)}$$

where A_h is the total damaged area of one potential hole, A is the rebar's area, l is spacing between damaged areas and $d_b = 0.75''$ (INDOT, 2020b) is the rebar diameter. The two in the numerator in the right expression accounts for the existence of two damaged areas that are separated by a spacing of l. Simplification of the above expressions leads to

$$d_h = \frac{1}{2\sqrt{\pi}} \quad \text{and} \quad l = \frac{d_h^2}{0.04 d_b} \qquad \text{(Eq. 2.20)}$$

both are in inches. The mean values of these variables for the standard construction case were set as the median between the hypothetical perfectly constructed handling (total absence of damaged areas, $d_h = l = 0$) and the thresholds defined above, that is:

$$\bar{d}_h = \frac{d_h}{2} \quad \bar{l} = \frac{l}{2} \qquad \text{(Eq. 2.21)}$$

while the standard deviation was set to be 50% of the mean value in each case. For the substandard construction scenario, we assume

$$\bar{d}_h = d_h \quad \bar{l} = l \qquad \text{(Eq. 2.22)}$$

with the same standard deviations as in the non-defective case.

A summary of the design parameters and their descriptive probability distributions is shown in Table 2.7.

2.3 Semi-Markov Process in the Physics-Based Deterioration Model

A semi-Markov process is a standard tool used in the next step in the prediction of condition states for civil engineering assets (Kleiner, 2001; Morcous et al., 2010; Thomas & Sobanjo, 2013; Zambon et al., 2019). The semi-Markov process consists of first determining, based on historical data, the probability of an asset (or component) of transitioning from one condition state to the next lower condition state (hereafter, *transition probabilities*). These values can then be arranged in a matrix for the calculation of the change of CR. Once generated, these matrices may be used to predict the condition state of the asset for each year in the future based on its current condition state.

The transition probabilities can be obtained either from historical data (Goyal, 2015) or from expert opinions in a Delphi process (Kleiner, 2001). However, as Zambon et al. (2019) showed, the availability of a physics-based or analytical model can be used to improve predictions when historical condition state data is lacking or incomplete. Moreover, this approach takes advantage of a broader spectrum of data that does not only include observations. For instance, information regarding the environmental and design parameters may be used to enrich the model.

To use a physics-based stochastic model to generate transition probability matrices, we followed three main steps: (1) physical or observational definition of the times that the deck resides in each CR (*sojourn* or *holding times*); (2) estimation of probability distributions for the time spent at each condition state; and (3) computation of the transition probabilities and assembly of them into matrices. The first step was achieved by defining a mapping between the responses generated by the analytical model from the previous section and INDOT's inspection guidelines. The second step required performing Monte Carlo simulations using the stochastic model and the sojourn time

TABLE 2.7
Probability distributions of the design parameters

Parameter	Mean (standard)	Mean (non-standard)	Standard Deviation
Diffusion Coefficient	22.97×10^{-12} ft/s^2	35.43×10^{-12} ft/s^2	22.97×10^{-12} ft/s^2
Initial Crack Width	0.003″	0.040″	0.003″
Concrete Cover	2.50″	1.50″	0.25″
Damaged Area Diameter	0.15″	0.30″	0.08″
Spacing Between Damaged Areas	0.375″	0.75″	0.19″

definitions from the previous step. Finally, the probabilities were determined, and the transition probability matrices were assembled. The details of these three steps are described in Sections 2.3.1 to 2.3.3.

2.3.1 Sojourn Time Mapping

A semi-Markov process describes the probability of a system being in one state or the next state depending on the time it has resided in its current state. In this study, the states are the CRs that can be assigned to a bridge deck. Consequently, the sojourn times for the deck are the times it resides at each CR. For example, if a deck spends 6 years in CR 8 before being assigned a 7, the sojourn time from 8 to 7 (T_2) is equal to 6 years. To define the sojourn times for the bridges in the state of Indiana, the average number of years bridge decks remained at each CR were calculated. The CR history of all the bridges in the state of Indiana was obtained from BIAS (2022). These average sojourn times, from now on *reference sojourn times*, with their respective adopted label appear in Table 2.8.

To map the physics-based model responses to these reference sojourn times, we performed a deterministic simulation of the standard construction case of each one of the decks under consideration. Three physical variables were chosen as indicators to represent the state of the deck at each sojourn time: (1) chloride concentration, (2) rebar section loss due to corrosion, and (3) crack width. Values are displayed from left to right in Table 2.9 in columns 2, 3, and 4, respectively. This table is for an example bridge (NBI number 79848), with the sojourn time level in column 1. These values are used to describe the physical state of the standard-construction decks under study at each sojourn time. Such values should be computed for each of the bridges constructed meeting standard requirements before proceeding with the non-standard construction analysis.

Using the mapping defined in Table 2.9 as a reference, we then determine the CR of each deck in our catalog at each timestep: for every time t, if any of the three indicators, $C(t)$, $\omega(t)$, *or* $\phi(t)$ has a value greater than its value at T_k but less than its value at T_{k+1}, then the corresponding sojourn time is T_k.

TABLE 2.8
Sojourn times of a deck throughout its entire lifespan

Sojourn Time Label	CR Change	Average Sojourn Time (Years)
T_1	9 to 8	4
T_2	8 to 7	8
T_3	7 to 6	10
T_4	6 to 5	8
T_5	5 to 4	8
T_6	4 to 3	8

TABLE 2.9
Mapping from the physical state of the bridge to the corresponding sojourn time

t	$C(t)$ (lb/yd^3)	$\omega(t)$ (*in.*)	$\Phi(t)$ (*in.*)
T_1	0.08	0.010	0.000
T_2	1.39	0.025	0.007
T_3	2.86	0.044	0.029
T_4	3.32	0.058	0.048
T_5	3.35	0.073	0.068
T_6	3.35	0.088	0.099

2.3.2 Monte Carlo Simulations

Given the complexity of the corrosion, carbonation and cracking processes contained in the developed scheme, there is no closed-form solution to determine each sojourn time's distribution. Thus, Monte Carlo simulations were performed by executing a large number (200) of simulations. For each simulation, the distribution of each physical parameter was sampled to generate realizations. Consequently, the value of each sojourn time varies from one simulation to another, thus generating a distribution from the ensemble of realizations.

A total of 200 realizations was executed per construction case, per bridge deck. Each sojourn time is assumed to follow a lognormal distribution (Zambon et al., 2019). Matlab's *fitdist* function was used to fit the simulated data of each sojourn time to determine the parameters of the lognormal distribution. The ensemble of Monte Carlo simulations was used to generate a probability distribution for each sojourn time, which is:

$$T_k \sim \text{Lognormal}(\mu_k,\sigma_k),\text{k}=1,\ldots,6 \qquad \text{(Eq. 2.23)}$$

2.3.3 Transition Probability Matrices

The probability distributions obtained in Section 2.3.2 were used to compute the transition probabilities needed for the semi-Markov process. The transition probability of the bridge deck staying in state k at time t, that is, the *stay-the-same transition probability,* is defined as (Goyal, 2015):

$$P_{kk}(t)=\frac{S_k(t+dt)dt}{S_k(t)} \qquad \text{(Eq. 2.24)}$$

where $S_i(t)$ is the survival function at time t. It is usually assumed that an infrastructure asset can only degrade from a CR to the immediate consecutive one (Kleiner, 2001). Also, assuming the process is Markovian, the following equality should hold:

$$\sum_{k=1}^{9}\sum_{k=2}^{9} p_{k(k-1)}(t)=1 \qquad \text{(Eq. 2.25)}$$

we obtain the probability of the deck transitioning from state k to state $k-1$ at time t:

$$P_{k(k-1)}(t) = 1 - P_{kk}(t) \qquad \text{(Eq. 2.26)}$$

The transition probability matrices (P-matrices) can then be assembled as:

$$P(t) = \begin{bmatrix} P_{99} & P_{98} & 0 & \cdots & 0 \\ 0 & P_{88} & P_{87} & \cdots & 0 \\ 0 & 0 & P_{77} & \cdots & 0 \\ \vdots & \vdots & \vdots & \ddots & \vdots \\ 0 & 0 & 0 & 0 & P_{11} \end{bmatrix} \qquad t = 1, 2, \ldots, T \text{ (Eq. 2.27)}$$

where T is the total number of years considered in the prediction. Therefore, using a timestep of 1 year, a total of T transition probability matrices are obtained per deck, per construction case. That is, 5 sets of 120 P-matrices would be obtained for a single bridge if 120 years of analysis were desired. The first set corresponds to the standard construction case, the remainder four sets for the substandard construction cases.

In the calculations of the P-matrices, 9 CRs and, thus, 9 condition states were considered. The condition states corresponding to the CR transitions from 3 to 2, 2 to 1, and 1 to 0 were arbitrarily selected and not used in the computation of the degradation curves described in Section 3. The purpose of their inclusion of the calculation was to avoid the bias that a probability transition of 1 in the condition state corresponding to 4 to 3 causes in the degradation curves.

Finally, notice that the transition probabilities given by Equation 2.27 are computed from survival functions which, by definition, are non-increasing (Kleinbaum, 2012). *Hence, the method presented here does not include maintenance actions or interventions that could improve the deck's grading in a given instant of time.*

3. DATA-DRIVEN DEGRADATION MODEL

As mentioned in Section 1, bridge asset engineers utilize prediction software to inform their budgetary planning needs. This prediction is updated yearly, and budgetary needs are planned 5 years into the future. This software tracks the needs regarding future preventative maintenance, repair, and new construction actions based on historical behavior of similar bridges. There are different ways to evaluate historical evidence and create an equation or set of equations for typical degradation patterns. The method chosen for this study is the approach introduced in Section 1 (Goyal, 2015). In this section we endeavor to familiarize the reader with the development of the data-driven model used in this study, introduce modifications made to the original structure for application to Indiana data, and this study in particular, and briefly discuss the results of the data-driven model.

3.1 Survival Analysis

The data-driven model in this study uses historical data and the underlying method originates from survival analysis (Goyal, 2015). Survival analysis is a statistical procedure for which the desired outcome is an estimate of the "time until an event occurs" (Kleinbaum, 2012). A common historical use for survival analysis is in medical applications, although it has more recently been adopted for bridge asset management.

In this project, we use the term *event* to describe the occurrence of a bridge deck being recorded as having a lower CR compared to the CR it was recorded as having in the previous inspection cycle. The term *survival time* refers to the time spent in a CR. For a bridge deck, rather than considering just a single event of interest and thus one survival time, a series of events must be considered since the event we have defined occurs multiple times over the lifespan of the bridge. Each reduction in CR of the deck is thus a separate event, and therefore has a corresponding survival time. Additionally, the external usage factors recorded at each inspection cycle found to significantly influence this survival time are termed *explanatory factors*. They are also sometimes referred to as *covariates* or *hazards*.

3.1.1 Survival Function

The following are the three primary steps comprising the survival analysis process: (1) estimating and interpreting survival functions and/or hazard functions; (2) comparing survival functions and/or hazard functions; and (3) assessing the effect of explanatory factors (hazards) on the survival time. The third step is typically paired with some type of mathematical model that can correctly address a multivariable problem, such as a regression model (Kleinbaum, 2012). The goal of a regression analysis is to describe the relationship between an explanatory factor (input), and the survival time (output).

Let T_s be the random variable representing the bridge deck survival time in a given CR. Then t denotes a specific value of the time of survival of the random variable, T_s. For example, if we are interested in knowing whether a certain bridge deck has lasted in CR 9 for 4 years, then $t = 4$ and we would evaluate whether $T_s > 4$. $S(t)$ is defined as the survival function and represents the probability that the bridge deck will be in a given CR longer than the specified value, t.

$$S(t) = P(T_s > t) \qquad \text{(Eq. 3.1)}$$

$$h(t) = \lim_{\Delta t \to 0} \frac{P(t \le T_s < t + \Delta t | T_s \ge t)}{\Delta t} \qquad \text{(Eq. 3.2)}$$

The survival function is a cumulative measure over time, and one could say that it focuses only on the bridge deck not failing. $h(t)$ is the hazard function that gives an instantaneous potential for the desired deck to degrade to the next CR, given that the bridge deck has survived in the current CR up until the current time, t. The hazard function contains a conditional probability

in the numerator, but because the denominator is a time interval, it makes $h(t)$ a conditional *failure rate* rather than a probability. One could say that the hazard function focuses on the bridge failing (the opposite of the survival function). The two functions can be derived from each other, and the formal relationship can be described as follows: If $\boldsymbol{h(t) = \gamma}$ then $\boldsymbol{S(t) = e^{-\gamma t}}$.

3.1.2 Cox Proportional Hazards Regression

When using a mathematical model to assess the effect of an explanatory factor on the survival time of a deck, a linear or logistic regression model is often used. The inputs of a linear regression model are data that include one or more explanatory factors (hazards), and the outcome is a continuous variable, β, called a "regression coefficient" that describes the impact of those explanatory factors (hazards). In survival analysis the output is called a *hazard ratio* and can be expressed as e^{β}. This hazard ratio represents the effect of one or more explanatory factors (hazards) on the final model. A hazard ratio value of 1 means there is no relationship between the explanatory factor and the survival time of a bridge deck, a hazard ratio greater than one (>1), means that the explanatory factor negatively affects (lowers) the survival time of a bridge deck, and a hazard ratio less than one (<1) means that explanatory factor positively affects (increases) the survival time of a bridge deck. Individual hazard ratios are then combined to accurately describe the overall effect on a specific bridge's degradation model.

One way to determine the hazard ratios, e^{β}, is through the Cox proportional hazards model (Kleinbaum, 2012). This analysis is analogous to that of a linear regression model, without the need to specify a particular form for the model. The desired model is also able to evaluate the effect of multiple explanatory factors, which is the reason we adopt this approach.

3.2 Indiana Data

The degradation model developed for the state of North Carolina, as described in Section 3.1, can be easily applied to the state of Indiana as the same type of data are required to be collected by all 50 states. The state of Indiana has 30 years of historical data available for approximately 17,500 bridges. To develop the degradation model used in this study, we modified the Matlab code from Goyal (2015), to reflect the differences in the data collected by the North Carolina Department of Transportation and those of INDOT.

3.2.1 Data Cleaning and Censoring

While it is impossible to know exactly how long a bridge deck remains in a specific CR (because a deck could degrade from one CR to another at any point during the 2-year inspection interval), the maximum amount of time it is recorded in that CR is taken as the duration. For example, if a given bridge deck had a CR of 7 in 2006, and a CR of 6 in 2008, 2010, 2012, 2014, 2016, followed by a CR of 5 in 2018, the duration of time the bridge remained in CR 6 would be calculated by subtracting 2008 from 2018, yielding 10 years.

Data may also be classified as censored or uncensored. *Uncensored* data are defined as observations of a certain CR that are fully observed. In other words, the full durations are known, and the data are considered reliable. An illustration of one uncensored observation is shown in Figure 3.1.

Censored data are interrupted in some way. There are different forms of censored data, the most common being left-censored or right-censored (Kleinbaum, 2012). In this study, the only form of censored data we see is right-censored. A *right-censored* CR observation is one in which the full duration of time that the bridge spent in that CR is not known exactly, due to some outside factor, therefore it could have been longer than the current observation length. A right-censored observation can occur for a number of reasons. Some examples of this type of an observation are as follows.

- The CR recorded for the bridge deck right before a maintenance action is performed, that alters the CR in some way.
- The first CR recorded in the analysis period, because the start of that CR observation is unknown as the analysis period is limited.
- The last CR recorded in the analysis period because the end of that degradation period is unknown as the analysis period is limited.

An illustration of a right-censored observation that occurred due to some maintenance action being performed that increased the CR is shown in Figure 3.2.

One additional and important matter to note is that the assigning of a CR to a bridge component is a subjective process. From day to day an individual's opinion can vary based on any number of outside factors. Thus, two bridges that are in a similar condition may ultimately be rated differently. In addition to individual subjectivity when assigning CRs, the federally mandated CR scale with options from 0–9 is not very descriptive, which leaves room for interpretation among inspectors. Due to the inherent subjectivity of the inspection process, certain criteria are applied to the dataset to remove unreliable data, even before they are determined to be censored or uncensored. One new criterion used herein to remove unreliable data is if the observation of a certain CR is less than or equal to 8 years, and if the observed CR has a CR the year before the observation starts that is equal to the CR the year after the observation ends, then the observation is considered unreliable and removed from the analysis completely. This additional criterion is adopted because sometimes subjectivity causes individual CRs to fluctuate between two values for some time before finally degrading to an even lower CR. This additional criterion will help create a dataset that is "clean" and consists of only reliable data.

Year	2008	2009	2010	2011	2012	2013	2014	2015	2016	2017	2018
CR	7	6	6	6	6	6	6	6	6	6	5

Figure 3.1 Observation of CR 6, illustrating an observation that is considered uncensored.

Year	2001	2002	2003	2004	2005	2006	2007	2008
CR	6	5	5	5	5	5	5	8

Figure 3.2 Observation of CR 6, illustrating an observation that is considered right-censored.

Year	1998	1999	2000	2001	2002	2003	2004
CR	7	6	6	6	6	6	7

Figure 3.3 Observation of CR 6, illustrating data considered unreliable.

TABLE 3.1
Basic dataset evaluation information

CR	Total No. Observations	No. Reliable Observations	No. Uncensored Observations	% Utilization Reliable Data	% Utilization Uncensored Data
9	3,065	2,361	1,196	77	39
8	9,640	8,511	3,441	88	36
7	14,280	13,376	3,238	94	23
6	11,922	11,072	2,367	93	20
5	7,270	6,549	1,275	90	18
4	2,688	2,301	466	86	17
3	553	452	89	82	16
2	95	69	9	73	9
1	22	18	3	82	14

An illustration of a CR observation that would be removed from the analysis dataset can be found in Figure 3.3.

Another benefit of using the Cox proportional hazards model is that it can incorporate both uncensored data and right-censored data. This option allows for much more data to be used in the analysis, which is likely to result in a more accurate final degradation model. Table 3.1 outlines how much information is available compared to how much is actually used in this study, after performing the censoring and cleaning process. Clearly the number of bridges with observations of CRs between 1 and 3 are extremely low in comparison to the other CRs. Additionally, the total number of reliable observations of CRs 1–3 is extremely low. With a dataset this large, and the small amount of data with a CR of 1, 2, or 3, it is not reasonable to formulate a reliable degradation model with these data. Based on the previous discussion and the fact that very few bridges are allowed to degrade to CR 4 anymore, it was determined that performing the analysis for CRs between 4 and 9 only was the most appropriate approach.

3.2.2 Hazard Group Determination and Categorization

The explanatory factors (hazard groups) of interest for the data-driven model in this study determined by the research team with input from INDOT are listed as follows:

- functional classification,
- wearing surface presence/type,
- average daily truck traffic,
- maximum span length,
- number of spans, and
- age of bridge.

Of the hazard groups evaluated, there are different options for further categorization within each hazard group. The division of the hazard group options is based on the coded value for each hazard. The coding values come from the FHWA recording and coding guide. For example, *functional classification* is divided into two options; whether the bridge is located on a non-interstate versus interstate road. So, *functional classifications* coded as 1 or 11 are considered the interstate option and all other coding options for functional classification are considered the non-interstate option. However, for *wearing surface presencel type* there are a total of 10 wearing surface types, so a bridge deck could be 1 of 10 coding options. For both age of the bridge and average daily truck traffic, there is a large range of possible data inputs. In order to reduce the number of options the degradation model has to work with, the full range of data inputs are evaluated and divided equally into 4 categories containing a range

TABLE 3.2
List of hazard groups and their individual options

Hazard Group	Options
Functional Classification	2, 6, 7, 8, 9, 12, 14, 16, 17, 19 = *Road System 1* 1, 11 = *Road System 2*
Wearing Surface Presence/Type	0 = *None* 1 = *Monolithic Concrete* 2 = *Integral Concrete* 3 = *Latex Concrete* 4 = *Low Slump Concrete* 5 = *Epoxy Overlay* 6 = *Bituminous* 7 = *Timber* 8 = *Gravel* 9 = *Other*
Average Daily Truck Traffic (vehicles)	$0 \leq ADTT\ 1 \leq 4$ $5 \leq ADTT\ 2 \leq 24$ $25 \leq ADTT\ 3 \leq 329$ $330 \leq ADTT\ 4$
Maximum Span Length (meters)	$0 \leq Max\ Span\ 1 \leq 7$ $8 \leq Max\ Span\ 2 \leq 14$ $15 \leq Max\ Span\ 3$
Number of Spans	1 = *Number Spans 1* >1 = *Number Spans 2*
Age of Bridge (years)	$0 \leq Age\ 1 \leq 16$ $17 \leq Age\ 2 \leq 26$ $27 \leq Age\ 3 \leq 44$ $45 \leq Age\ 4$

of values. The information about hazard group options and their associated coding numbers/input ranges can be found in Table 3.2.

For every hazard group and its corresponding set of options, there is always a baseline option that the remaining options are used to compare to in the calculation of the hazard ratios. Each of the baseline hazard options are assumed to have a hazard ratio value of 1.00, so if a bridge happens to have the same hazards that are applicable to it, as the baseline options, then the degradation behavior of that bridge would be the same as if the calculation had no hazard ratios applied to it. The baseline option is always taken as the first numerical coding option (example would be 0 = none for wearing surface presence/type) or the first option in the list (for example, ADTT1). The code is run initially with every hazard and its individual options, to determine which of all the hazard options are found to be statistically significant. The statistical significance of a hazard is determined by its *p*-value. The *p*-value is a common parameter calculated in all programs and functions associated with regression modeling and is automatically calculated within the *coxphfit.m* function within Matlab.

3.3 Hazard Ratios Calculation

Once initial significance is determined for each explanatory factor, the Cox proportional hazards model is run again with every possible combination of only those hazards deemed significant, and a final best combination is selected based on the best statistical fit with the least number of total hazards. During this best combination selection process, any hazard group option with a number of observations less than 1% of the total observations was excluded, as these hazard ratios may be unreliable due to the low amount of data used to determine their value. One additional exception is if one specific hazard is found to be significant in two consecutive combination runs, then it is automatically included in the final hazard selection (Goyal, 2015). The final set of hazard ratios computed for each CR between 4 and 9 is shown in Table 3.3.

3.4 Data Driven Model Validation

INDOT currently only uses uncensored historical data in their model development. When separating the reliable historical data from the unreliable historical data, and the right-censored historical data from the uncensored historical data, as described in Section 3.3.1, the amount of historical data that is left as uncensored per CR is on average 21% (Table 3.1). This value is consistent with the percentage of total data that INDOT currently uses in their historical data analysis, and the data-driven model is extracting a similar amount of historical data, compared to what INDOT views as reliable and usable in their current prediction

TABLE 3.3
Final hazard ratios for the state of Indiana

	CR4	CR5	CR6	CR7	CR8	CR9
Road System 2	1.0000	1.0000	1.0000	0.7536	0.8169	0.7426
Monolithic Concrete	1.0000	1.0000	0.7032	1.0000	1.0000	1.0000
Integral Concrete	2.3921	1.0000	1.0000	0.7471	1.0000	1.4003
Latex Concrete	1.0000	1.3825	1.0000	1.0000	1.0000	1.0000
Bituminous	2.0489	1.4686	1.0000	1.0000	1.0000	1.0000
ADTT 2	1.0000	1.0000	1.0000	1.0000	0.8540	1.0000
ADTT 3	1.0000	1.2519	1.4773	1.0000	1.0000	1.0000
ADTT 4	1.6830	1.2927	1.4553	1.2816	1.1172	0.7884
Max Span 3	1.0000	1.2177	1.0000	0.8696	1.0000	1.0000
Number Spans 2	1.0000	1.0000	1.0000	1.1083	1.0000	1.0000
Age 2	1.0000	1.0000	1.4005	0.8307	0.6426	1.7099
Age 3	1.0000	1.7709	1.8543	1.4032	1.8168	2.4305
Age 4	1.4877	2.1086	1.9336	1.4768	2.0180	1.9503

TABLE 3.4
Comparison of average time in each CR

CR	INDOT Expectation of Average Time in Each CR	Study Values of Average Time in Each CR
9	4	4
8	8	8
7	12	12
6	12	10
5	12	8
4	12	6

methods. However, the Cox proportional hazards model does incorporate the available historical right-censored data as well as the historical uncensored data, so our model uses on average 88% of the total amount of historical data available for bridges per CR, for CRs 4 through 9.

To validate the data-driven model developed in this study, we compare our calculated sojourn times for each CR to that of what INDOT currently observes. The expected values based on INDOT observations and the computed average values from the data used in this study are compared in Table 3.4. Our values are similar to what INDOT expects, and the differences could be explained by a difference in general censoring protocol used in our two different numerical models.

4. PREDICTIVE DEGRADATION MODEL DEVELOPMENT AND APPLICATION

A physics-based model can, in theory, be utilized to predict the degradation of a bridge deck over time. However, the physics-based model developed here is two-dimensional and alone has its limitations. *However, the physics-based model is necessary because it provides the ability to change the physical parameters of the bridge deck with a scientific basis and allows for reflecting construction defects in the degradation curve.* Furthermore, observations in the form of CRs from inspections are used to make decisions regarding intervention actions or replacement. Thus, in this study the physics-based model for standard construction (in Section 2) is linked to the data-driven model that reflects historical CRs by trained inspectors (in Section 3). This linkage empowers the predictive degradation model to capture the influence of defects on the degradation curves.

This linkage is done as follows. First, the stay-the-same transition probabilities are determined from the physics-based model, and the hazard ratios are determined for the data-driven model. Next, the two outcomes are combined to obtain a prediction of the future CRs of the bridge over time. The process of combining the two models and producing a prediction of the CRs of a given bridge is described further in this section.

4.1 Predictive Degradation Model Logistics

Hazard ratios can simply be applied to the already determined stay-the-same transition probabilities (Section 2.3.3) by raising the diagonal probability values to the corresponding hazard ratio, as defined in Equation 4.1. P^*_{kk} can be defined as the probability that a bridge deck will stay in CR k, given that it is already in CR k, where P_{kk} is the stay-the-same transition probability determined from the physics-based modeling and HR_k is the hazard ratio determined for this specific bridge deck in CR k. As explained in Section 2.3.3, we can then use Equation 4.2 to compute the probability that the bridge deck will degrade from CR k to CR *(k-1)* by subtracting the stay-the-same transition probability previously found from one.

$$P^*_{kk} = P^{HR_k}_{kk} \qquad \text{(Eq. 4.1)}$$

$$P^*_{k(k-1)} = 1 - P^{HR_k}_{kk} \qquad \text{(Eq. 4.2)}$$

4.2 Future Condition Rating Prediction

Prediction of future CR originates from the Markov chain approach (Goyal, 2015) and will be outlined herein.

Let the current CR of a bridge component be represented as a row vector, Z_0, with nine elements. Each element in the vector corresponds to the probability that the bridge component is in the associated CR (in reverse numerical order). Thus, the vector consists of zeros with a single entry with a value of one placed in the position associated with its current CR. Assume that when the bridge deck is constructed with no defects, it receives a CR of 9 after the first inspection. Thus, the initial vector is Z_0 = [1 0 0 0 0 0 0 0 0], essentially encoding the assumption that at the initial time (i.e., the first inspection) there is a 100% chance the bridge deck is at CR 9 and a 0% chance the bridge deck is at any other CR.

Let P_1 be the non-stationary stay-the-same transition probability matrix for the first year. Here the hazard ratios have already been applied to the transition matrix, as illustrated in Section 4.1.1. To determine the predicted condition state vector, Z_n after 1 year of life one would multiply the matrix, P_1 by the initial condition state vector, Z_0 (Equation 4.3), The form of the predicted condition state vector, Z_n, is similar to that of the initial condition state vector, Z_0 in that each element of Z_n represents the probability that the bridge deck will be in the corresponding CR n years in the future. Let R be a column vector, containing all possible CRs, which is expressed as R = [9 8 7 6 5 4 3 2 1]^T. The predicted future condition state (CR) of the bridge deck is expressed as E_n and is found by multiplying the Z_n [1 × 9] row vector by the column vector, R [9 × 1] (Equation 4.4).

$$Z_n = Z_{n-1} * P_n \qquad \text{(Eq. 4.3)}$$

$$E_n = Z_n * R \qquad \text{(Eq. 4.4)}$$

To estimate the CR at a time several years in the future, one would apply Equations 4.3 and 4.4 until the target number of years in the future is reached. The final calculation of future CR prediction, E_n yields a decimal value. Decimal values are acceptable for the purpose of creating a smooth degradation curve.

4.3 Validation of the Predictive Degradation Model

To validate the predictive degradation model, we compare the predicted lifetime of the bridge deck to the lifetime values that INDOT has historically observed. Here we introduce the term *native degradation*, which refers to only the act of degradation of the bridge deck, and it precludes any effects on CR that result from maintenance actions or interventions.

In reality, maintenance actions and interventions are performed on concrete bridge decks during their lifespan, some of which either improve the CR of the deck or extend the expected survival time of a particular CR of the deck. When the effects of maintenance actions and interventions are included, the behavior is referred to as *non-native degradation*. Discussions with INDOT personnel pointed out that a bridge deck will usually be replaced when it is believed to be halfway between CR 5 and 4. According to INDOT this is expected to occur approximately 40–50 years after construction, assuming only native degradation is taking place. In this study, exclusively native degradation is considered. Thus, all values associated with life expectancy and the subsequent cost analysis refers to those of concrete bridge decks experiencing native degradation. Furthermore, INDOT asset managers explained that the expected native degradation service life of a concrete bridge deck with standard construction is 40–50 years. The predictive degradation model is validated by determining when each of the case study bridges with standard construction reach the halfway point between CR 5 and 4 and comparing that to the time window of 40–50 years currently observed by INDOT asset managers. Table 4.1 confirms that our prediction of standard construction is reasonable as every bridge has an estimated time of rebuilding the deck between 40 and 50 years.

4.4 Application of the Predictive Degradation Model to the Case Study Bridges

To apply this method to the bridges in the case study, the physics-based deterioration, the data-driven and the cost models, were sequentially executed. First, the stay-the-same transition probabilities (Section 2) of each deck, coming from physical processes, were obtained. Next, the specific hazards applicable to the case study bridge were determined and the associated hazard ratios were combined (Section 3). Finally, the final set of applicable hazard ratios were applied to the specific stay-the-same transition probabilities for each year and the future CR prediction calculations were performed to obtain a predicted CR degradation over time, like that shown in Figure 4.1.

Table 4.2 provides the mean defect-related parameters for each bridge deck and each defect described in Section 2.1. The values for each bridge were inferred based upon their respective current CR and description in BIAS. Specifically, the mean values for the initial cracking are taken from the INDOT *Bridge Inspection Manual* (INDOT, 2020a), and the rebar handling

TABLE 4.1
Estimated native degradation service life of case study bridges

	Estimated Native Service Life (years)
4081	42
11980	41
15651	41
18911	41
19571	41
33440	42
36033	41
44080	41
50521	42
79848	42

damaged area diameter, cover and w/c ratio are taken from tolerance values from *Indiana Department of Transportation Standard Specifications 2020* (INDOT, 2020b) as described in Section 2.2.3. The standard deviations used here are the same as those used in Table 2.7.

Hazard ratios applied to a given bridge correspond to the specific hazards that are reported to be affecting the bridge over its life. To calculate the hazard ratios for an individual bridge, one must first identify which Indiana bridge hazards are applicable to a given bridge under consideration. This process requires evaluating the recorded hazard options from the historical data available on the FHWA website. To accurately represent the bridge over its history, the values used for the hazard assignment can be determined as follows. For hazards with pre-determined options (ex: wearing surface), we take the mode (the value that occurs most in the dataset) of all values recorded in the historic record of that particular bridge, as this would identify the value that represents the majority of the life of that bridge. For hazards defined with a varying numerical input (ex: average daily truck traffic), we take the average of all values recorded in the bridge's historic record. Once individual hazard assignment has been performed for the given bridge, the final hazard ratios

TABLE 4.2
Description of relevant features for the predictive simulation of the decks in the case study bridge set

NBI	CR	Relevant Observations	Initial Cracking	w/c Ratio	Cover	Rebar Handling (Damaged Area Diameter)	Initial Chloride Content
4081	9	"(…) hairline short longitudinal cracks at both ends of deck (…) Good condition."[1]	0.003″ (NS)	0.45 (S)	2.50″ (S)	0.15″ (S)	0
11980	6	"(…) longitudinal and transverse map cracking up to approximately 0.020" nominal width visible throughout topside of deck."[1]	0.020″ (NS)	0.45 (S)	2.50″ (S)	0.15″ (S)	0
15651	5	"Moderate width cracking throughout the deck, signs of water leaking through the deck and staining the slope walls underneath. Efflorescence forming on the bottom of the deck."[1]	0.030″ (NS)	0.45 (S)	2.50″ (S)	0.15″ (S)	1.69 lb/cuy
18911	8	"(…) deck also heavily cracked throughout."[2]	0.040″ (NS)	0.45 (S)	2.50″ (S)	0.15″ (S)	0
19571	7	"(…) slightly diagonal cracks with efflorescence."[1]	0.016″ (NS)	0.45 (S)	2.50″ (S)	0.15″ (S)	1.69 lb/cuy
33440	6	"Failed air test."[3]	0.020″ (NS)	0.60 (NS)	2.50″ (S)	0.15″ (S)	0
36033	8	"(…) the contractor was allowed to utilize a substitute concrete mix during the winter months provided they provide for special curing considerations (…) those considerations were not followed."[4]	0.012″ (NS)	0.60 (NS)	2.50″ (S)	0.15″ (S)	1.69 lb/cuy
44080	8	"There were issues with the rebar cover and rideability after the superstructure pour (…)."[5]	0.006″ (S)	0.45 (S)	2.50″ (S)	0.30″ (NS)	0
50521	9	"Deck (underside): no corrosion to metal forms."[1]	0 (S)	0.45 (S)	2.50″ (S)	0.15″ (S)	0
79848	5	"(…) some efflorescence on closure angles (of SIPs) in SE corner and at Pier 2 (NB) (…) Several transverse cracks visible under the deck at the center seam with efflorescent."[1] "(…) incorrect concrete was used in deck".	0.040″ (NS)	0.60 (NS)	2.50″ (S)	0.15″ (S)	1.69 lb/cuy

[1]Bridge Inspection Report, 01/06/2020 (available on BIAS).
[2]Correspondence with Mark Pittman, asset manager. 02/17/2021.
[3]Correspondence with Jason Heile, asset manager. 07/12/2021.
[4]Correspondence with Adam Post, asset manager. 07/12/2021.
[5]Correspondence with Christopher Wheeler, asset manager. 06/30/2021.

for that bridge must be determined. For each individual CR one must calculate the product of the applicable hazards. Table 4.3 contains the hazard group option assignment for the case study bridge #11980. Table 4.4 contains the final hazard ratio determination and the product calculation for the case study bridge #11980 to illustrate the process described above. Finally, Table 4.5 contains the calculated hazard ratios for each case study bridge for CRs 4 through 9. Recall that a hazard ratio value of 1 (shown in yellow) means there is no relationship between the explanatory factor (hazard) and the survival time of a bridge deck, a hazard ratio greater than one (>1, shown in red), means that the explanatory factor negatively affects (lowers) the survival time of a bridge deck, and a hazard ratio less than one (<1, shown in green) means that explanatory factor positively affects (increases) the survival time of a bridge deck. Individual hazard ratios are then combined to accurately determine the overall effect on the degradation model.

4.4.1 Loss of Life

Assuming native degradation in all instances, a sample predictive degradation curve is provided for case study bridge #11980 in Figure 4.1. Appendix A.2 provides the predicted degradation curves for each case study bridge. In Figure 4.1, the dashed black line corresponds to the predicted bridge degradation assuming it is built with standard construction, the solid black line assumes standard construction but with the addition of the hazard ratios determined in this study, and the solid red line corresponds to the predicted degradation pattern of the bridge built with its specific construction defect(s) and includes the same applied hazard ratios. The hazard ratios are applied to the stay-the-same transition probability matrices determined from the physics-based model. When following the prediction process outlined in Section 4.2, the future CR prediction calculations start from the current CR of

TABLE 4.3
Hazard group option assignment for case study bridge #11980

Hazard Group	Hazard Value	Hazard Group Option
Functional Classification	14	Road System 1
Wearing Surface	3	Latex Concrete
Average Daily Truck Traffic	547	ADTT 4
Maximum Span Length	29	Max Span 3
Number of Spans	3	Number Spans 2
Age	48	Age 4

TABLE 4.4
Final hazard ratio determination for case study bridge #11980

	CR4	CR5	CR6	CR7	CR8	CR9
Road System 1	1.0000	1.0000	1.0000	1.0000	1.0000	1.0000
Latex Concrete	1.0000	1.3825	1.0000	1.0000	1.0000	1.0000
ADTT 4	1.6830	1.2927	1.4553	1.2816	1.1172	0.7884
Max Span 3	1.0000	1.2177	1.0000	0.8696	1.0000	1.0000
Number Spans 2	1.0000	1.0000	1.0000	1.1083	1.0000	1.0000
Age 4	1.4877	2.1086	1.9336	1.4768	2.0180	1.9503
Π	2.5037	4.5886	2.8141	1.8239	2.2546	1.5375

TABLE 4.5
Final hazard ratios for case study bridges

	CR4	CR5	CR6	CR7	CR8	CR9
4081	1.6830	1.2927	1.0233	1.4203	1.1172	0.7884
11980	2.5037	4.5886	2.8141	1.8239	2.2546	1.5375
15651	1.6830	1.5741	1.4553	1.2351	1.1172	0.7884
18911	1.6830	1.5741	1.0233	1.2351	1.1172	0.7884
19571	1.0000	1.5245	1.0388	0.9637	1.0000	1.0000
33440	2.5037	4.5886	2.8141	1.3746	1.8418	1.1418
36033	1.6830	1.5741	1.0233	0.9308	0.9127	0.5855
44080	2.5037	3.7682	2.8141	1.5807	1.8418	1.1418
50521	1.0000	1.5245	1.0388	0.9637	1.0000	1.0000
79848	1.6830	1.5741	1.0233	1.2351	1.1172	0.7884

Note: HR < 1 equals green numbers. HR = 1 equals yellow numbers. 1 < HR < 1.5 equals blue numbers. 1.5 ≤ HR equals red text.

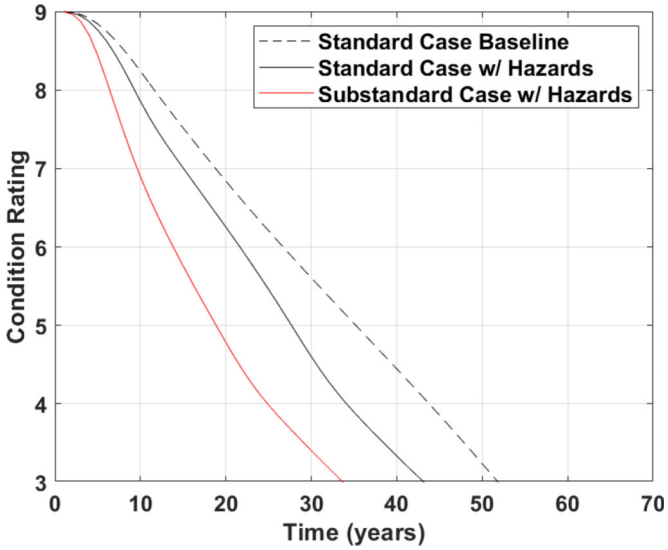

Figure 4.1 Degradation curve for case study bridge #11980.

TABLE 4.6
Estimated reconstruction years and life lost for case study bridges

	Estimated Reconstruction Year for Standard Construction	Estimated Reconstruction Year for Substandard Construction	Estimated Loss of Life (years)
4081	40	–	–
11980	33	23	10
15651	38	23	15
18911	39	19	20
19571	40	30	10
33440	33	24	9
36033	41	30	11
44080	33	32	1
50521	40	–	–
79848	40	17	23

the bridge, which may be a value other than nine. However, to facilitate comparison in this study, the degradation depicted is the estimated degradation from the first year of the life of a bridge deck, given that it started in CR 9, even though the bridge may have already been in service for some time. This simplification is made so that the case study bridges can be easily compared with the same starting point—immediately after construction—rather than the current CR which may be years after the initial construction.

The protocol that a bridge deck is replaced between CR 5 and 4 is applied here and used to generate a prediction of the estimated time to replacement for each case study bridge. Table 4.6 contains the predicted year when a bridge deck reconstruction would take place based on the average between the year at which each case study bridge is predicted to cross from CR 6 to 5 and the year at which each case study bridge is predicted to cross from CR 5 to 4. The last column provides the difference between the estimated year of bridge deck reconstruction for the standard construction and the substandard construction cases. Bridges that have a (-) in columns 2 and 3 do not contain defects, thus do not have a substandard construction case for comparison.

4.4.2 Sensitivity Analysis

The outcomes of the predictive degradation model given in Section 4.1 are degradation curves showing the loss of CR of the bridge with age, for either standard or substandard construction. In this section, the predictive degradation model from Section 4.1 is used to evaluate the sensitivity of the predictive degradation model to the different construction defects and hazard ratios evaluated in this study. A more detailed analysis that investigates the sensitivity of the model to different levels of each construction defect, as well as geographic region in the state of Indiana is included in Appendix A.3.

4.4.2.1 Sensitivity to defects. An individual degradation curve showing the variability between each of the construction defects studied was built.

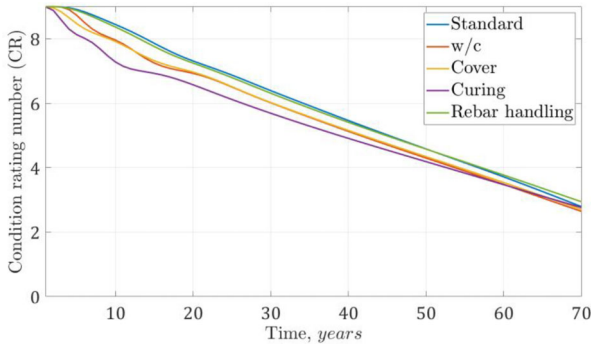

Figure 4.2 Comparison of a standard construction case with the worst-case scenario for each defect.

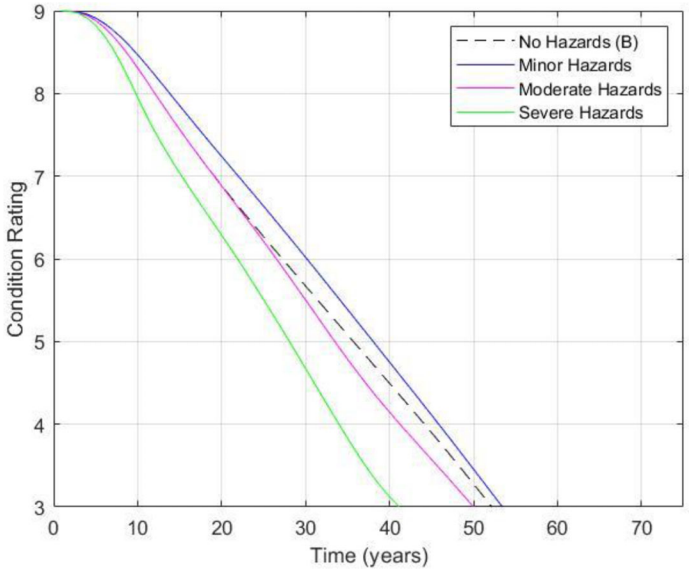

Figure 4.3 Sensitivity analysis for different hazard ratio combinations.

The standard construction case alongside the worst-case scenario for each defect is plotted in Figure 4.2—w/c of 0.60, 1.50″ concrete cover, 0.040″ initial crack width due to improper curing, and epoxy-coating damage at the top surface of the rebar. As can be seen, improper rebar handling is the least concerning defect of all of those considered. However, the life expectancy of the deck would greatly benefit from an improvement in the handling of epoxy-coated bars. This case is followed by the cases considering insufficient concrete cover and excessive water-cement ratio. These have very similar behavior after the first 15 years of life. Both reduce the life of the deck by around 3 years. Improper curing is the most important defect with a 10-year reduction in the life of the bridge deck.

4.4.2.2 Sensitivity to hazard ratios. Indiana bridges are subject to multiple external factors that could potentially speed up or slow down the degradation process over the life of the bridge. To better understand which external factors were significant to the degradation observed in the state bridges considered, a Cox proportional hazards regression was performed. Each individual external factor was assigned the term hazard group and the span of data values applicable to that group were divided into further subgroups called hazard group options. We evaluated the sensitivity of the final degradation curves to the presence of these hazard groups, by sequentially applying the effect of each hazard group to the same base degradation pattern. When comparing the individual hazard options (e.g., interstate versus non-interstate), often one single hazard option does not exhibit much variation in expected life loss/gain. The observed maximum variation is approximately 2 years in this study. That is, of course, for all hazard groups other than wearing surface presence/type and age. The hazard group age results in a variation of approximately 6 years among its respective hazard options. Another significant difference is that when the hazard ratios are combined for individual bridges (as most bridges are subject to multiple hazards at the same time), the effect of the hazard group greatly increases. See Figure 4.3 for an illustration of the difference in loss/gain of life that can happen from different levels of hazard combination. The curve representing "Negligible Hazards" has the hazards for "Road System 2" and

"5 ≤ ADTT ≤ 24" applied. The curve representing "Moderate Hazards" has the hazards for "Latex Concrete" and "25 ≤ ADTT ≤ 329" applied. The curve representing "Severe Hazards" has the hazards for "Bituminous," "330 ≤ ADTT," and "45 ≤ Age" applied.

5. COST MODEL DEVELOPMENT AND APPLICATION

The final task in this project is to compare the cost associated with a defective (non-standard) bridge as opposed to a non-defective (standard) one. To that end, a model to calculate the expected costs of a deck was adopted from Kleiner (2001) and adapted to fit the needs of this study.

5.1 Cost Model

The predictive degradation model input consists of the transition probability matrices, *P,* with the effect of hazard ratios applied, which then yields the predicted condition state vectors, Z_n. The vector, Z_n represents the probability of the bridge deck to be in each of the possible CRs (1–9) at year n. This value is then used to calculate lifecycle costs. The method chosen for the lifecycle cost calculation is adapted from Kleiner (2001), where there are three different cost equations (shown in this section with the original number as presented in Section 4) consisting of Equation 4.7 which is for calculating the estimated cost of interventions of the bridge deck; Equation 4.8 which is for calculating the estimated cost of replacement of the bridge deck; and, Equation 4.9a which is for calculating the total cost of the bridge deck (incorporating both intervention and replacement cost). The original Kleiner equation is that of Equation 4.9a, however it has been adapted to Equation 4.9b to be used in this study, by removing the effect of the exponential which includes the rate of inflation. Kleiner utilized this exponential to reflect the value of today's dollars at a future time, which is correct for a future payment. In this study, we are interested in knowing the difference in lifecycle costs in today's dollars, and therefore we do not need to account for inflation.

The use of these equations is introduced in Figure 1.3 and the process and application to this study are described below. The expected value of C_R, the cost of replacement, and the expected value of C_I, the vector of intervention costs associated with each condition rating in dollars, respectively, are found using Equations 4.7 and 4.8,

$$\mathbb{E}[C_I(t)] = C_I Z_{n(i)}(t) \qquad \text{(Eq. 4.7)}$$

$$\mathbb{E}[C_R(t)] = C_R Z_{n(r)}(t) \qquad \text{(Eq. 4.8)}$$

where $Z_n(t)$ is the predicted condition state vector at time t, $Z_{n(r)}$ is the (r-th) entry of the predicted condition state vector corresponding to the state at which the deck is likely to be replaced, $Z_{n(i)}$ is the (i-th) entry(s) of the predicted condition state vector of the remaining states, which are subject to future intervention.

The total expected cost at a time t years into the future could be then computed as C_T, based on Equation 4.9a. Because we need to compute the cost of the standard case and the substandard case in present day dollars, we use Equation 4.9b.

$$\mathbb{E}[C_T(t)] = \{\mathbb{E}[C_R(t)] + \mathbb{E}[C_I(t)]\}e^{(-rt)} \qquad \text{(Eq. 4.9a)}$$

$$\mathbb{E}[C_T(t)] = \mathbb{E}[C_R(t)] + \mathbb{E}[C_I(t)] \qquad \text{(Eq. 4.9b)}$$

5.2 Application of the Cost Model

To determine the estimated increase in the lifecycle cost of a bridge deck with defects, we need to first define the CR range of evaluation. The FHWA has guidelines for CR assignment with options ranging from 1 (imminent failure) to 9 (perfect) (FHWA, 1995). In reality, very few bridge decks are allowed to degrade below CR 5, even fewer go below CR 4, and virtually none will be allowed to degrade past CR 3. Moreover, according to INDOT personnel, the replacement of the deck is usually performed when the deck is between CR 5 and CR 4. However, since CR options exist starting with CR 9 all the way to CR 1, to avoid any unnatural skew in the predictive degradation model output, we use the full range of potential CR values to represent the potential lifecycle of the bridge deck and use CR 1 to indicate the end of the life of the bridge deck or the associated condition rating with replacement. Therefore, in Equation 4.7, $n(r)$ is taken as one and, consequently, $Z_n(i)(t) = [Z_9, Z_8, \ldots, Z_2]^T$. It is important to note that this method is consistent with the creation of the stay-the-same transition probability matrices, which include transition probabilities for all CR options 1–9 as well.

After defining the CR range of evaluation, we then determine at what point in time the cost values will be calculated and compared. It is necessary to choose the same point in time for both the standard construction and substandard construction cases so that the evaluation timeframe is equal. The selected time is chosen as the time at which the standard construction case for a given bridge deck is predicted to need replaced (degradation point halfway between CR 5 and 4). The estimated year of replacement for each of the case study bridges can be found in Table 4.6.

Finally, the determination of intervention and replacement costs will allow for the value assignment of variables C_R and C_I and then the final calculation of C_T. During our discussions with INDOT, the team was provided with a table that is used for preliminary cost estimate for deck maintenance and replacement actions including thin deck overlay, rigid deck overlay, and full

TABLE 5.1
Estimated total cost and cost difference for case study bridges (in present day dollars)

	C_T, Total Estimated Cost for Standard (STD) Construction Case	C_T, Total Estimated Cost for Substandard (SUB) Construction Case	Total Estimated Cost Difference (SUB – STD)
4081	$1,175,800	$1,175,800	–
11980	$1,820,200	$1,835,700	$15,500
15651	$1,481,600	$1,750,900	$269,300
18911	$1,245,800	$2,054,800	$809,000
19571	$1,070,100	$1,124,100	$54,000
33440	$1,497,000	$1,531,400	$34,400
36033	$3,963,200	$4,299,800	$336,600
44080	$1,969,400	$1,976,800	$7,400
50521	$1,529,000	$1,529,000	–
79848	$5,404,500	$9,453,000	$4,048,500

deck replacement. These costs are based on the type of roadway the bridge is located on and the area of the deck. Thus, once the user knows if the roadway that the bridge is located on is an interstate roadway or a non-interstate roadway, the applicable range of deck square footage is determined to then find a per square foot approximation for the cost of the three action items mentioned previously. The values in this table are used for the determination of the C_R and C_I values for each case study bridge.

The C_I vector must be determined based on the typical set of maintenance actions performed over the service life of a concrete bridge deck. After discussions with multiple INDOT personnel, we have created a baseline estimate for this. This baseline is reflected in the cost intervention vector by following the typical pattern of no intervention actions while the bridge experiences CR 9, followed by the first thin deck overlay application while the bridge experiences CR 8, followed by a second thin deck overlay application while the bridge experiences a CR 7, and finally one rigid deck overlay application while the bridge experiences CR 6. However, one cannot simply assign the cost of the maintenance action to the CR value in the vector. At each time, one must sum the cost of all interventions performed at previous CR values and add it to the current CR value cost to reflect the accumulation of intervention actions in a deck's life and thus a lifecycle cost of maintenance actions for a bridge deck over its service life.

The C_R value is approached in a similar manner. The estimated cost for deck replacement found in the table provided to us by INDOT, is multiplied by the deck square footage, yielding the replacement cost, which is then added to the total intervention cost reflected in CR2. Previous intervention costs must be included because, before the bridge deck is replaced, multiple intervention actions have been performed over its lifetime. Including the price of those intervention actions in the replacement cost reflects this assumption. The computed total cost values can be found in Table 5.1, along with the calculated difference in those costs. All cost values are shown in present day dollars. A positive difference in the last column of Table 5.1 indicates the additional cost that could be assigned to the defects during construction.

For a graphical representation of the application of the cost calculation, see Figure 5.1 where case study bridge #11980 (second from the top in Table 5.1) is used as an example. Here, solid lines represent the standard construction case, and dashed lines represent the substandard construction case. Two red lines are associated with the expected value of the intervention costs, C_I, two blue lines are associated with the expected value of the replacement cost, C_R, and two pink lines correspond to the total cost, C_T. Lastly, the horizontal black lines are included for a visual illustration of the two total cost values used in the comparison. Please note that not all lines may be visible in a given bridge's cost curve graph because in some cases the calculated cost of replacement is near zero for a large portion of the timeline (the bridge does not reach CR1 until later). However, we are using the year determined for INDOT practice replacement, which is halfway between CR5 and CR4, causing the C_R curve to lie on the x-axis. In this case, the intervention cost and total cost are identical (and overlapping) for some time. Also take note of the possibility for the C_I curve to decrease after some time. This is because the probability of the bridge being in one of the CRs assigned to an intervention action decreases, and the probability of the bridge being in the CR assigned to the replacement action increases. The reduction in intervention cost reflects this logical progression.

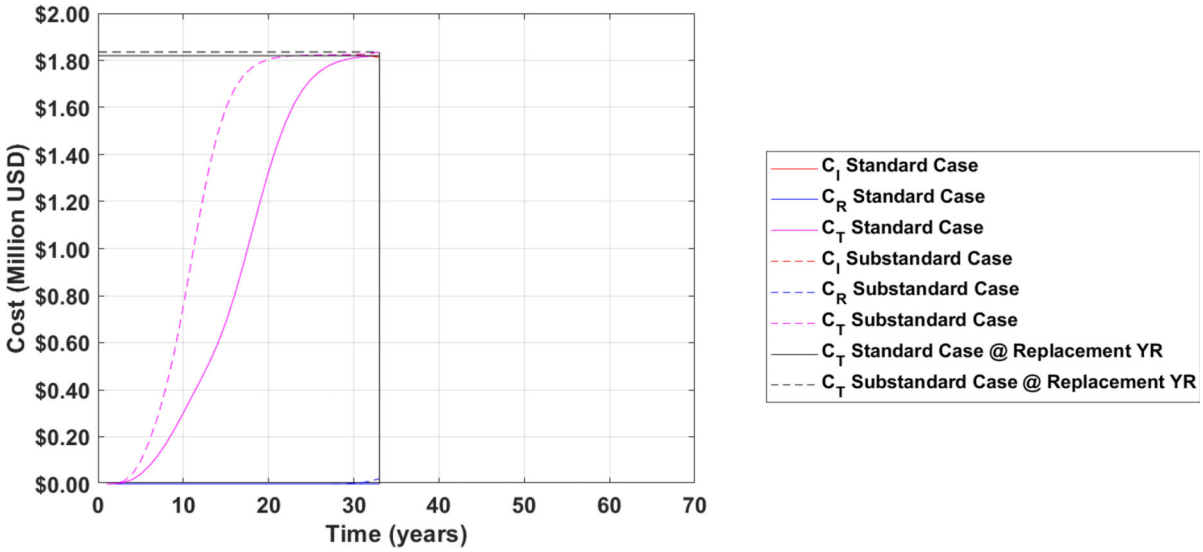

Figure 5.1 Present day cost curves for case study bridge #11980.

6. CLOSING REMARKS

A proposed implementation plan is presented in Section 6.1. The plan is supported by the final recommendations from the study in Section 6.2.

6.1 Implementation

Based on the findings of this study, the following plan is suggested for implementation.

- Clarify and improve standards for handling of epoxy-coated bars.
- Evaluate procedures for inspection during construction and examine lessons learned and possible improvements based on that experience (Section 6.2.3).
- Enhance the robustness of the approach presented; additional data could be collected as described in Sections 6.2.1 and 6.2.2.
- Implement the approach developed in this study and monitor a broader sample of bridges in the state to refine estimated costs.

6.1.1 Introduction to Additional Cost Estimation Tool

A computational tool to make an approximation of the estimated additional cost associated with substandard construction of a concrete bridge deck was developed. *Such a tool is aimed to serve as an estimation instrument and by no means replaces a comprehensive evaluation of the hazards or a formal economic analysis.*

The following assumptions were considered for its programming.

1. Indiana was divided into three regions: south, center and north (see Section A3.1).
2. The standard construction cases used for comparison are those following *Indiana Department of Transportation Standard Specifications 2020* (INDOT, 2020b) (see Table 2.2).
3. The maximum number of simultaneous defects that can be considered is two.
4. The severity of each defect is taken as the worst possible scenario (see Subsection 2.1.7).
5. The values used to determine hazard group options are up-to-date at the time the tool is being used. These values are selected by the user; the user must ensure the information is up-to-date.
6. The price per square foot estimations is up to date at the time the tool is developed. These values are input by the user; the user must ensure the information is up-to-date at the time of use.

Table 6.1 shows a summary of how each defect was modelled inside the tool (for more details, see Section 2). The last column shows possible additional uses or situations in which each defect option can be selected within the tool. *Please notice that the formulation of the physics-based model (Section 2) was not specifically developed for these additional uses or situations. Thus, the results coming from the tool for these cases should be taken as a rough approximation.*

In addition to cost assessment, the provided tool can serve as an educational and training resource to show inspectors and asset managers how defective construction practices impact the long-term cost of the bridge deck. This will motivate inspectors to enforce construction stage specifications on the contractors. Moreover, an awareness of the lifelong performance and cost impact of a defect will improve the quality of the reports made during construction. Finally, the tool can be used as a rationale to change the epoxy-coated rebar-handling policies and the rebar-placing signaling on the construction site.

6.2 Final Recommendations

During the refinement of the models, our research team identified missing data that would have improved the accuracy of the process. In this section,

TABLE 6.1
Summary of defect modelling and additional uses for the additional cost estimation tool

Defect	Modelling	Subsection	Uses/Situations
Improper Curing	It was assumed that the primary consequence of improper curing was shrinkage. Hence, to account for this defect an early cracking of the deck was simulated by modifying the diffusion coefficient.	2.1.7.1	In addition to improper curing, this option may be appropriate to evaluate the performance of decks with early cracking of unknown origin.
Insufficient Concrete Cover	The concrete layer above the upper rebar was shortened in the model.	2.1.7.2	In addition to insufficient concrete cover, this option may be used for decks already showing some degree of wearing or spalling.
Water/Cement Ratio	The diffusion coefficient of the concrete deck was set to be greater if it has a higher w/c ratio (see Table 2.5).	2.1.7.3	In addition to an excessive water/cement ratio, this option can be used for decks with segregation issues.

a summary of the outcomes from the model analyses is presented. Some suggestions about data that could be collected to improve the modeling of the related phenomena are given and, when available, possible methods to gather such data. These recommendations are presented in Section 6.2.1 to improve the physics-based model, and in Section 6.2.3 for the data driven model. Section 6.2.3 provides a compilation of recommendations from the INDOT personnel that interacted with the research team over the course of this study. These recommendations represent the first-hand experience from experienced INDOT personnel and add great value to the findings and recommendations from the research team.

6.2.1 Recommendations for Data Relevant to the Physics-Based Model

The following are two categories of information related to the physics-based model: (1) parameters, that is, variables and constants that help to describe, for example, environmental processes or deterioration mechanisms; and (2) inputs and outputs, that is, histories of data generated by the proposed model. The items in category (1) are usually static scalars that, treated deterministically, do not change throughout the simulation; or random variables with a given distribution that vary for each realization (or run) if treated stochastically. The items in category (2) are streams of data with a value at each time step.

6.2.1.1 Parameters. Some recommendations to improve the accuracy of the parameters used in the physics-based model are summarized in Table 6.2. These recommendations are mainly focused on data-collection suggestions.

6.2.1.2 Inputs and outputs. The following are three main outcomes from the physics-based model that serve as indicators of the performance of the deck.

1. Chloride concentration at rebar level, C, in *lb/cuy* or kg/m^3.
2. Rebar loss due to corrosion, ϕ, in *in* or *mm*.
3. Crack width due to factors other than corrosion, ω, in *in* or *mm*.

At the beginning of each simulation, the three indicators listed above are computed for a deterministic run and matched with the CR evolution of a bridge deck with standard construction (see Table 6.3). The substandard cases are then evaluated based on the mapping generated by the standard case. The transition times between each CR and the next one was obtained based on the expertise of INDOT asset managers and bridge inspectors.

Histories of the three outcomes listed above would have been helpful to calibrate the model, i.e., to adjust the numerical simulation results to be as close as possible to the measured results from the bridges in the state of Indiana. Although some chloride profile histories were provided, the number of sampled bridges (8, see Table A.3.2) was too low to produce a significant average value and the timespan of the sampling was too short to get a clear tendency in the results. In the case of the crack width and corrosion rate histories, the information was either nonexistent or difficult to obtain. Unfortunately, crack widths from the visual inspections are not accurate enough as they are seldom accompanied by quantitative measurements.

6.2.2 Recommendations for Data Relevant to the Data-Driven Model

One of the main obstacles of a data-driven model is unreliable data. Data can be unreliable for a number of reasons including the standards for collection, the rates of collection, and the quality and quantity of the data collected. The current method of data collection used by INDOT is based on the 1–9 CR scale. This approach is not precise and leads to subjective decision-making in the final assigned CR. There is also limited guidance for the type, quality, or quantity of data collected during these routine inspections, further leading to the subjective nature of the results. Changes to the inspection process would aid to improve results from

TABLE 6.2
Recommended actions for improving parameter accuracy

Parameter	Recommendation
CO_2 Concentration in Ambient Air	While all the other environmental parameters were easily obtained via the NBI (FHWA, 2023), there were no data available for this parameter in the state of Indiana. The nearest location with known information was used instead (Homer, Illinois; NOAA, 2023). Given its importance in the modeling and quantifying the carbonation process of concrete decks, it is strongly recommended to include a source of information for this parameter in the bridge inventory database.
Average Surface Chloride Concentration	This parameter serves as a boundary condition for the physics-based model. Given its high impact in the model's outcomes, a reliable estimate of this quantity is desirable. In the absence of it, the procedure described in Section 2.1.1 was adopted.
Deicing Salts Chloride Concentration	A more refined model would take the deicing salts application rate or amount and transform it in surface chloride concentration. Although our team was able to obtain some registers for this information, it could be significantly improved.
Chloride Diffusion Coefficient Values	This constant governs the penetration of the chlorides through the concrete during the simulations. The accuracy of the model could be improved if samples of this magnitude for different decks at different times were available. The values used in this project were obtained from the literature (see Section 2.1.1 for details).
Corrosion Rate	As in the case of the chloride diffusion coefficient, samples of the corrosion rate for the decks of the state of Indiana would have been helpful to increase the fidelity of the physics-based model. The value used for this report was obtained from the literature (see Section 2.1.1 for details).

TABLE 6.3
Mapping from the indicators of the physics-based model to the corresponding change in CR number

CR Change	$C(t)$ (lb/yd^3)	$\omega(t)$ $(in.)$	$\Phi(t)$ $(in.)$
9 to 8	0.08	0.010	0.000
8 to 7	1.39	0.025	0.007
7 to 6	2.86	0.044	0.029
6 to 5	3.32	0.058	0.048
5 to 4	3.35	0.073	0.068
4 to 3	3.35	0.088	0.099

inspections, and eventually led to more effective asset management and more refined data-driven models. However, to improve the data-driven models for future use at least 20 years, based on the research conducted in this study, of data are required. Thus, it is recommended to implement changes to the bridge inspection process as follows.

- The current routine bridge inspection procedure requires only two photos of the bridge be taken and documented per inspection. These photos seldom provide tangible information to document the condition of the bridge or instances of deterioration. Hence, we recommend INDOT consider, for the purposes of improving the deck modeling, covering the entire surface using high-definition digital images to allow zooming on critical areas. We also recommend INDOT consider providing a simple sketch of the bridge to mark in what order the photos were taken and in what location in relation to the bridge, to ensure an accurate documentation of deterioration progression over time and ensure the correct assignment of CRs.
- For data-driven models to be beneficial, the data used in the creation of the model must be as accurate as is practically feasible. It may be the case that some data item values reported based on the requirements of the FHWA's *Recording and Coding Guide* may not be accurately updated with each submission. This oversight can influence model development and application if the values of data items like average daily traffic and average daily truck traffic, for example, are not accurately updated in each submission. We recommend ensuring all data values are up to date in the submission of at least every routine bridge inspection.
- Training of the bridge inspectors of course benefits data collection procedures as it prepares all bridge inspectors to perform high quality inspections. However, during the interviews with INDOT personnel, it was also emphasized the importance of providing the inspectors with adequate tools and training on the use of the tools in the inspection.
- Stay-in-place metal forms present an obstacle to the routine bridge inspection process because they obstruct line-of-sight to the underside of the concrete bridge deck. Being able to see and accurately assess the condition of the bridge deck from underneath the bridge is vital to the management of the bridge deck during its life. Therefore, we recommend the use of either (1) removable deck forms, or (2) clear stay-in-place forms when building a bridge deck.
- Develop and refine language to aid bridge inspectors in understanding both the differences and similarities between abrasion and wearing on a bridge deck, and how to evaluate the presence of each on a wearing surface versus a deck. This clarification will allow for better distinction between wearing surface and deck in the assigned CRs, as well as keeping bridge asset managers up to date on the abrasion and wearing patterns present on their bridges.

6.2.3 Recommendations Based on Input from INDOT

Throughout the study, the team met with INDOT personnel from various departments to better understand the processes involved in the construction,

inspection, and management of concrete bridge decks under INDOT ownership. During this knowledge gathering process, INDOT personnel shared with the research team their concerns and suggestions for improvement in relation to each of their respective job duties. Those concerns and suggestions for improvement are summarized below, in order of priority assigned by the interviewees.

- Include the respective INDOT district Bridge Asset Engineers/Managers in the final bridge inspection for determination of acceptance of a newly constructed bridge by INDOT.
- Adapt INDOT business rules to allow for changing preventative maintenance practices, without these business rules being the sole policy hindering the life expectancy of a bridge component. In other words, adapt the preventative maintenance business rules so that they are not the sole indicator of replacement of a component if the component's condition does not point to the same decision.
- Consider expanding the material testing specification to include taking additional concrete samples from the beginning of the batch prior to concrete placement to test for minimum quality requirements before a significant portion of the concrete is poured.
- Incorporate the use of alternatives to deicing salt that mitigate corrosion.
- Determine a more appropriate way to adequately code data item categories from the FHWA *Recording and Coding Guide* when new data item options are present for INDOT. An example would be making silica fume overlays their own category, rather than placing them in the "other" category or an improperly labeled category. This addition allows for proper data analysis on the performance of said data item in the future.
- Assign an inspector to perform inspections of the INDOT in-house maintenance department's work, ensuring all maintenance actions are following craftsmanship quality standards and material standards.
- Incorporate more specific and clearer epoxy-coated rebar handling instructions. An example of more clear storage instruction may include "Coated bars or bundles shall be stored above the ground on wooden or padded supports with timbers placed between bundles when stacking is necessary. Space the supports sufficiently to prevent sags in the bundles" (ASTM D3963). An example of more clear handling instructions may include "All systems for handling coated steel reinforcing bars shall have padded contact areas…. All bundles of coated steel reinforcing bars shall be lifted with a strong back, spreader bar, multiple supports, or a platform bridge to prevent bar-to-bar abrasion from sags in the bundles of coated steel reinforcing bars" (ASTM 775).

REFERENCES

AASHTO. (2017). *AASHTO LRFD bridge design specifications* (8th ed.). American Association of State Highway and Transportation Officials.

ACI Committee 308. (2016). *Guide to external curing of concrete* (ACI 308-16). American Concrete Institute.

ACI Committee 318. (2016). *Building code requirements for structural concrete and commentary* (ACI 318-16/ACI 318R-16). American Concrete Institute.

ACI Committee 318. (2022). *Building code requirements for structural concrete and commentary* (ACI 318R-95/ACI 318-95). American Concrete Institute.

ACI Committee 365. (2017). *Report on service life prediction* (ACI 365.1R-17). American Concrete Institute.

Barrett, T. J., Miller, A. E., & Weiss, W. J. (2015). *Documentation of the INDOT experience and construction of the bridge decks containing internal curing in 2013* (Joint Transportation Research Program No. FHWA/IN/JTRP-2015/10). West Lafayette, IN: Purdue University. https://doi.org/10.5703/1288284315532

Cavalline, T. L., Whelan, M. J., Tempest, B. Q., Goyal, R., & Ramsey, J. D. (2015). *Determination of bridge deterioration models and bridge user costs for the NCDOT bridge management system* (Report No. FHWA/NC/2014-07). North Carolina Department of Transportation.

Chen, D., & Mahadevan, S. (2008, March). Chloride-induced reinforcement corrosion and concrete cracking simulation. *Cement and Concrete Composites*, *30*(3), 227–238. https://doi.org/10.1016/j.cemconcomp.2006.10.007

Chen, X., Yu, A., Liu, G., Chen, P., & Liang, Q. (2020). A multi-phase mesoscopic simulation model for the diffusion of chloride in concrete under freeze–thaw cycles. *Construction and Building Materials*, *265*, 120223. https://doi.org/10.1016/j.conbuildmat.2020.120223

Claisse, P. A. (2020). *Transport properties of concrete: Modelling the durability of structures*. Woodhead Publishing.

Cox, D. R. (1972). Regression models and life-tables. *Journal of the Royal Statistical Society: Series B (Methodological)*, *34*(2), 187–202.

Enright, M. P., & Frangopol, D. M. (1998). Probabilistic analysis of resistance degradation of reinforced concrete bridge beams under corrosion. *Engineering Structures*, *20*(11), 960–971.

Faber, M. H. (2000). Reliability based assessment of existing structures. *Progress in Structural Engineering and Materials*, *2*(2), 247–253.

FHWA. (1995, December). *Recording and coding guide for the structure inventory and appraisal of the nation's bridges* (Report No. FHWA-PD-96-001). Federal Highway Administration. https://www.fhwa.dot.gov/bridge/mtguide.pdf

FHWA. (2012, February). *Bridge inspector's reference manual* (Publication No. FHWA NHI 12-049). Federal Highway Administration. https://www.dot.state.mn.us/bridge/pdf/insp/birm/birmchapt0-cover.pdf

FHWA. (2019). *Bridge component condition forecast—Base models*. Federal Highway Administration. Retrieved March 18, 2020, from https://www.fhwa.dot.gov/bridge/nbi.cfm

FHWA. (2023, January 23). *National bridge inventory (NBI)*. Federal Highway Administration. Retrieved April 10, 2022, from https://www.fhwa.dot.gov/Data/SelectedBridges

Glass, G. K., & Buenfeld, N. R. (2000). Chloride-induced corrosion of steel in concrete. *Progress in Structural Engineering and Materials*, *2*(4), 448–458.

Goyal, R. (2015). *Development of a survival based framework for bridge deterioration modeling with large-scale application to the North Carolina bridge management system* [Doctoral dissertation, University of North Carolina at Charlotte].

Holland, T. (1998, December 1). Chloride limits in the ACI 318 building code requirements. *Concrete Construction*. https://www.concreteconstruction.net/business/producers/chloride-limits-in-the-aci-318-building-code-requirements_o

INDOT. (2013). *Indiana design manual*. Indiana Department of Transportation. Retrieved October 28, 2021, from https://www.in.gov/indot/design-manual/

INDOT. (2020a). *Bridge inspection manual*. Indiana Department of Transportation. Retrieved October 28, 2021, from https://www.in.gov/dot/div/contracts/standards/bridge_inspection/inspector_manual/index.htm

INDOT. (2020b). *Indiana Department of Transportation standard specifications 2020*. Indiana Department of Transportation. Retrieved October 28, 2021, from https://www.in.gov/dot/div/contracts/standards/book/sep19/sep.htm

Ji, Y., McCullouch, B., & Zhou, Z. (2020). *Evaluation of anti-icing/de-icing products under controlled environmental conditions* (Joint Transportation Research Program Publication No. FHWA/IN/JTRP-2020/22). West Lafayette, IN: Purdue University. https://doi.org/10.5703/1288284317253

Jiang, W.-Q., Shen, X.-H., Xia, J., Mao, L.-X., Yang, J., & Liu, Q.-F. (2018). A numerical study on chloride diffusion in freeze-thaw affected concrete. *Construction and Building Materials*, *179*, 553–565.

Jiang, Y., Saito, M., & Sinha, K. C. (1988). Bridge performance prediction model using the Markov chain. *Transportation Research Record*, *1180*, 25–32.

Jin, W. L., Yan, Y. D., & Wang, H. L. (2010). Chloride diffusion in the cracked concrete. *Fracture mechanics of concrete and concrete structures-assessment, durability, monitoring and retrofitting of concrete structures* (pp. 880–886).

Kassir, M. K., & Ghosn, M. (2002). Chloride-induced corrosion of reinforced concrete bridge decks. *Cement and Concrete Research*, *32*(1), 139–143. https://doi.org/10.1016/s0008-8846(01)00644-5

Kim, S., Frangopol, D. M., & Soliman, M. (2013). Generalized probabilistic framework for optimum inspection and maintenance planning. *Journal of Structural Engineering*, *139*(3), 435–447.

Kim, Y.-Y., Lee, K.-M., Bang, J.-W., & Kwon, S.-J. (2014). Effect of W/C ratio on durability and porosity in cement mortar with constant cement amount. *Advances in Materials Science and Engineering*, 1–11. https://doi.org/10.1155/2014/273460

Kleinbaum, D. G., & Klein, M. (2012). *Survival analysis: A self-learning text* (3rd ed.). Springer.

Kleiner, Y. (2001). Scheduling inspection and renewal of large infrastructure assets. *Journal of Infrastructure Systems*, *7*(4), 136–143.

Leiva Maldonado, S. L., & Bowman, M. D. (2019). *Life-cycle cost analysis for short- and medium-span bridges* (Joint Transportation Research Program Publication No. FHWA/IN/JTRP-2019/09). West Lafayette, IN: Purdue University. https://doi.org/10.5703/1288284316919

Li, D., Wei, R., Li, L., Xiaotao, G., & Xuming, M. (2019). Pitting corrosion of reinforcing steel bars in chloride contaminated concrete. *Construction and Building Materials*, *199*, 359–368.

Liu, H., & Yunfeng, Z. (2020). Bridge condition rating data modeling using deep learning algorithm. *Structure and Infrastructure Engineering*, *16*(10), 1447–1460.

Mangat, P. S., & Molloy, B. T. (1994). Prediction of long term chloride concentration in concrete. *Materials and Structures*, *27*(6), 338–346.

Martín-Pérez, B., Zibara, H., Hooton, R. D., & Thomas, M. D. A. (2000). A study of the effect of chloride binding on service life predictions. *Cement and Concrete Research*, *30*(8), 1215–1223. https://doi.org/10.1016/s0008-8846(00)00339-2

McCullouch, B. (2010). *Snow and ice removal and anti-icing synthesis study* (Joint Transportation Research Program Publication No. FHWA/IN/JTRP-2010/18). West Lafayette, IN: Purdue University.

Morcous, G., Lounis, Z., & Cho, Y. (2010). An integrated system for bridge management using probabilistic and mechanistic deterioration models: Application to bridge decks. *KSCE Journal of Civil Engineering*, *14*, 527–537. https://doi.org/10.1007/s12205-010-0527-4

NOAA. (2023, June 10). *GML data finder* [Webpage]. Earth System Research Laboratories Global Monitoring Laboratory. Retrieved April 10, 2022, from https://gml.noaa.gov/dv/data/index.php

Olek, J., & Liu, R. (2001). *Development and evaluation of cement-based materials for repair of corrosion-damaged reinforced concrete slabs* (Joint Transportation Research Program Publication No. FHWA/IN/JTRP-2000/10). West Lafayette, IN: Purdue University.

O'Reilly, M., Darwin, D., Browning, J. P., & Locke, C. E., Jr. (2011, January). *Evaluation of multiple corrosion protection systems for reinforced concrete bridge decks* (SM Report No. 100). University of Kansas Center for Research.

Purdue University. (n.d.). *Freeze-thaw events in Indianapolis: Indianapolis International Airport (KIND)* [Webpage]. Indiana State Climate Office. Retrieved May 18, 2022, from https://ag.purdue.edu/indiana-state-climate/tools/miscellaneous-climate-tools/freeze-thaw-events-in-indianapolis/

Ryan, T. W., Mann, J. E., Chill, Z. M., & Ott, B. T. (2012, February). *Bridge inspector's reference manual* (Publication No. FHWA NHI 12-049). Federal Highway Administration. https://www.dot.state.mn.us/bridge/pdf/insp/birm/birmchapt0-cover.pdf

Sajedi, S., & Huang, Q. (2019). Reliability-based life-cycle-cost comparison of different corrosion management strategies. *Engineering Structures*, *186*, 52–63.

Samples, L. M., & Ramirez, J. A. (2000a, February). Field investigation of concrete bridge decks in Indiana- Part 1: New construction and initial field investigation of existing bridge decks. *Concrete International*, *22*(2), 53–56. American Concrete Institute.

Samples, L. M., & Ramirez, J. A. (2000b, March). Field investigation of concrete bridge decks in Indiana: Part 2: Detailed investigation of existing decks. *Concrete International*, *22*(3), 59–63. American Concrete Institute.

Stewart, M. G., Xiaoming, W., & Nguyen, M. N. (2011). Climate change impact and risks of concrete infrastructure deterioration. *Engineering Structures*, *33*(4), 1326–1337.

Takiya, H., Naoko, W., Tamotsu, K., & Seichi, S. (2014). Effects of water-to-cement ratio and temperature on diffusion of water in hardened cement pastes. *Journal of Nuclear Science and Technology*, *52*(5), 728–738. https://doi.org/10.1080/00223131.2014.979902

Thomas, O., & Sobanjo, J. (2013). Comparison of Markov chain and semi-Markov models for crack deterioration on flexible pavements. *Journal of Infrastructure Systems*, *19*(2), 186–195.

Ueda, T., Hasan, M., Nagai, K., Sato, Y., & Wang, L. (2009). Mesoscale simulation of influence of frost damage on mechanical properties of concrete. *Journal of Materials in Civil Engineering*, *21*(6), 244–252.

Vu, K. A. T., & Stewart, M. G. (2000). Structural reliability of concrete bridges including improved chloride-induced corrosion models. *Structural Safety*, *22*(4), 313–333.

Wang, J., Ng, P.-L., Su, H., & Du, J. (2019). Meso-scale modelling of stress effect on chloride diffusion in concrete using three-phase composite sphere model. *Materials and Structures*, *52*(55), 1–23.

Wang, X.–Y., & Zhang, L.-N. (2016). Simulation of chloride diffusion in cracked concrete with different crack patterns. *Advances in Materials Science and Engineering*. https://doi.org/10.1155/2016/1075452

Weather Atlas. (n.d.). *Climate and monthly weather forecast South Bend, IN* [Webpage]. Weather U.S. Retrieved October 28, 2021, from https://www.weather-us.com/en/indiana-usa/south-bend-climate

Weather Underground. (2021). *South Bend, IN weather history*. IBM. Retrieved October 28, 2021, from https://www.wunderground.com/history/daily/KSBN/date/2021-10-25

Wiss, J. (2005). *Service life extension of northern bridge decks containing epoxy-coated reinforcing bars* (Research Series No. 12). Concrete Reinforcing Steel Institute.

Xu, J., & Li, F. (2017). A meso-scale model for analyzing the chloride diffusion of concrete subjected to external stress. *Construction and Building Materials*, *130*, 11–21.

Zambon, I., Vidović, A., Strauss, A., & Matos, J. (2019). Condition prediction of existing concrete bridges as a combination of visual inspection and analytical models of deterioration. *Applied Sciences*, *9*(1), 148. https://doi.org/10.3390/app9010148

Zhang, M., Ye, G., & van Breugel, K. (2014). Multiscale lattice Boltzmann-finite element modelling of chloride diffusivity in cementitious materials. Part II: Simulation results and validation. *Mechanics Research Communications*, *58*, 64–72.

Zhu, H., Huo, Q., Fan, J., Pang, S., Chen, H., & Yi, C. (2020). The depth–width correlation for shrinkage-induced cracks and its influence on chloride diffusion into concrete. *Materials*, *13*(12), 2751. https://doi.org/10.3390/ma13122751

APPENDIX

Appendix A. Detailed Results for the Case Study Bridges

APPENDIX A. DETAILED RESULTS FOR THE CASE STUDY BRIDGES

A.1 Case Study Catalog

NBI number:	4081	**Year built:**	2017
Asset name:	015-43-10215	**Current deck CR:**	9

Nominal case criteria:

Cast-in-place, concrete deck:	☑
No overlay/membrane:	☑
Epoxy-coated rebars:	☑
Monolithic concrete wearing surface:	☑
Continuous span	☑
Deck concrete class C	☑

Bridge's picture

Location:	41.28917	-85.85689
	Latitude	*Longitude*

ADTT:	2888	**Number of spans:**	3
Wearing surface:	Monolithic concrete	**Max span length (m):**	13
Functional class:	Non-Interstate		

	Available	Not available
Structural drawings:	☑	☐
Condition reports:	☑	☐

	Steel	Concrete	Prestressed
Type of superstructure:	☐	☐	☑

Defects identified either during construction or via regular inspections:

A few transverse hairline cracks across Bents 1& 2 (CS2-129sft); map cracking in North Bound lane at South end (CS2-72sft); hairline short longitudinal cracks at both ends of deck (CS2-202sft); Concrete barrier walls; (under metal railing); hairline cracking under each post; stay-in-place (SIP's); Good condition; missing downspout in Span A SW corner.

NBI number:	11980	**Year built:**	1973
Asset name:	037-47-05934	**Current deck CR:**	6

Nominal case criteria:

Cast-in-place, concrete deck:	☑
No overlay/membrane:	☑
Epoxy-coated rebars:	☑
Monolithic concrete wearing surface:	☑
Continuous span	☑
Deck concrete class C	☑

Bridge's picture

Location:	38.88164	-86.52092
	Latitude	*Longitude*

ADTT:	547	**Number of spans:**	3	
Wearing surface:	Latex Concrete	**Max span length (m):**	29	
Functional class:	Non-Interstate			

	Available	Not available
Structural drawings:	☑	☐
Condition reports:	☑	☐

	Steel	Concrete	Prestressed
Type of superstructure:	☑	☐	☐

Defects identified either during construction or via regular inspections:

Topside exhibited longitudinal and transverse map cracking up to approximately 0.020" nominal width visible throughout topside of deck. Underside SIP metal forms exhibited no visible deterioration or moisture staining.

NBI number:	15651	**Year built:**	2018
Asset name:	041-45-02808	**Current deck CR:**	5

Nominal case criteria:

Cast-in-place, concrete deck:	☑
No overlay/membrane:	☑
Epoxy-coated rebars:	☑
Monolithic concrete wearing surface:	☑
Continuous span	☑
Deck concrete class C	☑

Bridge's picture

Location:	41.53165	-87.47118
	Latitude	*Longitude*

ADTT:	1928	**Number of spans:**	3	
Wearing surface:	None	**Max span length (m):**	20	
Functional class:	Non-Interstate			

	Available	Not available
Structural drawings:	☑	☐
Condition reports:	☑	☐

	Steel	Concrete	Prestressed
Type of superstructure:	☐	☑	☐

Defects identified either during construction or via regular inspections:

Moderate width cracking throughout the deck, signs of water leaking through the deck and staining the slope walls underneath. Efflorescence forming on the bottom of the deck. There are several large and small coring holes in all four lanes. throughout the deck. Several of the cracks run through the lane, bridge walls and sidewalks. Per the BAE water runs through the cracks in a rain event.

NBI number:	18911	**Year built:**	2018
Asset name:	051-45-09797 SBL	**Current deck CR:**	8

Nominal case criteria:

Cast-in-place, concrete deck:	☑
No overlay/membrane:	☑
Epoxy-coated rebars:	☑
Monolithic concrete wearing surface:	☑
Continuous span	☑
Deck concrete class C	☑

Bridge's picture

Location:	41.58724	-87.24044
	Latitude	*Longitude*

ADTT:	1854	**Number of spans:**	3	
Wearing surface:	Monolithic concrete	**Max span length (m):**	23	
Functional class:	Non-Interstate			

	Available	Not available
Structural drawings:	☑	☐
Condition reports:	☑	☐

	Steel	Concrete	Prestressed
Type of superstructure:	☑	☐	☐

Defects identified either during construction or via regular inspections:

There is hair line transverse cracking in the wearing surface.

NBI number:	19571	**Year built:**	2013
Asset name:	054-77-08692	**Current deck CR:**	7

Nominal case criteria:

Cast-in-place, concrete deck:	☑
No overlay/membrane:	☑
Epoxy-coated rebars:	☑
Monolithic concrete wearing surface:	☑
Continuous span	☑
Deck concrete class C	☑

Bridge's picture

Location:	39.07571	-87.3866
	Latitude	*Longitude*

ADTT:	218	**Number of spans:**	3
Wearing surface:	Monolithic concrete	**Max span length (m):**	15
Functional class:	Non-Interstate		

	Available	Not available
Structural drawings:	☑	☐
Condition reports:	☑	☐

	Steel	Concrete	Prestressed
Type of superstructure:	☐	☑	☐

Defects identified either during construction or via regular inspections:

Deck coping fascias at both piers exhibited full depth vertical to slightly diagonal cracks with efflorescence.

NBI number:	33440	**Year built:**	1966
Asset name:	I64-18-05205 BEBL	**Current deck CR:**	6

Nominal case criteria:

Cast-in-place, concrete deck:	☑
No overlay/membrane:	☑
Epoxy-coated rebars:	☑
Monolithic concrete wearing surface:	☑
Continuous span	☑
Deck concrete class C	☑

Bridge's picture

Location:	38.16686	-87.66206
	Latitude	*Longitude*

ADTT:	532	**Number of spans:**	3	
Wearing surface:	Latex Concrete	**Max span length (m):**	16	
Functional class:	Interstate			

	Available	Not available
Structural drawings:	☑	☐
Condition reports:	☑	☐

	Steel	Concrete	Prestressed
Type of superstructure:	☐	☐	☑

Defects identified either during construction or via regular inspections:

The deck underside is not visible due to the placement of SIP metal forms; There is rust and deterioration of a form in Span B and C right below a cores drilled in the deck approximately 2 SFT each. Deck rating based on surface condition on the forms and on transverse cracking observed at coping areas.

NBI number:	36033	**Year built:**	2017
Asset name:	I65-106-10142 NBL	**Current deck CR:**	8

Nominal case criteria:

Cast-in-place, concrete deck:	☑
No overlay/membrane:	☑
Epoxy-coated rebars:	☑
Monolithic concrete wearing surface:	☑
Continuous span	☑
Deck concrete class C	☑

Bridge's picture

Location:	39.70355	-86.10815
	Latitude	*Longitude*

ADTT:	11153	**Number of spans:**	3	
Wearing surface:	Monolithic concrete	**Max span length (m):**	45	
Functional class:	Interstate			

	Available	Not available
Structural drawings:	☑	☐
Condition reports:	☑	☐

	Steel	Concrete	Prestressed
Type of superstructure:	☑	☐	☐

Defects identified either during construction or via regular inspections:

SIP forms

NBI number:	44080	**Year built:**	1964
Asset name:	33-04944 FWBL	**Current deck CR:**	8

Nominal case criteria:

Cast-in-place, concrete deck:	☑
No overlay/membrane:	☑
Epoxy-coated rebars:	☑
Monolithic concrete wearing surface:	☑
Continuous span	☑
Deck concrete class C	☑

Bridge's picture

Location:	40.07973	-86.90422
	Latitude	*Longitude*

ADTT:	2074	**Number of spans:**	4	
Wearing surface:	Latex Concrete	**Max span length (m):**	13	
Functional class:	Interstate			

	Available	Not available
Structural drawings:	☑	☐
Condition reports:	☑	☐

	Steel	Concrete	Prestressed
Type of superstructure:	☐	☑	☐

Defects identified either during construction or via regular inspections:

Bridge was opened to traffic fall of 2019, no obvious concerns were noted for the 2020 inspection.

NBI number:	50521	**Year built:**	2020
Asset name:	I465-132-09971	**Current deck CR:**	9

Nominal case criteria:

Cast-in-place, concrete deck:	☑
No overlay/membrane:	☑
Epoxy-coated rebars:	☑
Monolithic concrete wearing surface:	☑
Continuous span	☑
Deck concrete class C	☑

Bridge's picture

Location:	39.92452	-86.18406
	Latitude	*Longitude*

ADTT:	127	**Number of spans:**	2	
Wearing surface:	Monolithic concrete	**Max span length (m):**	34	
Functional class:	Non-Interstate			

	Available	Not available
Structural drawings:	☑	☐
Condition reports:	☑	☐

	Steel	Concrete	Prestressed
Type of superstructure:	☐	☐	☑

Defects identified either during construction or via regular inspections:

Deck (underside): no corrosion to metal forms.

NBI number:	79848	**Year built:**	2014
Asset name:	031-71-08944	**Current deck CR:**	5

Nominal case criteria:

Cast-in-place, concrete deck:	☑
No overlay/membrane:	☑
Epoxy-coated rebars:	☑
Monolithic concrete wearing surface:	☑
Continuous span	☑
Deck concrete class C	☑

Bridge's picture

Location:	41.60839	-86.25681
	Latitude	*Longitude*

ADTT:	2026	**Number of spans:**	3
Wearing surface:	Monolithic concrete	**Max span length (m):**	58
Functional class:	Non-Interstate		

	Available	Not available
Structural drawings:	☑	☐
Condition reports:	☑	☐

	Steel	Concrete	Prestressed
Type of superstructure:	☑	☐	☐

Defects identified either during construction or via regular inspections:

Barrier Walls: widely-to-moderately spaced, hairline vertical cracks {CS2, 50%}; Top: see Wearing Surface; Underside: galvanized steel stay-in-place deck forms (SIPs); widely-spaced transverse cracks with light efflorescence visible on copings (moderate-spacing at supports); light rust and galvanic reaction at several places on SIPs (likely due to rusty or damaged scr1ews); some efflorescence on closure angles (of SIPs) in SE corner and at Pier2 (NB); Several transverse cracks visible under the deck at the center seam with efflorescent.

A.2 Performance Results for Case Study Bridges

Bridge NBI#:	4081	**Estimated Loss of Life:**	N/A
Region:	North	**Estimated Additional Cost:**	N/A
Defect Classification:	None		

Defect Notes:

"(…) hairline short longitudinal cracks at both ends of deck (…) Good condition."

Hazard Ratios:

CR4	CR5	CR6	CR7	CR8	CR9
1.6830	1.2927	1.0233	1.4203	1.1172	0.7884

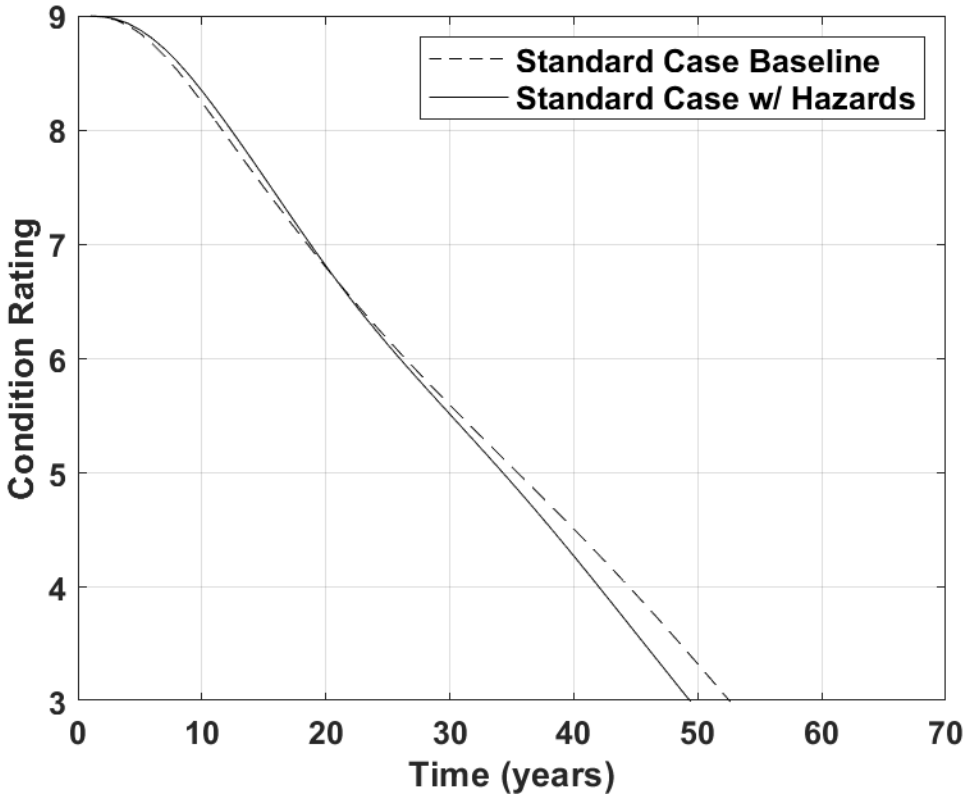

Figure A.1 Degradation curve for case study bridge #4081.

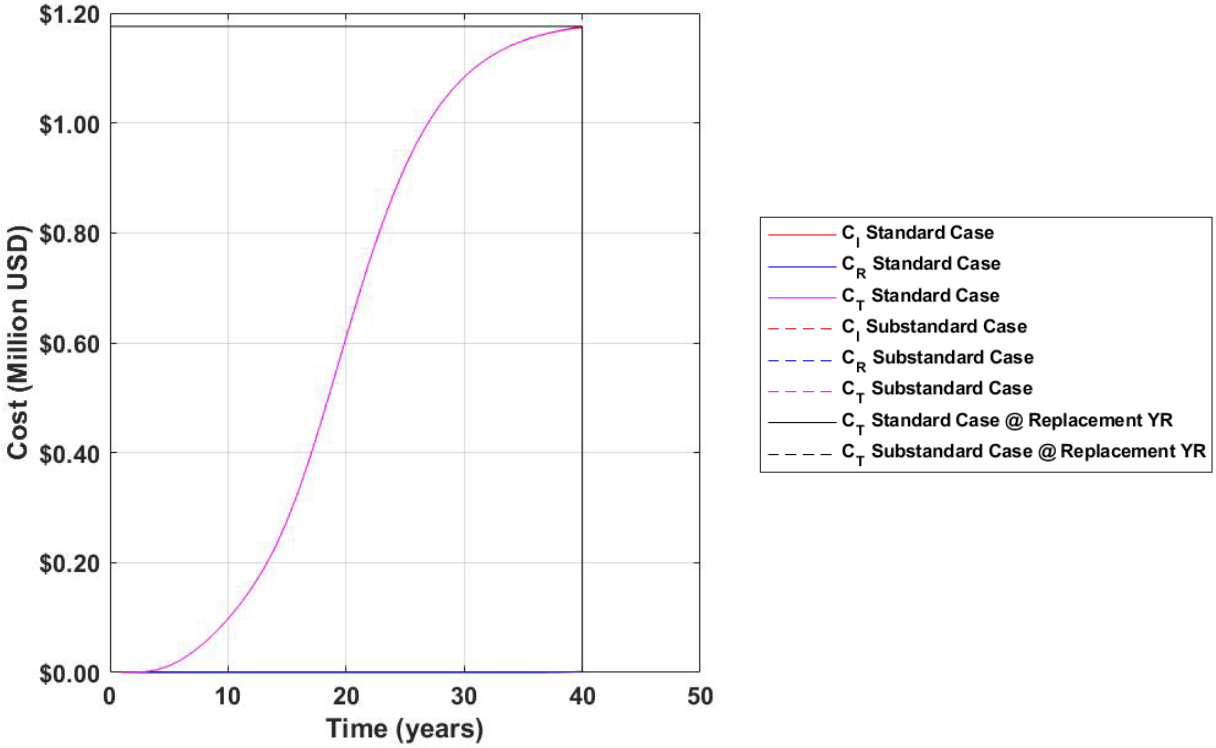

Figure A.2 Present day cost curve for case study bridge #4081.

Bridge NBI#:	11980	**Estimated Loss of Life:**	10 years
Region:	South	**Estimated Additional Cost:**	$15,500
Defect Classification:	Improper curing		

Defect Notes:

"(…) longitudinal and transverse map cracking up to approximately 0.020" nominal width visible throughout topside of deck."

Hazard Ratios:

CR4	CR5	CR6	CR7	CR8	CR9
2.5037	4.5886	2.8141	1.8239	2.2546	1.5375

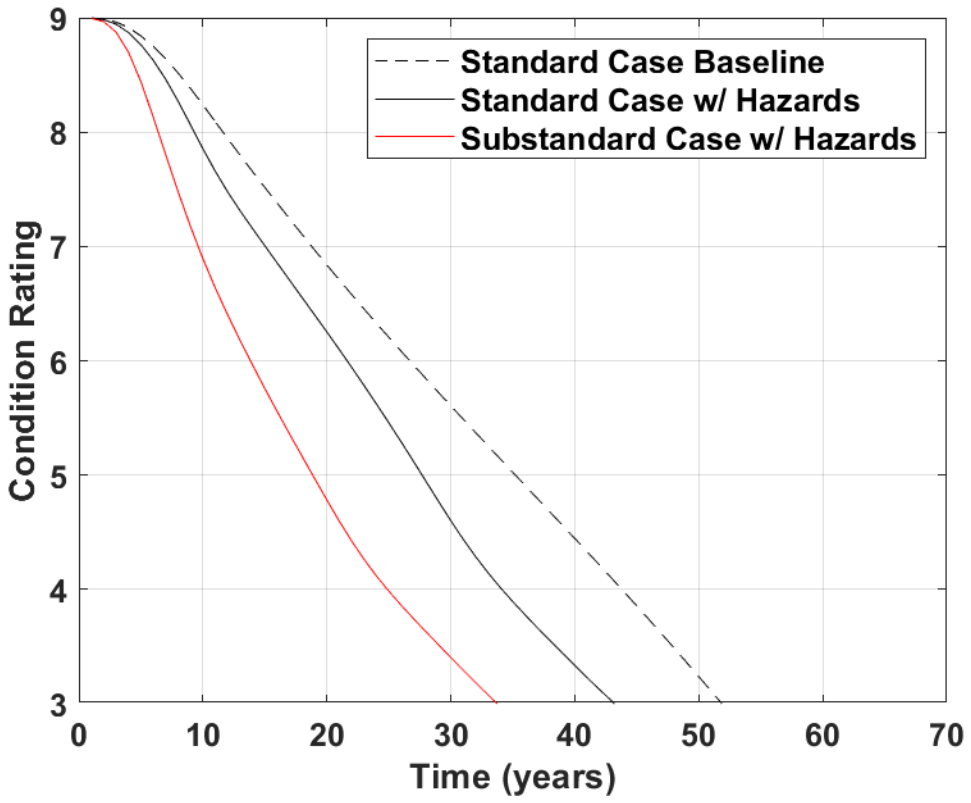

Figure A.3 Degradation curve for case study bridge #11980.

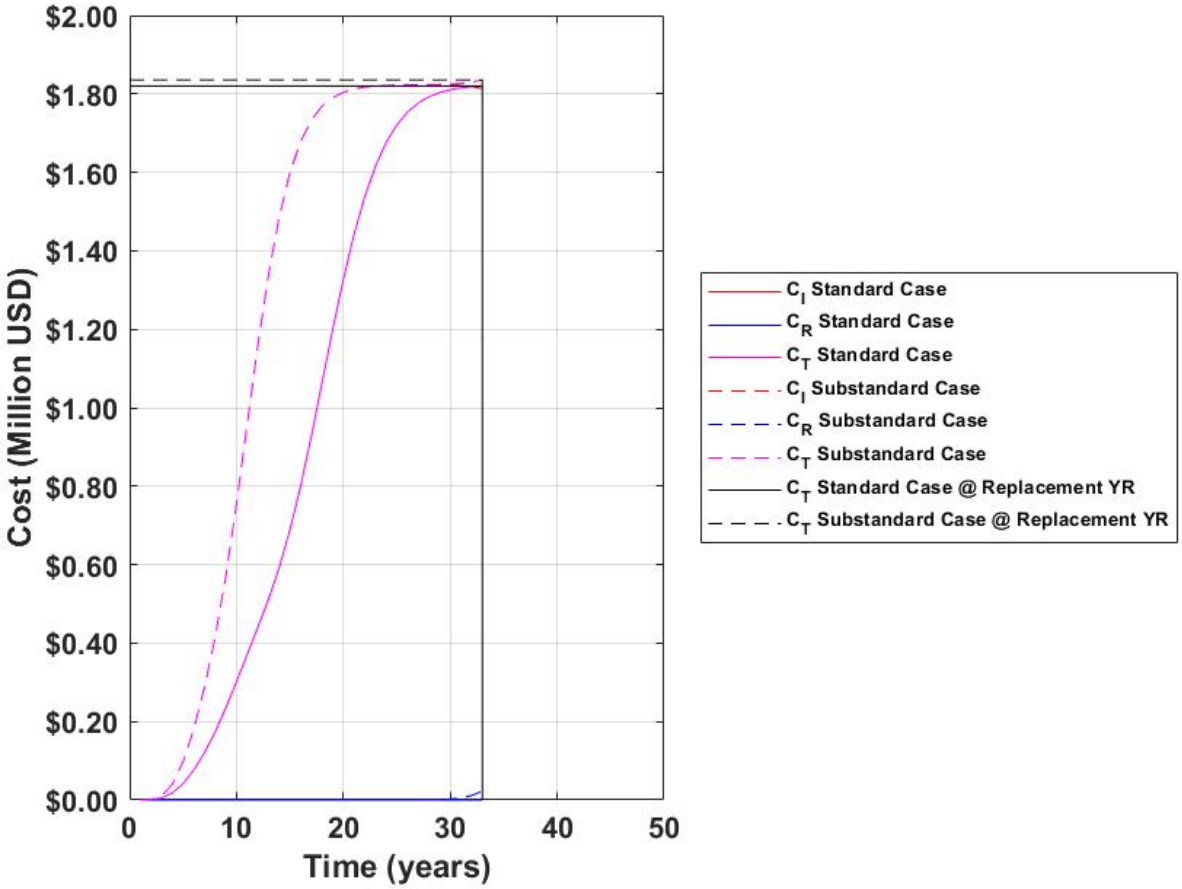

Figure A.4 Present day cost curve for case study bridge #11980.

Bridge NBI#:	15651	**Estimated Loss of Life:**	15 years
Region:	North	**Estimated Additional Cost:**	$269,300
Defect Classification:	Improper curing		

Defect Notes:

"Moderate width cracking throughout the deck, signs of water leaking through the deck and staining the slope walls underneath. Efflorescence forming on the bottom of the deck."

Hazard Ratios:

CR4	CR5	CR6	CR7	CR8	CR9
1.6830	1.5741	1.4553	1.2351	1.1172	0.7884

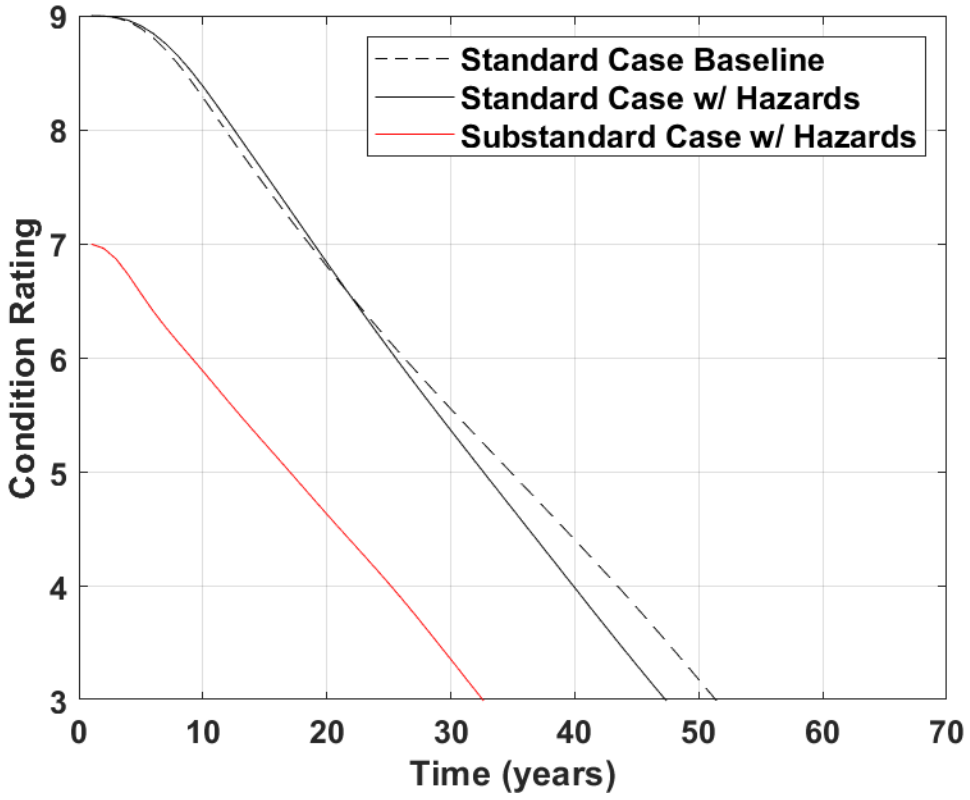

Figure A.5 Degradation curve for case study bridge #15651.

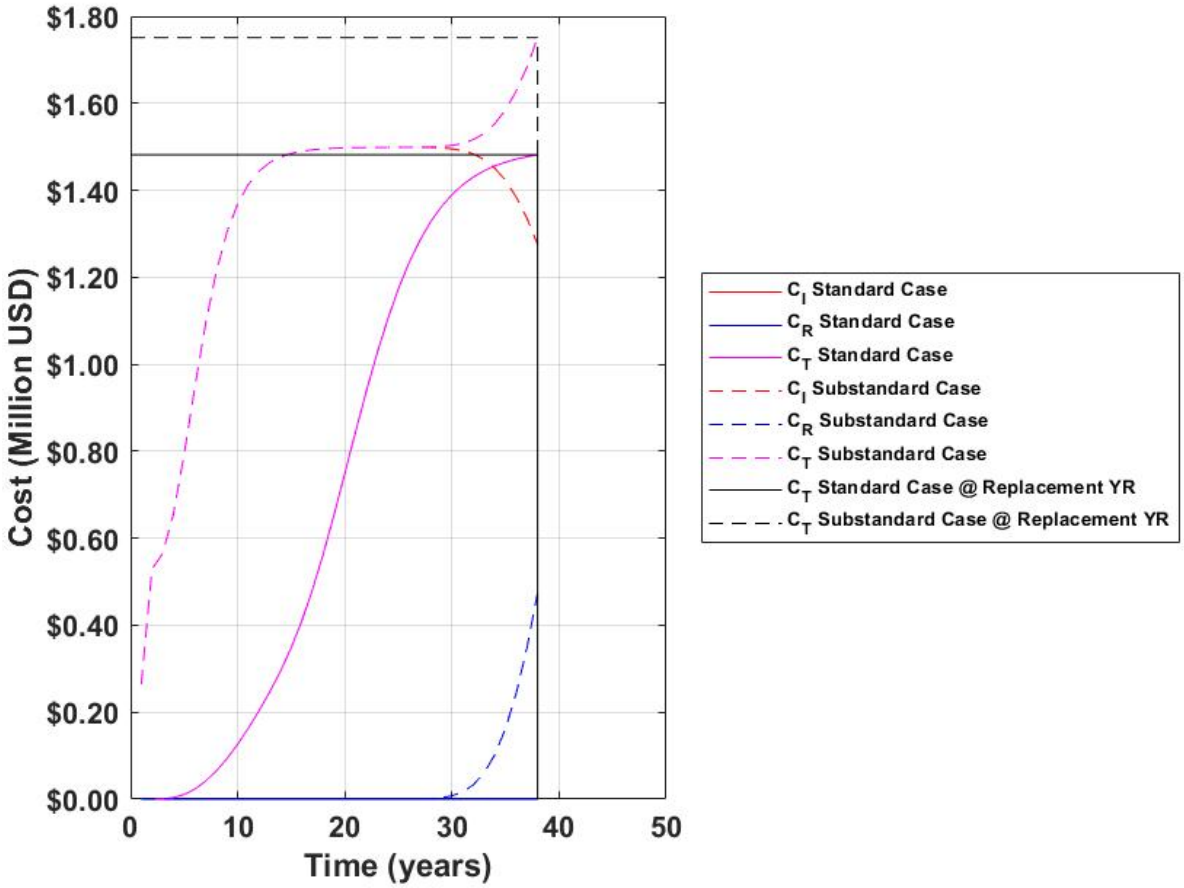

Figure A.6 Present day cost curve for case study bridge #15651.

Bridge NBI#:	18911	**Estimated Loss of Life:**	20 years
Region:	North	**Estimated Additional Cost:**	$809,000
Defect Classification:	Improper curing		

Defect Notes:

"(…) deck also heavily cracked throughout."

Hazard Ratios:

CR4	CR5	CR6	CR7	CR8	CR9
1.6830	1.5741	1.0233	1.2351	1.1172	0.7884

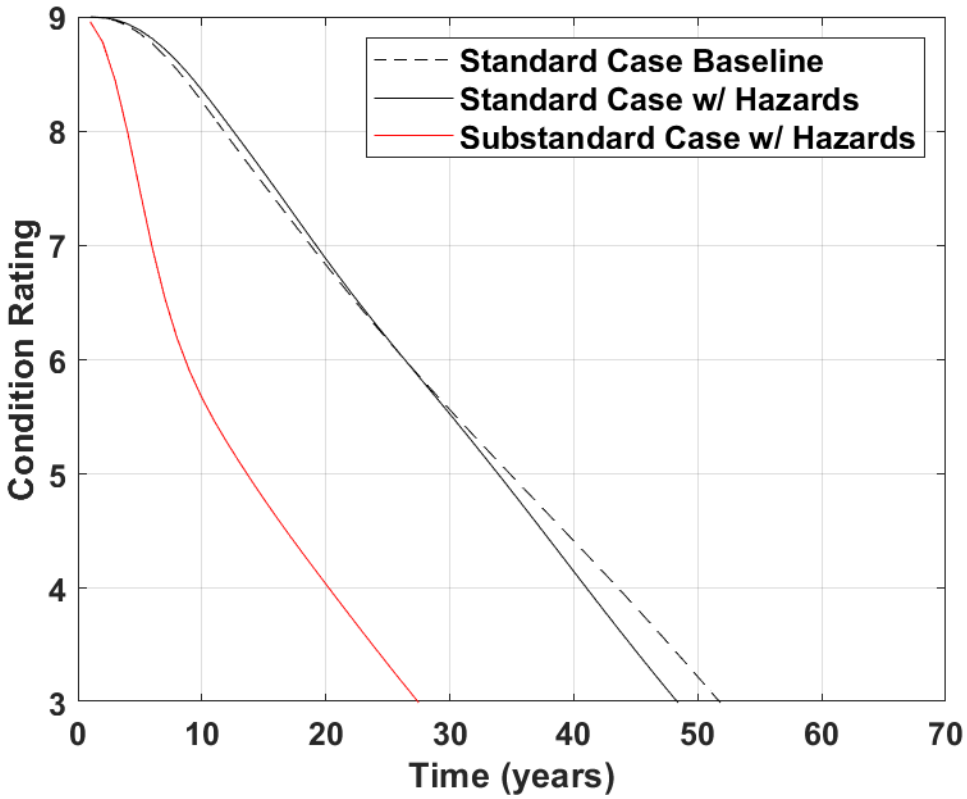

Figure A.7 Degradation curve for case study bridge #18911.

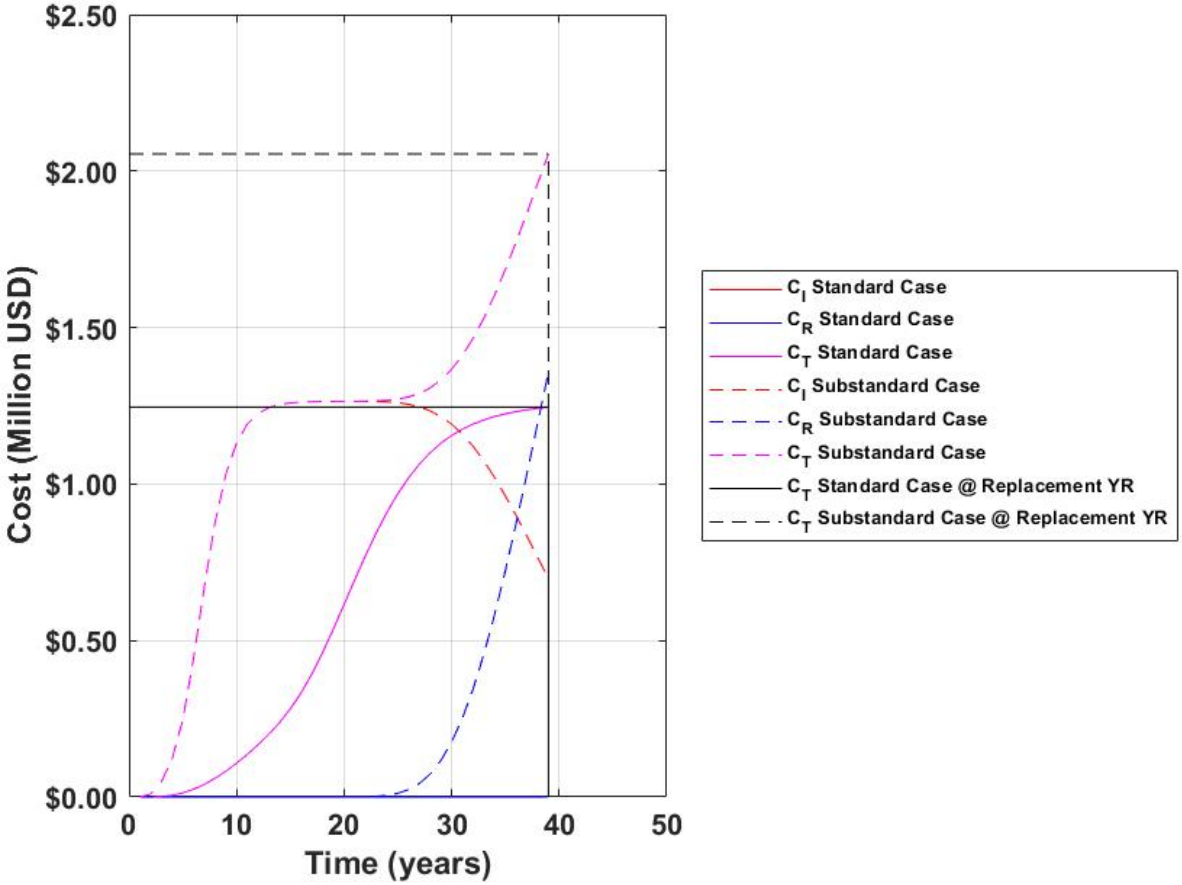

Figure A.8 Present day cost curve for case study bridge #18911.

Bridge NBI#:	19571	**Estimated Loss of Life:**	10 years
Region:	South	**Estimated Additional Cost:**	$54,000
Defect Classification:	Improper curing		

Defect Notes:

"(…) slightly diagonal cracks with efflorescence."

Hazard Ratios:

CR4	CR5	CR6	CR7	CR8	CR9
1.0000	1.5245	1.0388	0.9637	1.0000	1.0000

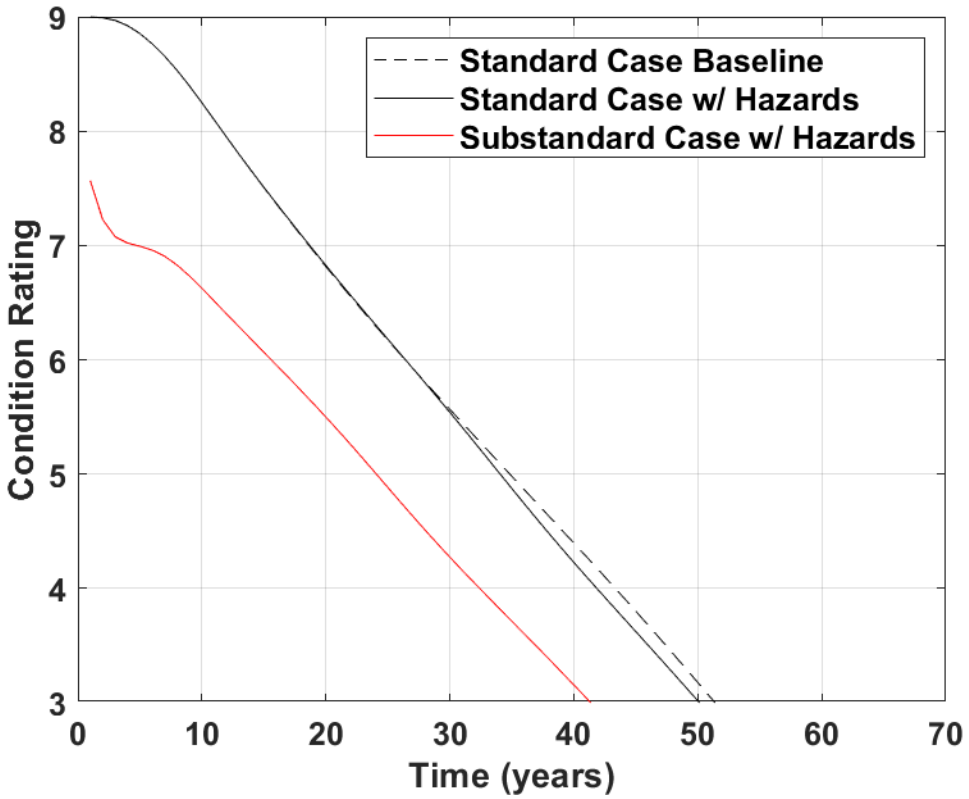

Figure A.9 Degradation curve for case study bridge #19571.

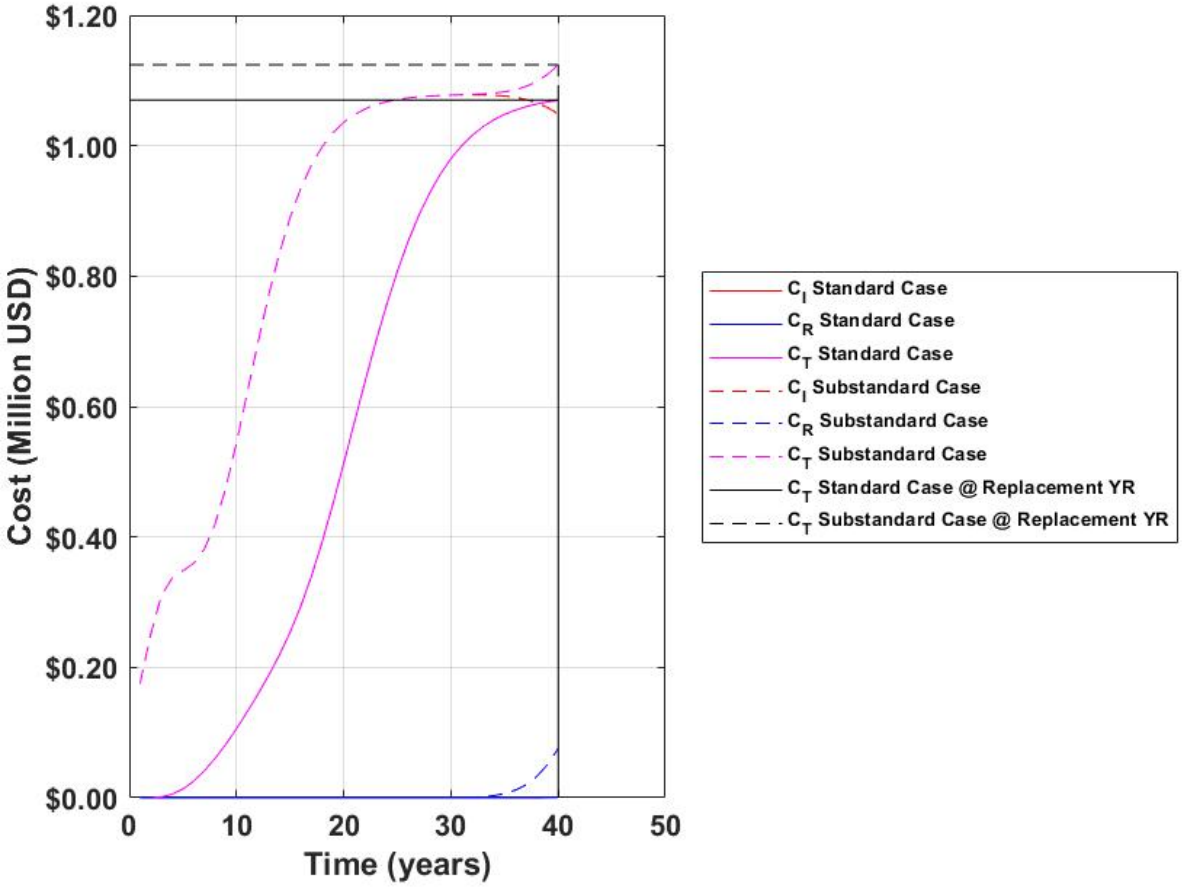

Figure A.10 Present day cost curve for case study bridge #19571.

Bridge NBI#: 33440 **Estimated Loss of Life:** 9 years

Region: South **Estimated Additional Cost:** $34,400

Defect Classification: Non-standard w/c ratio

Defect Notes:

"Failed air test."

Hazard Ratios:

CR4	CR5	CR6	CR7	CR8	CR9
2.5037	4.5886	2.8141	1.3746	1.8418	1.1418

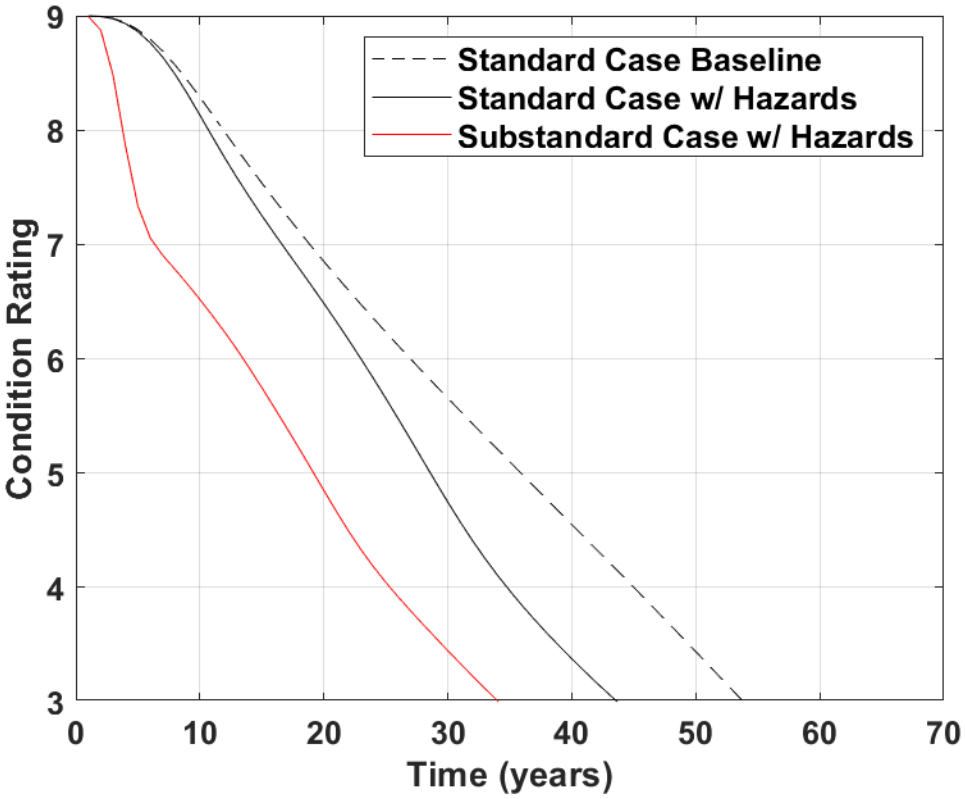

Figure A.11 Degradation curve for case study bridge #33440.

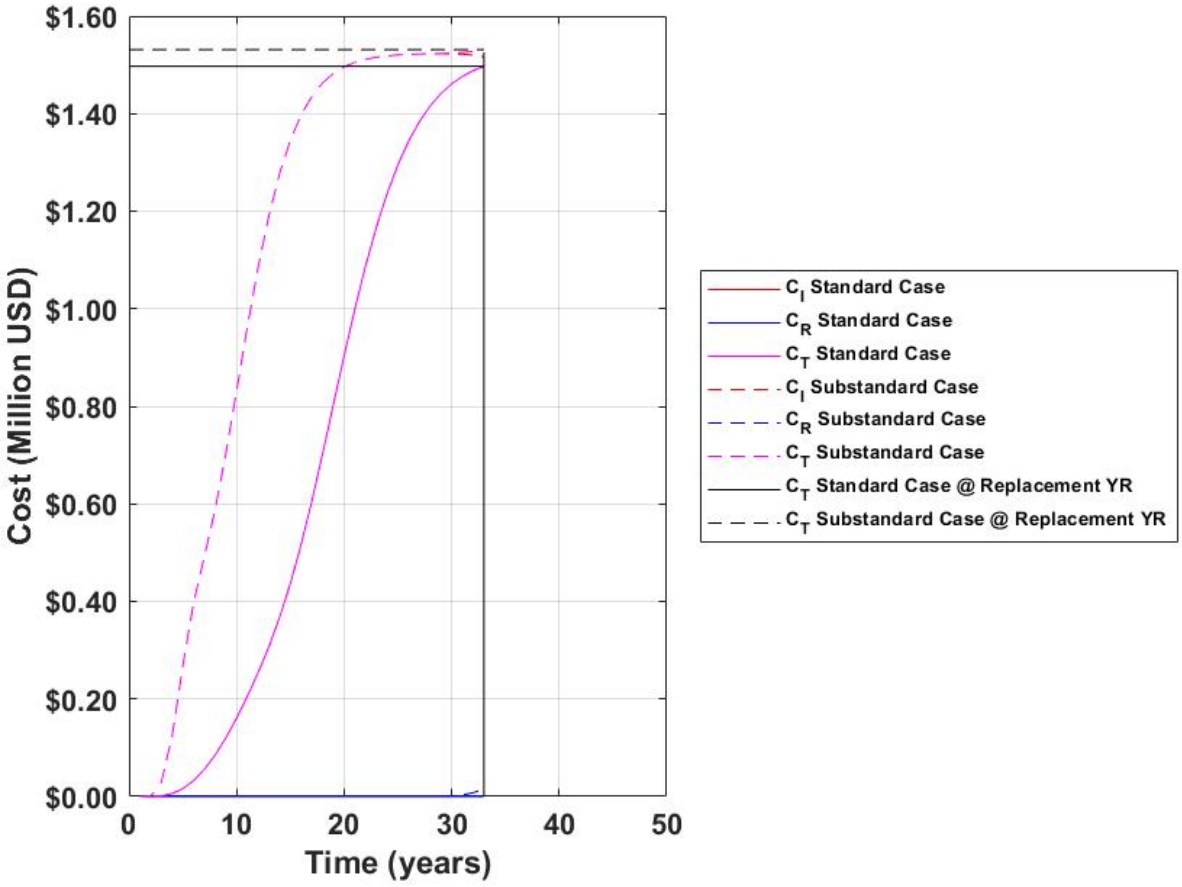

Figure A.12 Present day cost curve for case study bridge #33440.

Bridge NBI#:	36033	**Estimated Loss of Life:**	11 years
Region:	Middle	**Estimated Additional Cost:**	$336,600
Defect Classification:	Non-standard w/c ratio & improper curing		

Defect Notes:

> "(…) the contractor was allowed to utilize a substitute concrete mix during the winter months provided they provide for special curing considerations (…) those considerations were not followed."

Hazard Ratios:

CR4	CR5	CR6	CR7	CR8	CR9
1.6830	1.5741	1.0233	0.9308	0.9127	0.5855

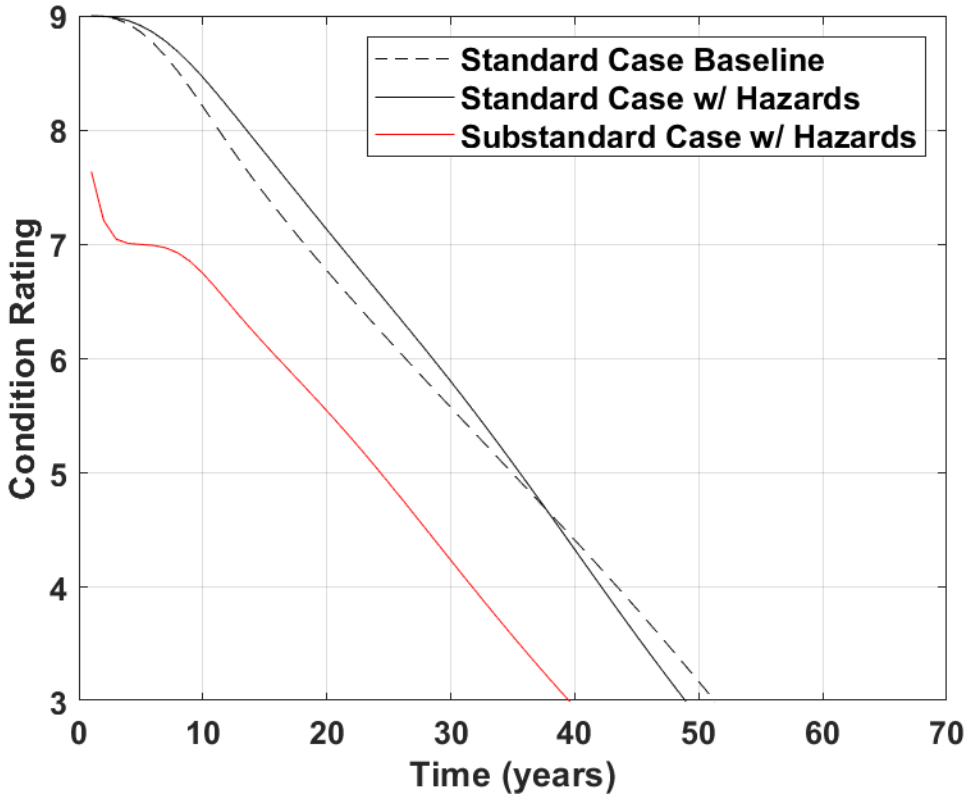

Figure A.13 Degradation curve for case study bridge #36033.

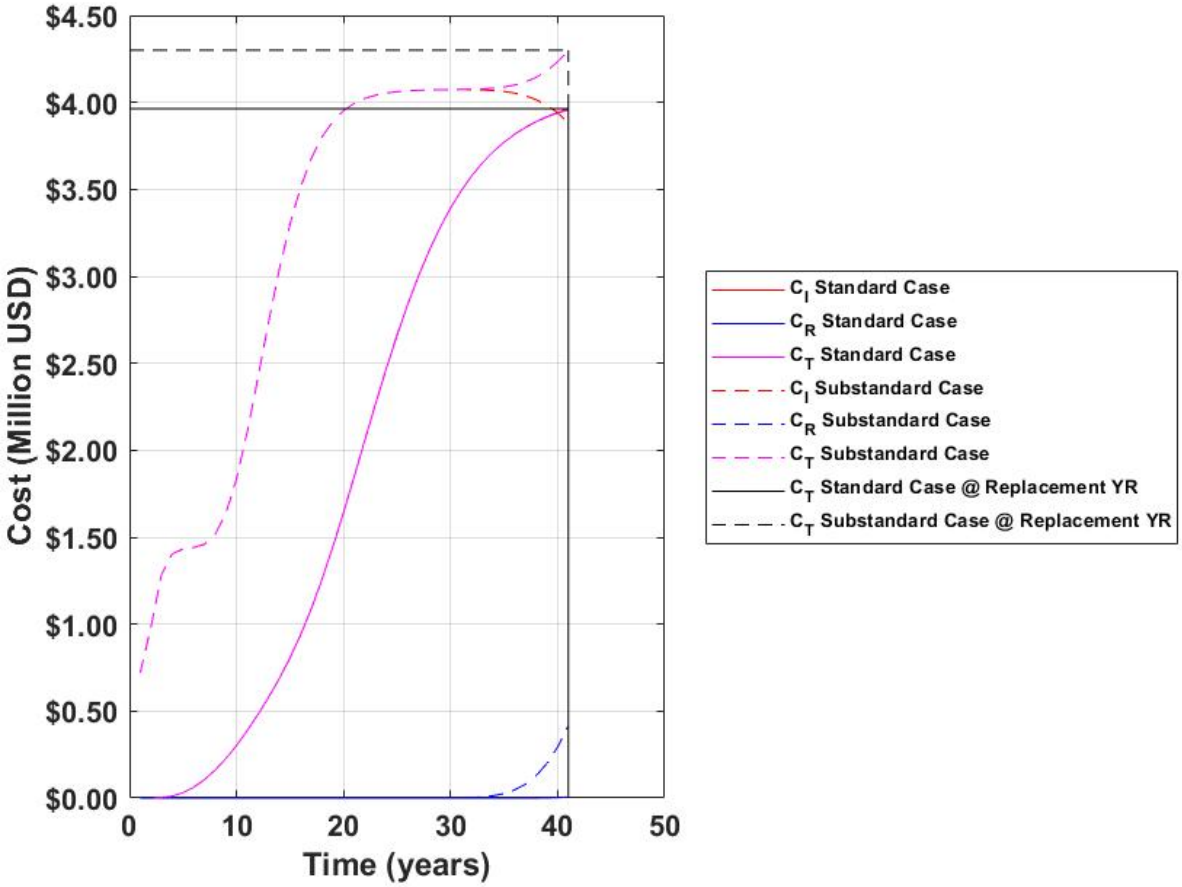

Figure A.14 Present day cost curve for case study bridge #36033.

Bridge NBI#: 44080 **Estimated Loss of Life:** 1 year

Region: Middle **Estimated Additional Cost:** $7,400

Defect Classification: Improper rebar handling

Defect Notes:

"There were issues with the rebar cover and rideability after the superstructure pour (…)."

Hazard Ratios:

CR4	CR5	CR6	CR7	CR8	CR9
2.5037	3.7682	2.8141	1.5807	1.8418	1.1418

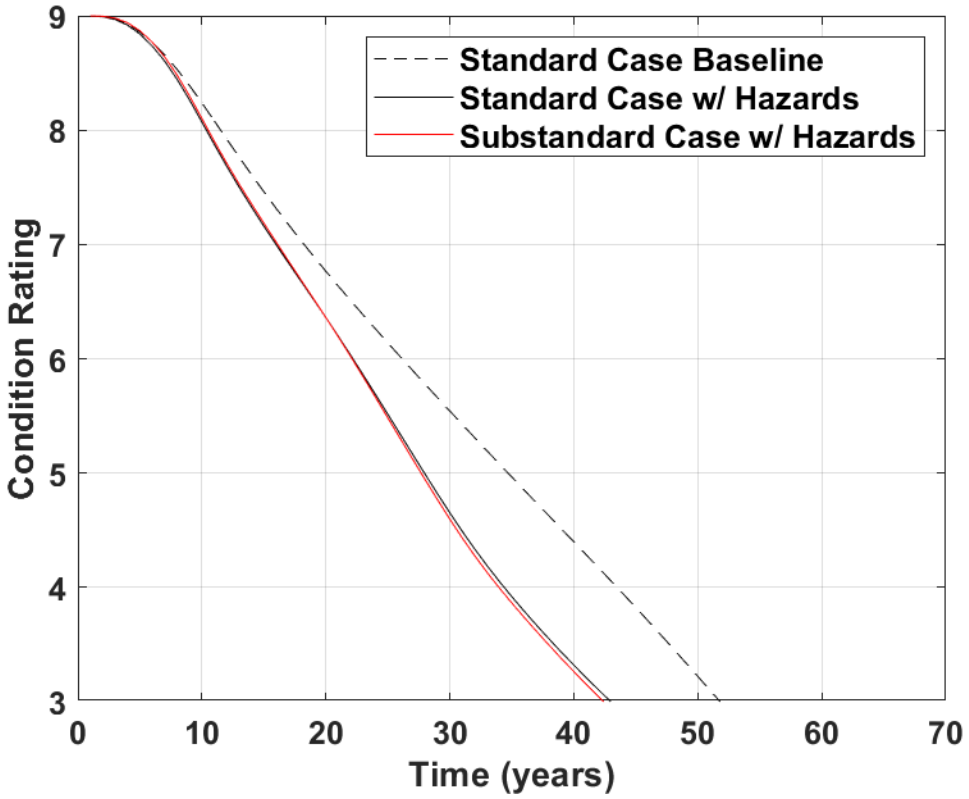

Figure A.15 Degradation curve for case study bridge #44080.

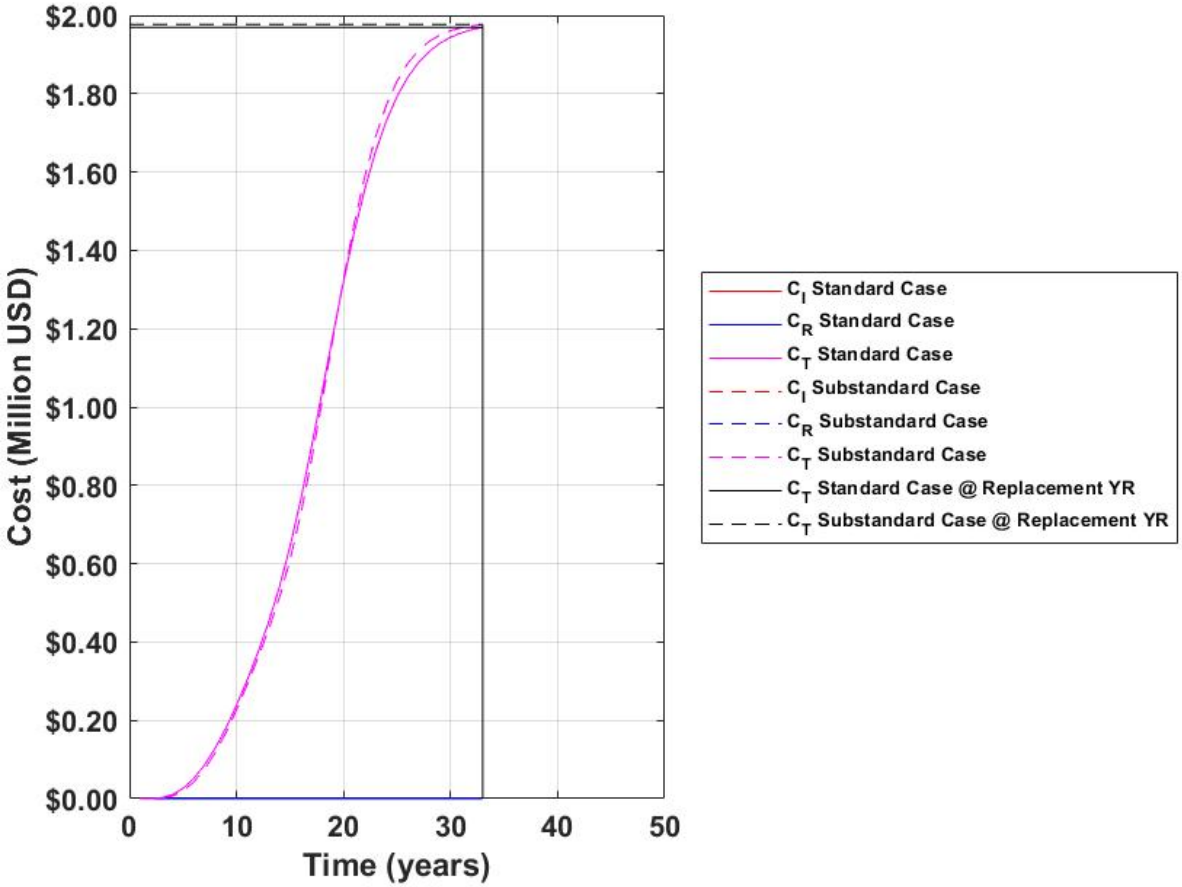

Figure A.16 Present day cost curve for case study bridge #44080.

Bridge NBI#:	50521	**Estimated Loss of Life:**	N/A
Region:	Middle	**Estimated Additional Cost:**	N/A
Defect Classification:	None		

Defect Notes:

"Deck (underside): no corrosion to metal forms."

Hazard Ratios:

CR4	CR5	CR6	CR7	CR8	CR9
1.0000	1.5245	1.0388	0.9637	1.0000	1.0000

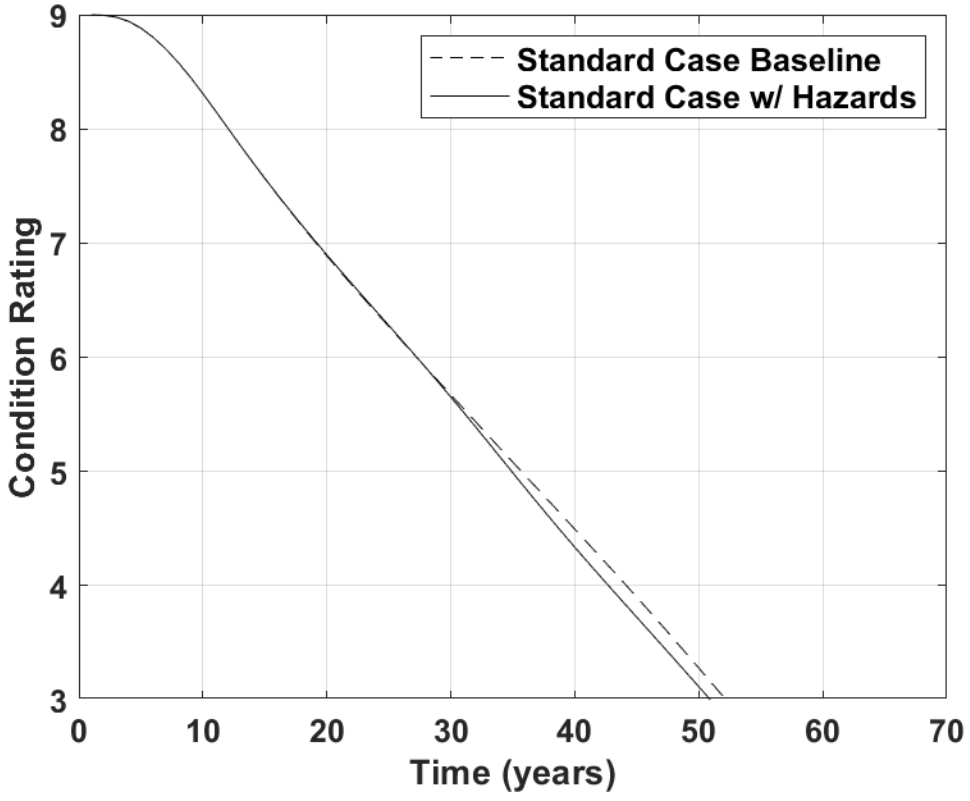

Figure A.17 Degradation curve for case study bridge #50521.

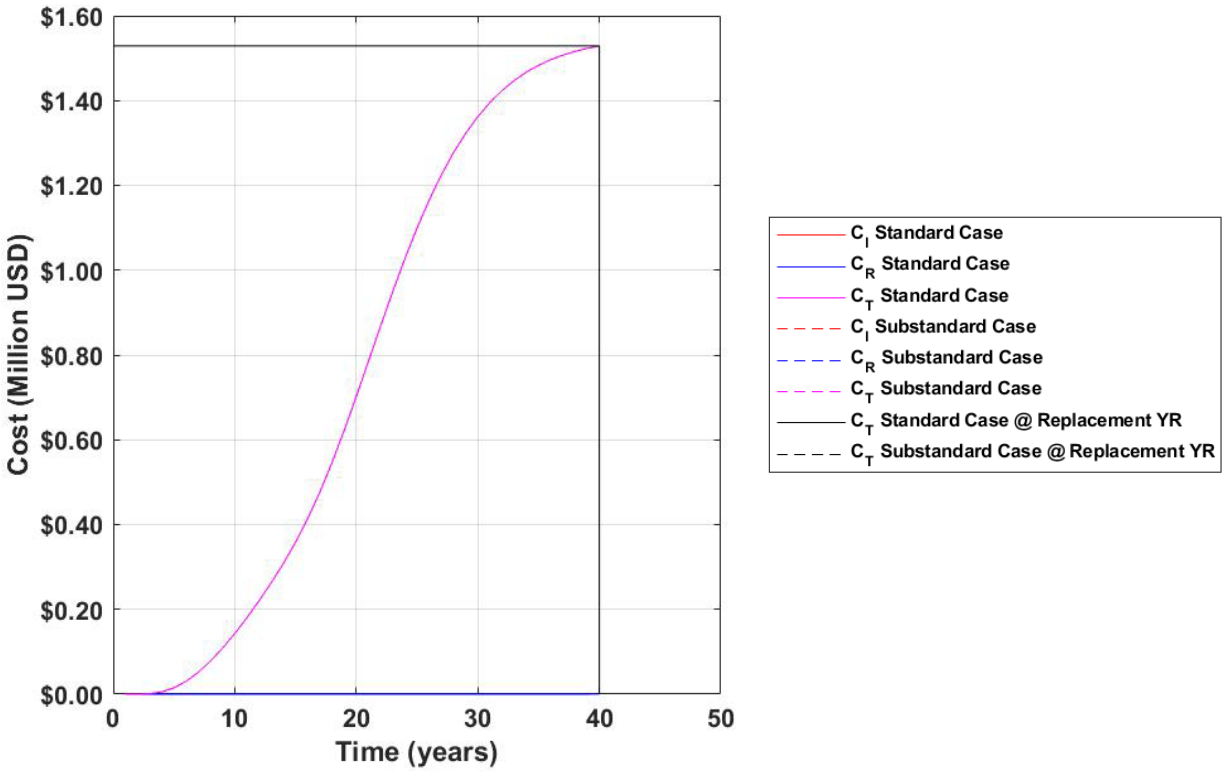

Figure A.18 Present day cost curve for case study bridge #50521.

Bridge NBI#:	79848	**Estimated Loss of Life:**	23 years
Region:	North	**Estimated Additional Cost:**	$4,048,500
Defect Classification:	Non-standard w/c ratio & improper curing		

Defect Notes:

"(…) some efflorescence on closure angles (of SIPs) in SE corner and at Pier2 (NB) (…) Several transverse cracks visible under the deck at the center seam with efflorescent."

"(…) incorrect concrete was used in deck."

Hazard Ratios:

CR4	CR5	CR6	CR7	CR8	CR9
1.6830	1.5741	1.0233	1.2351	1.1172	0.7884

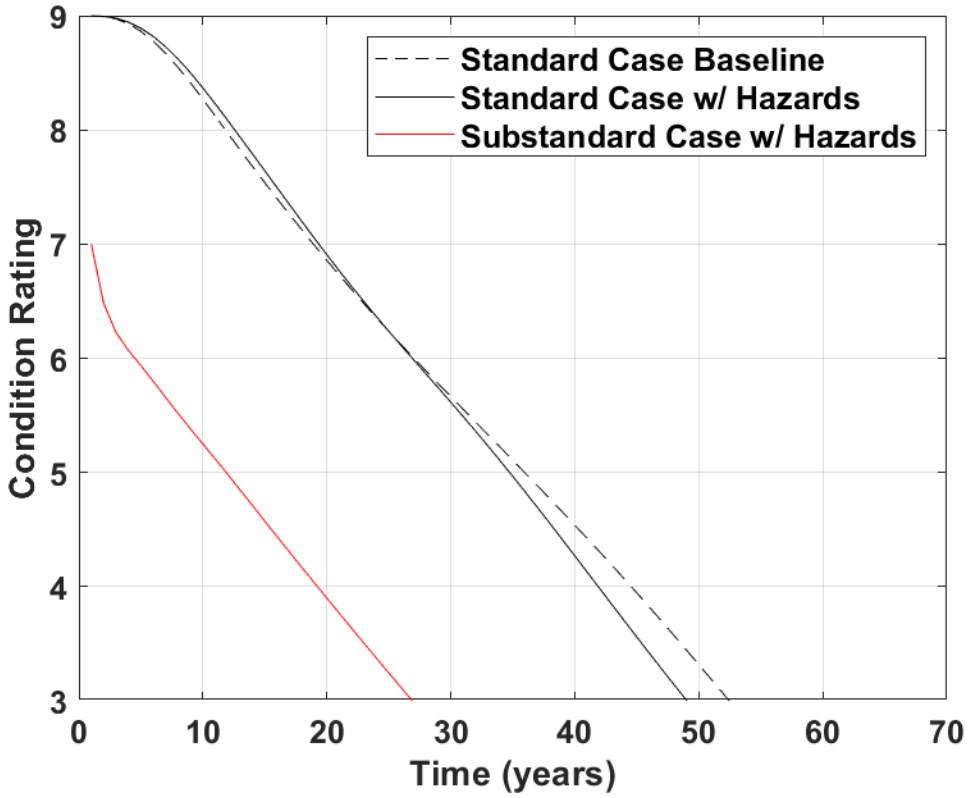

Figure A.19 Degradation curve for case study bridge #79848.

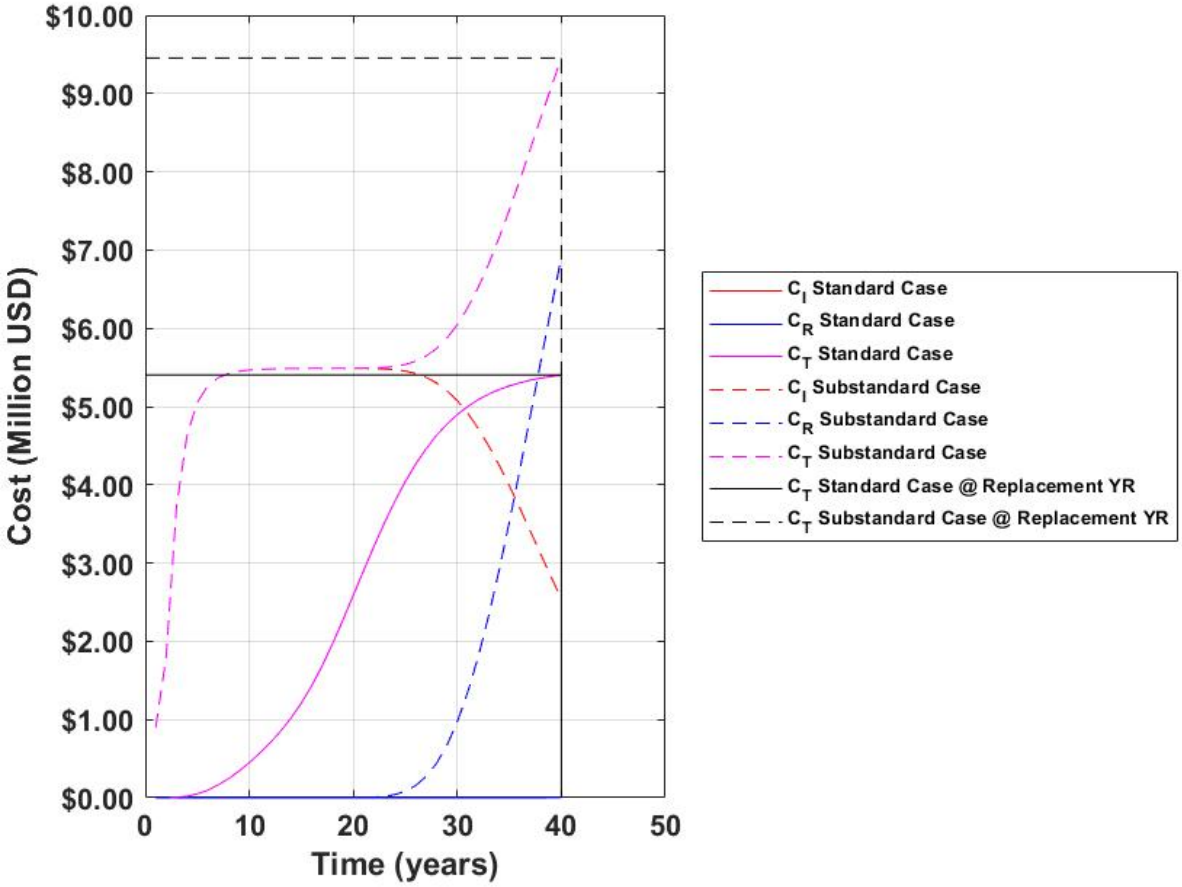

Figure A.20 Present day cost curve for case study bridge #79848.

A.3 Detailed Sensitivity Analysis

The variation of behavior with the region –a category that includes changes in environmental parameters and deicing salts pouring rates– and with different levels of intensity in each hazard ratio are also evaluated. In all the sensitivity studies, one parameter is varied while the others are fixed.

During this study, three main categories were considered as key influencers of the deck performance: (1) geographic region in the state where the deck is located; (2) defects during the construction stage; and (3) the factors not represented in a physical model but implicitly contained in the archived performance data of the bridge (also known as *external factors*).

In the first category, the variations from one region to another are represented by changes in the environmental parameters (relative humidity, number of freeze-thaw cycles, etc.) and in the rates of application of deicing salts. In the second category, the variations are caused by the defect-related parameters exposed in Section 2.1: water/cement ratio (which implies a change in diffusion coefficient), clear cover to the top mat of deck reinforcement, curing (whose representative parameter is the initial crack width) and rebar handling (modeled using pitting holes' diameter and spacing). Finally, the third category contains the hazard ratios related to each hazard group presented in Section 3: functional classification, wearing surface presence/type, average daily truck traffic, maximum span length, number of spans, and age of bridge. These three categories and related parameters are summarized in Table A.1.

In the following sections, the sensitivity of the predictive degradation model to each category is analyzed. For the region analysis, three non-defective bridges from the North, Center and South of Indiana were considered and compared. For the remainder of the categories, the bridge with asset number 50521 (considered as non-defective) was used as a baseline and the parameter under study was varied accordingly.

A.3.1 Sensitivity to Region

The environmental factors corresponding with each bridge were obtained from the NBI (2022) and the Global Monitoring Laboratory of NOAA (2022). Such factors (relative humidity, number of days of driving rain, number of freeze-thaw cycles, etc.) play an important role in the carbonation and freeze-thaw cycle modeling in the PBM.

On the other hand, there is a direct relationship between the deicing salt application rate and the chloride concentration at the surface of the deck (Martín-Pérez et al., 2000; Kassir, 2000). Given that the number of salts applied throughout Indiana vary depending on the weather conditions (McCullouch, 2010; Ji et al., 2020), the surface chloride concentration in the deck also varies. In this project, the state of Indiana was divided into three regions: North, South, and Center. To account for this variation in surface chloride concentration, it has been assumed that the bridges located in each one of these regions are exposed to similar weather conditions and thus a similar annual application rate of deicing salts. Further, it was assumed that the northernmost region of Indiana shares weather properties similar to those of the snowbelt region of the USA. Under the aforementioned assumption, the time vs. surface chloride concentration curve given by Kassir and Ghosn (2000) can be used (see Figure A.21).

Table A.2 Categories of the predictive degradation model with their respective phenomena and representative parameters

Category	**Phenomenon**	**Parameters/Data source**
Region	Environmental changes	Relative humidity
		Number of freeze-thaw cycles
		Number of rainy days
		Number of winter days
		CO_2 concentration in ambient air
	Deicing salts pouring rates	Surface chloride concentration
Defects	Water/cement ratio	w/c ratio
		Diffusion coefficient
	Cover	Cover
	Curing	Initial crack width
	Rebar handling	Pitting hole diameter
		Pitting hole spacing
External Factors (Hazard Groups)	Functional classification	Item 26[1]
	Wearing surface presence/type	Item 108[1]
	Average daily truck traffic	Item 29 & 109[1]
	Maximum span length	Item 48[1]
	Number of spans	Item 45[1]
	Age of bridge	Item 27[1]

[1] Refers to the item number in the *FHWA Recording and Coding Guide*.

Figure A.21 shows that the value of the surface chloride concentration stabilizes at around 15 years. Unfortunately, the available information for the state of Indiana is not as comprehensive as the one given in Figure A.21: our research team could access the registers of 8 bridges with yearly samples of chloride concentration in a time span of 3 to 7 years after construction. The information provided is summarized in Table A.2.

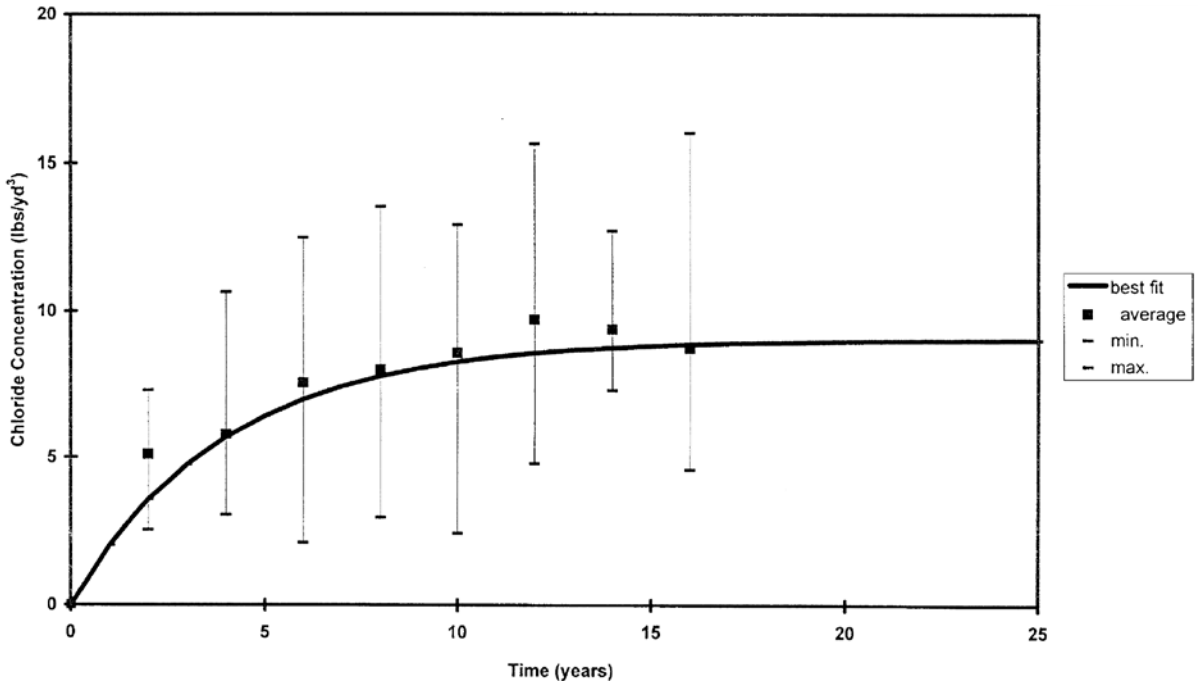

Figure A.21 Exponential representation of the surface chloride concentration data in the snowbelt region (from Kassir & Ghosn, 2000).

The average surface chloride concentration at 7 years coming from the data given by INDOT is 16.53 *lb/cuy* (9.80 kg/m^3). In the snowbelt region (Figure A.21), the corresponding value at 7 years is approximately 7 lb/cuy (4.15 kg/m^3). Considering the same stabilization period as the one observed in the snowbelt and assuming a linearly proportional relationship, it can be assumed that the stabilized surface concentration value for the Indiana North region bridges is 20.66 lb/cuy (12.25 kg/m^3).

Table A.2 Chloride concentration data provided by INDOT personnel[1]

		SURFACE CHLORIDE CONCENTRATION (*lb/cuy*)				
STRUCTURE	**NBI**	**3 Years**	**4 Years**	**5 Years**	**6 Years**	**7 Years**
Str. No. 27-A WB Bendix Rd.	47650	09.36	08.52	09.54	12.27	13.90
Str. No. 30-5 NB Fir Rd.	47850	05.74	03.17	09.23	12.31	13.81
Str. No. 30-6 EB Cleveland Rd.	47860	09.23	09.33	11.07	15.15	17.12
Str. No. 49-64-2562 NB	17976	02.44	02.48	03.58	–	–
Str. No. 49-64-2562 SB	17977	02.32	02.76	02.95	02.65	–
Str. No.49-64-2563 NB	17978	10.17	11.96	13.01	15.80	–
Str. No. 49-64-2563 SB	17979	15.68	18.79	17.28	18.07	21.45
Str. No. 49-64-2564 NB	17985	01.41	05.36	17.47	–	–
Str. No. 49-64-2564 SB	17986	07.93	13.09	09.89	17.67	–
Str. No. 49-64-6678 SB	17983	05.00	05.63	08.84	14.18	–
Str. No. 49-64-6679 NB	17988	05.79	07.87	10.99	13.75	16.37
Str. No. 49-64-6679 SB	17986	03.66	06.26	05.34	05.90	–

[1] Information provided by Tommy Nantung on May 27, 2022.

For the Center and South region, the deicing salt usage reports for the 2008, 2009 and 2010 bridges were used[1]. A summary of this information is presented in Table A.3. Assuming a proportional relationship between the salt usage and the surface chloride concentration and taking the district of LaPorte as a reference to equate with the conditions of the snowbelt region, the chloride concentration for each district can be obtained. These values are shown in the last column of Table A.3.

Table A.3 Summary of deicing salt usage per district in the period 2008–2010

District	**Region**	**Deicing Salt Usage, Short-Ton (average of 3 years)**	**Proportional Surface Chloride Concentration, lb/cuy (kg/m^3)**
Fort Wayne	North	79,873	16.02 (9.49)
LaPorte	North	102,605	20.66 (12.25)
Crawfordsville	Center	62,241	12.53 (7.43)
Greenfield	Center	79,619	16.02 (9.49)
Seymour	South	50,617	10.18 (6.03)
Vincennes	South	69,417	13.97 (8.28)

To perform a sensitivity analysis of the models to the geographic region, all the non-environment related parameters in the physics-based model were fixed, i.e., the only parameters that were free to vary throughout the stochastic simulation are the ones appearing in Table A.4. To guarantee replicability from one simulation to another, the random number generator seed was set to 1. The surface chloride concentration was considered a fixed parameter taking the values of LaPorte for the North region, Crawfordsville for the Center, and Seymour for the South. The degradation curves associated with the three regions are shown in Figure A.22. It can be seen that the decks in the northern region degrade faster than those in the South and Center. This behavior is a consequence of the greater number of deicing salts used in such area. We can see that the degradation due to the region can accelerate between 3 or 4 years as the deck approaches a CR value of 4.

Table A.4 Varying parameters for the region sensitivity analysis

Parameter	Source	Observations
Surface chloride concentration	As described in Section 2.1.1.	North: LaPorte value. Center: Crawfordsville value. South: Seymour value.
Average relative humidity (%)	NBI (2022)	–
Number of freeze thaw cycles	NBI (2022)	The maximum number of the historical records was also used.
Number of rainy days	NBI (2022)	–
Number of winter days (days with temperature below 0°C)	NBI (2022)	–
CO_2 concentration in ambient air	Global Monitoring Laboratory of NOAA (2022)	No information for the state of Indiana. Data from the closest location (Homer, IL) was used.

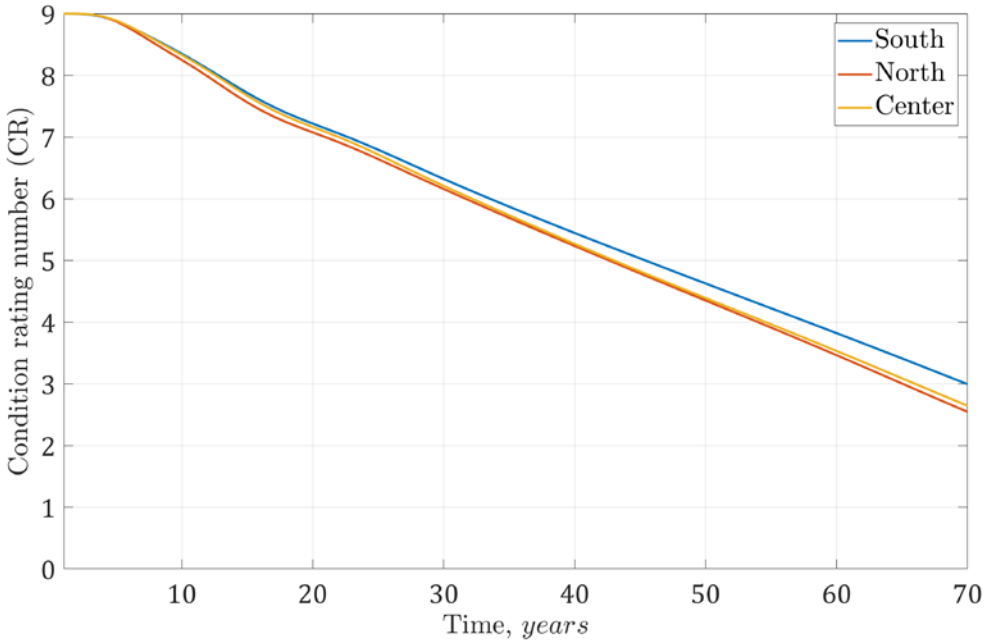

Figure A.22 Change in degradation trend with regional variations.

A.3.2 Sensitivity to Defects

The same strategy used to evaluate the region-related parameters was used with the defect-related ones: an individual degradation curve showing their variability was built. This set of parameters and the different cases contemplated here are shown in Table 4.12, where D stands for chloride's diffusion coefficient, c for the concrete cover of the deck, ω_0 for initial crackwidth and d_h and l_h for pitting holes' diameter and spacing, respectively. For each parameter, a standard case was determined, and 4 to 5 substandard cases were defined. In the case of the w/c ratio, the substandard cases correspond to the different scenarios given by Kim et al. (2014). For the concrete cover, the substandard cases were arbitrarily defined as ¼" decrements with respect to INDOT's standard of 2.50". With respect to curing, the standard and substandard cases correspond to the indicated crack widths as a function of the CR given in the INDOT Bridge Inspection Manual (2020). Finally, the allowed ("standard") diameter of pitting holes and spacing for the

rebar handling defect were taken from the INDOT Standards and Specifications (2020); the substandard cases were defined based on observational data taken from our team during an in-site visit (see Figure A.23). As in the region analysis, the random number generator seed was set to 1, thus the only changes between one curve and another beneath the same defect group are due to the change in the associated parameter's mean.

Table A.5 Summary of defective cases and its associated model parameters' means

Defect	**Case**	**Associated Parameter's Mean**
w/c ratio	0.45 (standard)	$D = 22.96 \times 10^{-12}\ ft/s^2$ ($7.00 \times 10^{-12} m/s^2$)
	0.50	$D = 24.60 \times 10^{-12}\ ft/s^2$ ($7.50 \times 10^{-12} m/s^2$)
	0.55	$D = 29.52 \times 10^{-12}\ ft/s^2$ ($9.00 \times 10^{-12} m/s^2$)
	0.60	$D = 35.43 \times 10^{-12}\ ft/s^2$ ($10.80 \times 10^{-12} m/s^2$)
Cover	2.50" (standard)	$c = 2.50"$ ($63.5\ mm$)
	2.25"	$c = 2.25"$ ($57.15\ mm$)
	2.00"	$c = 2.00"$ ($50.80\ mm$)
	1.75"	$c = 1.75"$ ($44.45\ mm$)
	1.50"	$c = 1.50"$ ($38.10\ mm$)
Curing	CR 9 (standard)	$\omega_0 = 0.006"$ ($0.1524\ mm$)
	CR 8	$\omega_0 = 0.012"$ ($0.3048\ mm$)
	CR 7	$\omega_0 = 0.016"$ ($0.4064\ mm$)
	CR 6	$\omega_0 = 0.020"$ ($0.5080\ mm$)
	CR 5	$\omega_0 = 0.030"$ ($0.7620\ mm$)
	CR 4	$\omega_0 = 0.040"$ ($1.016\ mm$)
Rebar handling	Allowed (standard)	$d_h = 0.25"$ ($06.35\ mm$) $l_h = 0.375"$ ($9.525\ mm$)
	Spread corrosion	$d_h = 0.0375"$ ($0.9525\ mm$) $l_h = 0.375"$ ($9.525\ mm$)
	Corrosion at tip	$d_h = 0.1875"$ ($4.7625\ mm$) $l_h = 0.375"$ ($9.525\ mm$)

(a) (b)

Figure A.23 Photographs of the types of rebar damage observed on site: (a) spread holes; (b) corrosion at tips.

Figure A.24 shows the resultant degradation curves for the different w/c ratio values. As expected, the standard case, i.e., w/c of 0.45, shows the highest life expectancy of all. Specifically, the maximum gap between the curves occurs around CR 7. The standard case gets to CR 7 at approximately 24 years, while the substandard, w/c of 0.60 case, does this in 19 years. With no maintenance actions, the difference then shrinks to 4 years and remains roughly constant until the end of the service life of the deck. *This result may suggest that when an anomaly in the water-cement ratio is detected, enhanced surveillance and maintenance of the deck on its first 20 years of existence is of great importance.* Even if the water-cement ratio of the deck is not below the standard at the time of construction, a special care to avoid water infiltrations and possible applications of preventive overlays may help to close the gap and keep the degradation curve close to the standard one.

Figure A.25 shows the variations in loss of life with differences in concrete cover. INDOT's standard is 2.50". It can be observed that a loss of a quarter of an inch at the time of construction already takes 1 year of life from the bridge. It is worth noticing that the cases in which the concrete cover is 2.00", 1.75" and 1.50" all collapse to the same degradation curve after the first 10 years of life, in other words, *a reduction of half an inch is as bad as a reduction of a whole inch*. The difference between these cases and the standard one can be as high as 4 years. *This lack of differentiation between one or another defective case, and the noticeable change after just a quarter of an inch reduction, suggest that the tolerances regarding the concrete cover of the deck should be strictly enforced*.

Figure A.26 shows the degradation curves for different curing scenarios in terms of the resultant crack width. Here there is a different behavior based on the severity of the defect. *The loss of life can be as high as 10 years at a CR of 7.* The worst performance occurs before the first 20 years of life, so any measure to avoid water infiltration—like sealant or overlay application—at this stage is critical to keep the deck in good shape. From 20 years onwards, the loss of life is primarily due to the rebar corrosion and rust expansion. At this point, sealing the cracks is no longer an option to preserve the integrity of the deck because the

corrosion process has already started. Thus, in this latter stage of the corrosion process, more invasive measures, such as hydro-demolition and rigid deck overlay application, are more suitable.

Figure A.27 shows the results for the different rebar handling scenarios given in Table A.5. The standard case has the same behavior as the corrosion at tips one. On the other hand, the spread corrosion case has a longer lifespan: the difference as big as 12 years. *It can be concluded that the damage at the tips of the bars should be minimized. The storage and placing of the epoxy-coated bars plays an important role in such effort.* On the other hand, the fact that the "Allowed" (standard) case (0.25" diameter, 0.375" spacing) shows worse behavior than the substandard "Spread corrosion" case *suggests that the specifications should be modified. It is strongly recommended to state such standard in terms of the diameter allowed and the spacing or spread allowed between the pitting holes.*

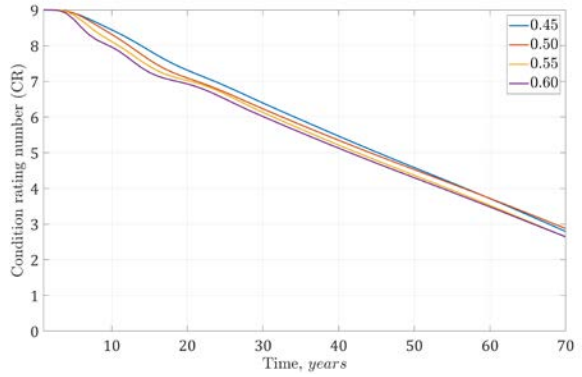

Figure A.24 Sensitivity analysis for changes in water-cement ratio

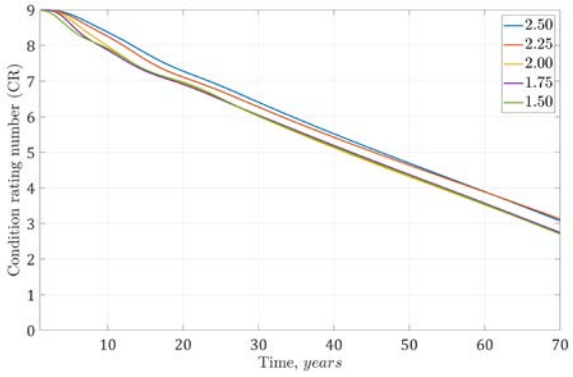

Figure A.25 Sensitivity analysis for changes in concrete cover

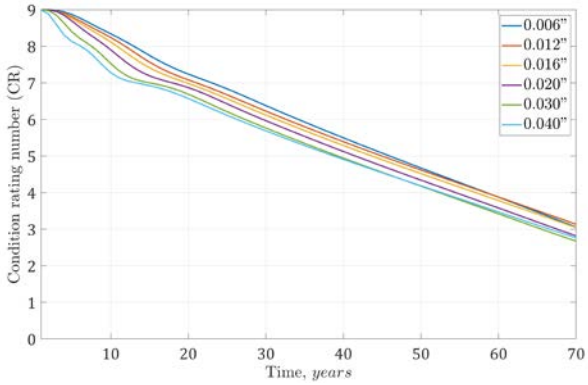

Figure A.26 Sensitivity analysis for changes in initial crack width due to improper curing

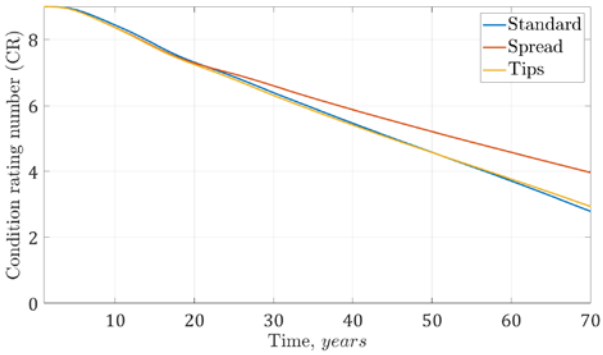

Figure A.27 Sensitivity analysis for different improper rebar handling scenarios

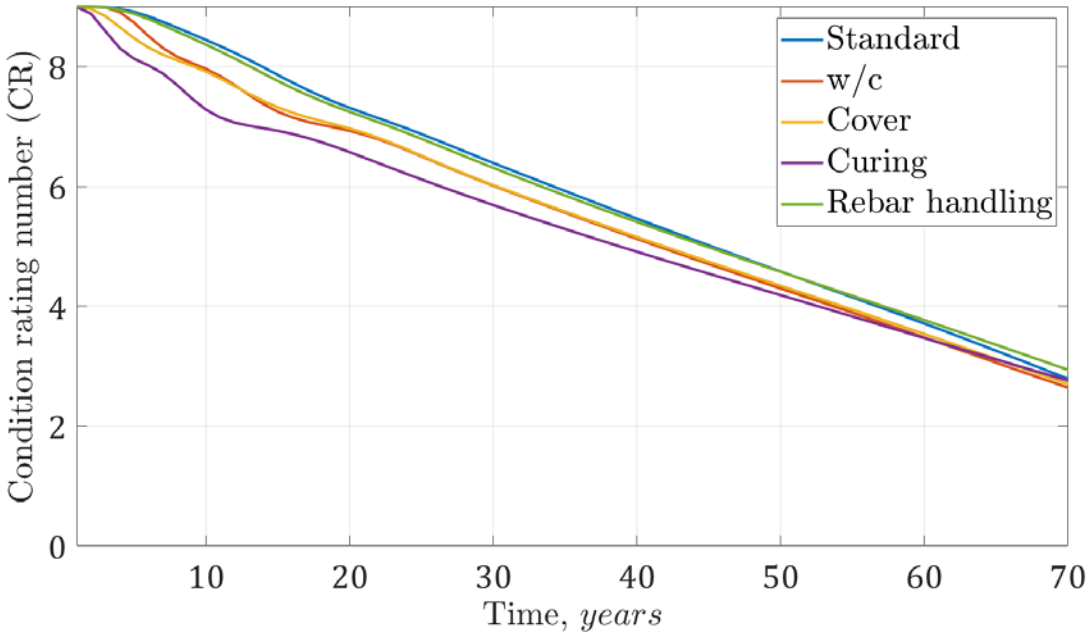

Figure A.28 Comparison of a standard construction case with the worst case scenario of each defective case.

Finally, the standard construction case alongside the worst-case scenario for each defect was plotted in Figure A.28: w/c of 0.60, 1.50" of concrete cover, 0.040" of initial crack width due to improper curing, and epoxy-coating damage at the tip of the rebars. As can be seen, improper rebar handling is the least concerning defect of those considered. However, and as mentioned before, the life expectancy of the deck would be greatly benefitted from an improvement in the rebar coating manipulation. This case is followed by the cases considering insufficient concrete cover and excessive water-cement ratio which have very similar behavior after the first 15 years of life. Both reduce the life of the deck by around 3 years. Clearly, improper curing is the most impactful defect with a 10-year reduction in the life of the bridge deck.

Finally, the case of combined defects was studied. Figures A.29 and A.30 shows the degradation curves for simultaneous occurrence of improper curing and two defects: excessive water-cement ratio and insufficient concrete cover, respectively. The initial crack width due to shrinkage cracking was set to 0.040", which corresponds to the worst-case curing scenario. Given that the worst case for the rebar handling defect is very close to the standard construction case, such comparison is not shown. It can be seen from Figures A.29 and A.30 that improper curing, whose representative parameter is the initial cracking ω_0, has a dominant behavior over the other two defects. Therefore, the avoidance of such defect should be prioritized during construction.

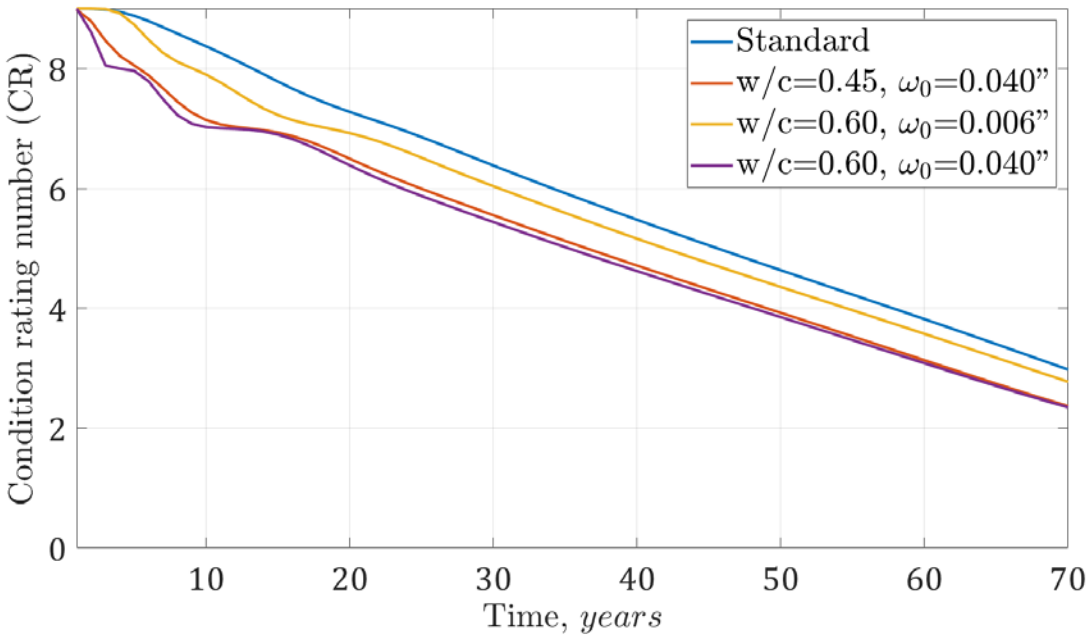

Figure A.29 Degradation curves for different combinations of improper curing and water-cement ratio.

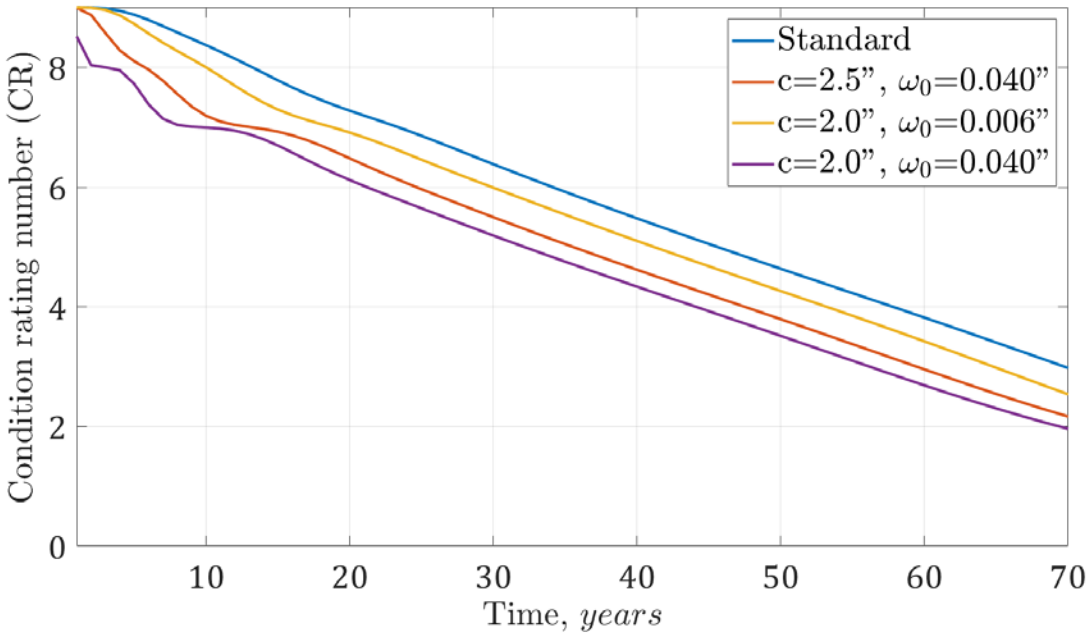

Figure A.30 Degradation curves for different combinations of improper curing and insufficient concrete cover.

A.3.3 Sensitivity to Hazard Ratios

Indiana bridges are subject to multiple external factors that could potentially speed up or slow down the degradation process over the bridge's life. In order to better understand which external factors were significant to the degradation pattern observed within the state, a Cox Proportional Hazards Regression was performed. Each individual external factor was assigned the term hazard group and the span of data values applicable to that group were divided into further subgroups called hazard group options. We evaluated the sensitivity of the final degradation curves to the presence of these hazard groups, by applying one at a time, the effect of a hazard group option to the same base degradation pattern. The transition probabilities obtained from the physics-based model of one of the case study bridges that is considered non-defective (NBI #50521) was used. The resulting degradation curves for each hazard group and its respective options are included in its own plot (see Figures A3.11–A3.16), where each line represents a different option for that hazard group. Any hazard options in the group that is not shown has been determined to have no impact on final degradation. Thus, that case had the same degradation curve as the baseline indicated with a (B) in the corresponding legend. Table A.6 provides the final hazard ratios calculated in this study.

Table A.6 Hazard ratios for the state of Indiana

	CR4	**CR5**	**CR6**	**CR7**	**CR8**	**CR9**
Interstate	1.0000	1.0000	1.0000	0.7536	0.8169	0.7426
Monolithic Concrete	1.0000	1.0000	0.7032	1.0000	1.0000	1.0000
Integral Concrete	2.3921	1.0000	1.0000	0.7471	1.0000	1.4003
Latex Concrete	1.0000	1.3825	1.0000	1.0000	1.0000	1.0000
Bituminous	2.0489	1.4686	1.0000	1.0000	1.0000	1.0000
$5 < \text{ADTT} \leq 24$	1.0000	1.0000	1.0000	1.0000	0.8540	1.0000
$25 < \text{ADTT} \leq 329$	1.0000	1.2519	1.4773	1.0000	1.0000	1.0000
$330 \leq \text{ADTT}$	1.6830	1.2927	1.4553	1.2816	1.1172	0.7884
$15 \leq \text{Max Span}$	1.0000	1.2177	1.0000	0.8696	1.0000	1.0000
Multi-Span	1.0000	1.0000	1.0000	1.1083	1.0000	1.0000
$17 < \text{Age} \leq 26$	1.0000	1.0000	1.4005	0.8307	0.6426	1.7099
$27 < \text{Age} \leq 44$	1.0000	1.7709	1.8543	1.4032	1.8168	2.4305
$45 \leq \text{Age}$	1.4877	2.1086	1.9336	1.4768	2.0180	1.9503

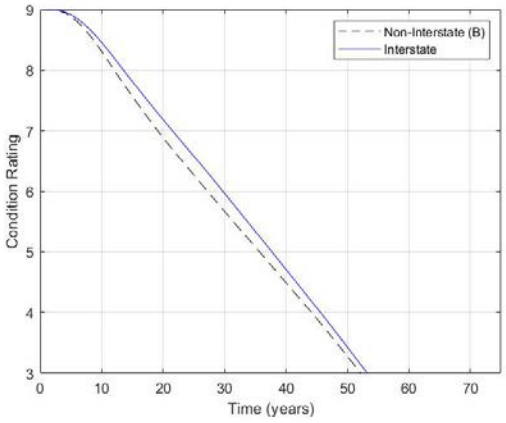

Figure A.31 Degradation curve for functional classification comparison

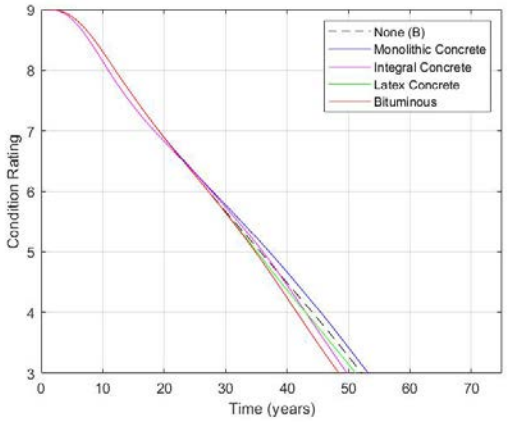

Figure A.32 Degradation curve for wearing surface presence/type comparison

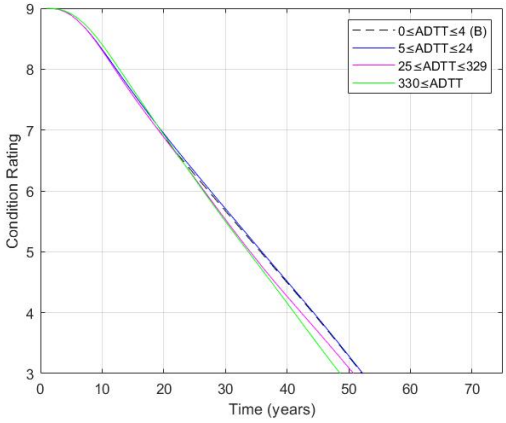

Figure A.33 Degradation curve for average daily truck traffic comparison

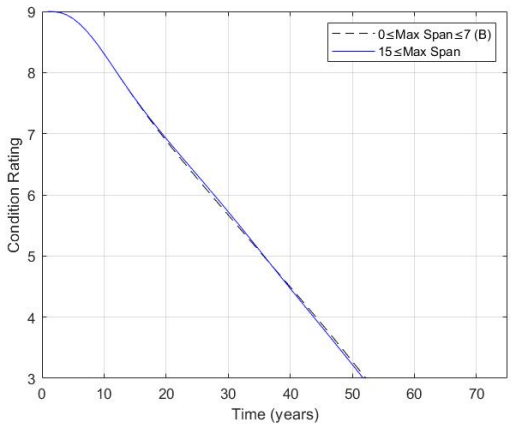

Figure A.34 Degradation curve for maximum span length comparison

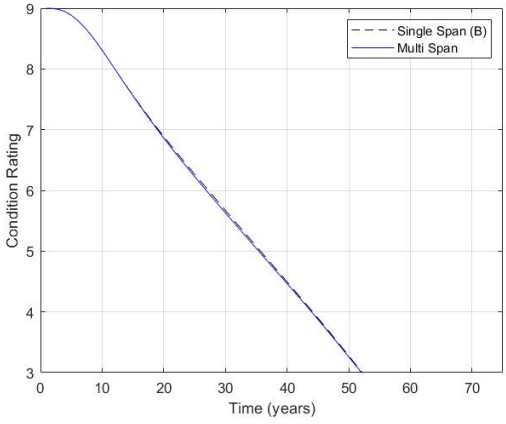

Figure A.35 Degradation curve for number of spans comparison

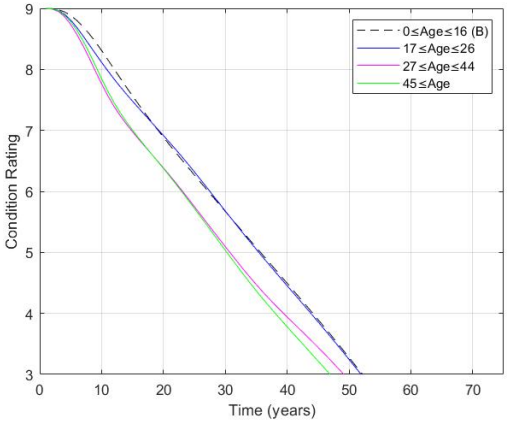

Figure A.36 Degradation curve for age comparison

When comparing the individual hazard options (i.e., interstate versus non-interstate), often one single hazard option does not exhibit much variation in expected life lost/gained. The observed maximum variation is approximately 2 years in this study. That is, of course, for all hazard groups other than wearing surface presence/type and age. The hazard group age results in a variation of approximately 6 years among its respective hazard options. Another difference to note is when the hazard ratios are combined for individual bridges (as most bridges are subject to multiple hazards at the same time), the effect of the hazards greatly increases. See Figure A.37 for an illustration of the difference in loss/gain of life that can happen from different levels of hazard combination. The curve representing "Negligible Hazards" has the hazards for "Road System 2" and "$5 \leq$ ADTT ≤ 24" applied. The curve representing "Moderate Hazards" has the hazards for "Latex Concrete" and "$25 \leq$ ADTT ≤ 329" applied. The curve representing "Severe Hazards" has the hazards for "Bituminous," "$330 \leq$ ADTT," and "$45 \leq$ Age" applied.

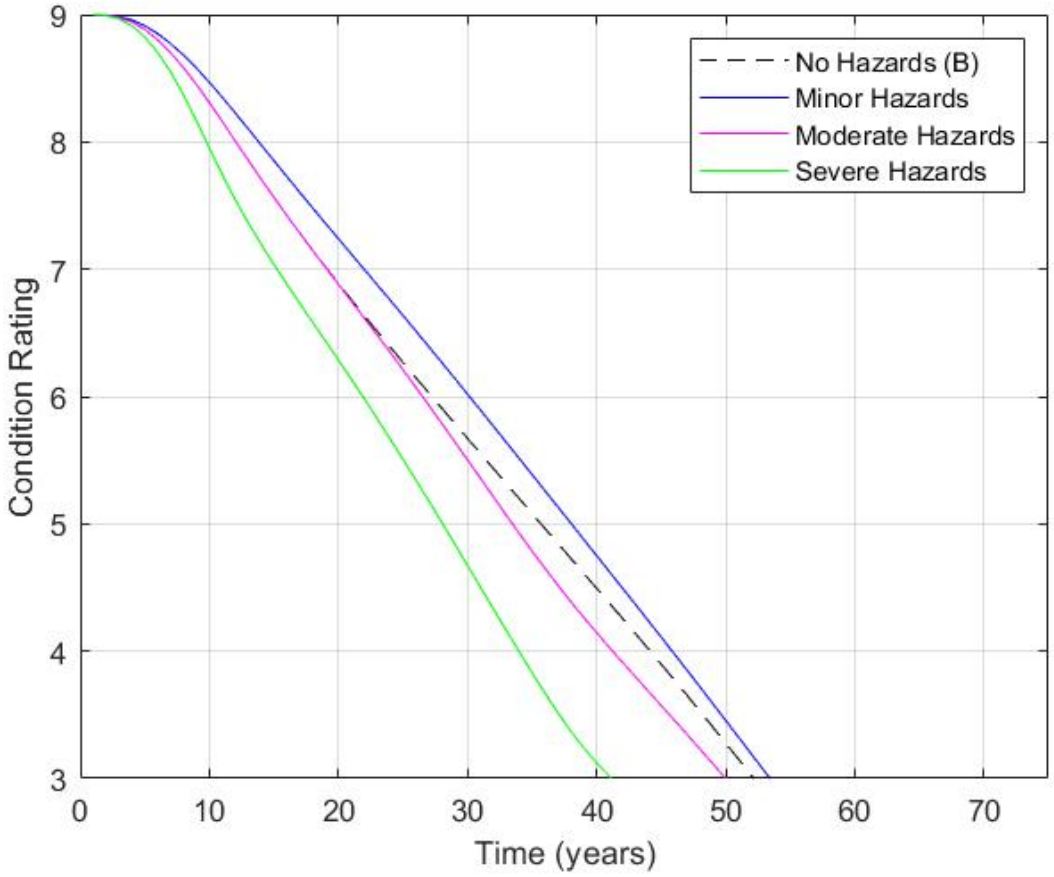

Figure A.37 Sensitivity analysis for different hazard ratios combinations.

Appendix A.4 Nomenclature

Symbol	Meaning
A_h	Rebar damaged area
a_f	Fraction of corroded area
b_c	Curing time regression parameter
C	Chloride concentration
C_I	Cost of interventions
C_R	Cost of replacement
C_T	Total cost
c	Concrete cover
c_a	Ambient CO_2 concentration
c_l	Reference CO_2 concentration
D	Diffusion coefficient
D_{FT}	Freeze-thaw cycles-modified chloride diffusion coefficient
d_b	Rebar diameter
d_h	Rebar pitting diameter
E_n	n^{th} Estimated future condition rating
E_w	Equivalent weight of steel
$E[\,x\,]$	Expected cost of x
f_e	Regression parameter for k_e
g_e	Regression parameter for k_e
HR_k	k^{th} Hazard Ratio
$h(t)$	Hazard function
i_{corr}	Current density
k_a	Ambient CO_2
k_c	Curing factor
k_e	Relative humidity factor
k_{NAC}	Carbonation rate
l	Rebar pitting spacing
l_f	Fraction of corroded length
$\bar{m}$	Mean value of the crack width slope for the state's bridges
P_{kk}	k^{th} Stay-the-same transition probability (physics-based model)
P^*_{kk}	k^{th} Stay-the-same transition probability (data-driven model)
$P^*_{k(k-1)}$	Transition probability
P_n	n^{th} Transition probability matrix

Symbol	Meaning
R	Condition rating column vector
R_c	Random corrosion rate of steel
RH_a	Reference relative humidity.
RH_l	Relative humidity of ambient air
r	Discount rate (rate of inflation)
r_c	Corrosion rate of steel
$S(t)$	Survival function
T	Ambient temperature
T_k	k^{th} sojourn time
T_s	Survival Time
t	Instantaneous time
t_c	Curing time
t_i	Time to initiation
t_s	Time to spalling
t_1	Time to first repair
$W(t)$	Wetting events' factor
Z_n	n^{th} Condition state vector
β	Regression coefficient
ϕ	Rebar loss due to corrosion
ϕ_c	Critical rebar loss due to corrosion
ρ	Steel's density
σ	Standard deviation of the crack width slope for the state's bridges

Appendix A.5 Glossary

Term	Definition
AASHTO	American Association of State Highway and Transportation Officials
ACI	American Concrete Institute
BIAS	Bridge Inspection Application System
CR	Condition Rating
INDOT	Indiana Department of Transportation
FHWA	Federal Highway Administration
NBI	National Bridge Inventory
Baseline	The estimated current degradation pattern used by INDOT that does not include the effects of physical, chemical, or environmental parameters and is based solely on historical condition rating patterns
Construction Defect	A material or workmanship error during the construction of a concrete bridge deck
Data Censoring	The process of assigning the title “censored” or “uncensored” to a historical condition rating assignment
Data Cleaning	The process of removing unreliable data from the data set
Data-Driven Degradation Model	Simulation of the state of the concrete deck over time using historical data gathered during inspections to account for relevant external usage factors
Degradation	The loss of condition rating value over time
Deterioration	The process of a concrete bridge deck losing effectiveness over time
Future Condition State	The future condition rating of a bridge deck based on the predictive degradation model calculations
Hazard Group	The collection of all coding options of a specific external factor (hazard)
Hazard Ratio	A value used to compare the effect on overall bridge deck degradation of an individual hazard group option
Intervention	Any action taken by INDOT that effects the condition rating of a bridge deck, can include but is not limited to; thin deck overlay, rigid deck overlay, crack sealing.
Native Degradation	Degradation with no interventions and/or maintenance actions performed on the deck during its lifespan
Non-Stationary Transition Probability Matrices	A set of stay-the-same transition probability matrices, one for every year into the future the condition rating of the bridge deck will be predicted
Physics-Based Deterioration Model	Simulation of the chemical and physical properties in concrete and the environmental factors that influence this behavior
Service Life	The total time a bridge deck is in service to the public. This time begins immediately after construction and ends when the bridge deck, superstructure, or whole bridge is replaced
Snow Belt	Region in the US and Canada next to the Great Lakes characterized by heavy snowfall during winter.
Sojourn Time	Time that the deck spends in a certain condition rating number before transitioning to the next one
Standard Construction	Indicates that the concrete bridge deck was constructed meeting all the material and workmanship criteria imposed by INDOT
Stay-The-Same Transition Probability	The probability of a bridge deck to stay in the condition rating it is currently in, in the next inspection cycle
Substandard Construction	One or more of the material and/or workmanship criteria imposed by INDOT was not fulfilled during construction

Time to First Repair	Time it takes for the first rust-induced crack to appear on the surface of the deck
Time to Initiation	Time it takes for the chlorides to reach the rebar level of the deck
Time to Spalling	Time it takes for the deck to crack after the chlorides have reached the rebar level
Transition Probability	The probability of a bridge deck to transition from the current condition rating to the next lowest condition rating, in the next inspection cycle
Uncensored Data	Historical condition rating observation that is potentially shorter than it would have been if (1) the observation had not been interrupted by a maintenance action or (2) the timeframe of the dataset was not cutting off the beginning or end of the condition rating observation
Unreliable Data	Condition rating assignments that have been influenced by subjectivity in the inspection process or have been coded incorrectly

About the Joint Transportation Research Program (JTRP)

On March 11, 1937, the Indiana Legislature passed an act which authorized the Indiana State Highway Commission to cooperate with and assist Purdue University in developing the best methods of improving and maintaining the highways of the state and the respective counties thereof. That collaborative effort was called the Joint Highway Research Project (JHRP). In 1997 the collaborative venture was renamed as the Joint Transportation Research Program (JTRP) to reflect the state and national efforts to integrate the management and operation of various transportation modes.

The first studies of JHRP were concerned with Test Road No. 1—evaluation of the weathering characteristics of stabilized materials. After World War II, the JHRP program grew substantially and was regularly producing technical reports. Over 1,600 technical reports are now available, published as part of the JHRP and subsequently JTRP collaborative venture between Purdue University and what is now the Indiana Department of Transportation.

Free online access to all reports is provided through a unique collaboration between JTRP and Purdue Libraries. These are available at http://docs.lib.purdue.edu/jtrp.

Further information about JTRP and its current research program is available at http://www.purdue.edu/jtrp.

About This Report

An open access version of this publication is available online. See the URL in the citation below.

Criner, N. M., Salmeron, M., Zhang, X., Dyke, S. J., Ramirez, J. A., & Wogen, B. E. (2023). *Predictive analytics for quantifying the long-term costs of defects during bridge construction* (Joint Transportation Research Program Publication No. FHWA/IN/JTRP-2023/08). West Lafayette, IN: Purdue University. https://doi.org/10.5703/1288284317615